الجمهورية الجزائرية الديمقراطية الشعبية
People's Democratic Republic of Algeria

Ministry of Higher Education and Scientific Research
University Abdelhamid Ibn Badis Mostaganem

وزارة التعليم العالي والبحث العلمي
جامعة عبد الحميد بن باديس مستغانم

Faculty of Exact Sciences and Computer Science
كلية العلوم الدقيقة والإعلام الآلي

Department of Chemistry
قسم الكيمياء

Thesis

Submitted in candidacy for the degree of

LMD Doctorate

In Materials Sciences

Option: Organic Chemistry and Environnement

Elaboration and characterization of algae biomass-derived materials and their applications

Submitted by: Radhia ELONG

Board of examiners

Mr. Aissa BELOUATEK	Professor	University of Mostaganem	Chairperson
Mr. Amine HARRANE	Professor	University of Mostaganem	Examiner
Mr. Youcef BOUHADDA	Professor	University of Mascara	Examiner
Mr. Mahmoud BELALIA	Professor	University of Mostaganem	Supervisor
Mrs. Louiza BELKACEMI	Professor	Higher School of Agronomy, Mostaganem	Co-Supervisor

22/10/2026

البحث عن الحقيقة أشرف الممن , والمعرفة هي عبادة للخالق.

ابن رشد.

ملخص

تهدف هذه الدراسة إلى إبراز تركيب مواد حيوية المصدرلم تنشر مسبقا، مشتقة من مصادر محلية متجددة عبر مسارات تركيب صديقة للبيئة، أسفرت عن مركبات ذات نشاط مضاد للأكسدة ومضاد للبكتيريا، مع تطبيقات محتملة في مجالات الصناعات الصيدلانية والمنتجات الغذائية الصحية.

في هذا السياق، يركز العمل الحالي على تثمين طحالب *Cystoseira stricta* التي تم جمعها من الساحل الجزائري الغربي، من خلال استخلاص مختلف عديدات السكاريد: الفوكويدان، ألجينات الصوديوم، السليلوز، والسليلوز المتبلور الدقيق، مع تقييم تأثير حجم جسيمات العينة ونسبة السائل إلى الصلب، وتغير فترة جمع العينة على مردود الاستخلاص. أشارت النتائج إلى أن حجم جسيمات 150ميكرومتر ونسبة صلب /سائل بقدار 1:30، والحصاد خلال شهر فبراير أعطت أفضل النتائج للألجينات والفوكويدان.

على عكس السليلوز، تحقق أفضل مردود في شهر سبتمبر. كما تم تقييم خصائص المستخلصات الفيزيوكيميائية بتحاليل مطيافية الأشعة تحت الحمراء و الأشعة السينية والمسح الحراري و المجهر الإلكتروني وتقييم نشاطها المضاد للبكتيريا. علاوة على ذلك، تم تحضير ألجينات الصوديوم الموظّف بأنهيدريد الماليك بهدف تركيب مادة جديدة بخصائص معدّلة ونشاط مضاد للأكسدة محسن بحيث بلغ مقدار الإستبدال 0.93 في حين بلغ نصف التركيز المثبط الأقصى 55.6 مغ/مل. كما استُخدم ألجينات الصوديوم المعدّل في تركيب طلاء صالح للأكل للحفاظ على الفراولة الطازجة. أظهرت التركيبة حجم قطرات على المقياس النانومتري مع استقرار عالٍ وفقاً لتحليل تشتت الضوء. علاوة على ذلك، أثبت الطلاء فعالية كبيرة بوصفه حاجزاً ضد الأكسدة والجفاف من خلال الاختبار على الفراولة الطازجة. وكتطبيق ثالث لألجينات الصوديوم، تم تطوير هيدروجيل على أساس الألجينات لتغليف السيفالكسين عبر تقنية التبلور الأيوني. كانت الحبيبات المحضرة شبه كروية ويُقدَّر متوسط حجمها بـ 807 ميكرومتر، وبلغت كفاءة الاحتجاز أثبتت دراسة ملف الإطلاق للسيفالكسين أن حركية الرتبة الأولى هي النموذج الأفضل اتباعاً. وقد أُثبت من خلال .51.45% الاختبارات المضادة للبكتيريا أن التغليف الدقيق حافظ على توافر العامل الفعّال وفعاليته.

تُمهّد النتائج المهمة لهذه المبادرة البحثية الطريق لدراسات عديدة تتعلق باستخدام عديدات السكاريد الطحلبية في تطبيقات أخرى كتصنيع المواد المركبة النانونية.

الكلمات المفتاحية:

الطحالب، الكتلة الحيوية، الاستخلاص، المواد الحيوية المصدر، التغليف، الطلاء الصالح للأكل، النشاط المضاد للبكتيريا، النشاط المضاد للأكسدة.

Abstract

This study aims to highlight the synthesis of previously unreported bio-based materials derived from local renewable source through environmentally friendly synthesis routes, yielded compounds with notable antioxidant and antibacterial activities, with prospective applications in pharmaceuticals and nutraceuticals.

In this context, the present work focuses on the valorisation of *Cystoseira stricta* brown macroalgae, harvested from west Algerian coast, by extracting several polysaccharides: Fucoidan, sodium alginate, cellulose and microcrystalline cellulose with the evaluation of the effect of particle size, liquid to solid ratio and harvesting period variation on their extraction yield. The findings were suggested a particle size of 150 µm, Solid/Liquid ratio 1:30, and harvesting during February yielding the best results for alginate and fucoidan. Contrary to cellulose, best yield was achieved in September. The physico-chemical characteristics of the extracts were investigated through FTIR, XRD, DSC/ATG, SEM and their antibacterial activity was also evaluated. In addition, sodium alginate has chosen to be functionalized with maleic anhydride with the aim of synthesizing a new material with modified properties and enhanced antioxidant activity where the substitution degree reached 0.93, while the half-maximal inhibitory concentration (IC50) was 55.6 mg/mL. Esterified sodium alginate has been also used in the synthesis of edible coating for fresh strawberries preservation. The formulation showed droplet size in nanometric scale with high stability according to DLS analysis. Furthermore, the developed coating exhibited remarkable effectiveness as a protecting barrier against fruit oxidation and dehydration, thereby extending fruit shelf life. As third application of sodium alginate, alginate-based hydrogel for cephalexin encapsulation via ionotropic gelation technique was also developed. The prepared beads were nearly spherical and their average size was estimated to be 807±0.097 µm and the entrapment efficiency was 51.45±0.83%. The study of cephalexin released profile proved that the first-order kinetics was the best followed modal. It was demonstrated via antibacterial assays that the microencapsulation has maintained the availability and the effectiveness of the active agent.

The significant findings of this research initiative pave the way for several studies regarding the use of algal polysaccharides in other applications such as the fabrication of nanocomposites.

Keywords:

Algae, biomass, extraction, bio-based materials, encapsulation, edible coating, antibacterial activity, antioxidant activity.

Résumé

Cette étude vise à mettre en lumière la synthèse de matériaux biosourcés non rapportés précédemment, dérivés d'une source renouvelable locale par des voies de synthèse respectueuses de l'environnement, ayant produit des composés dotés d'activités antioxydantes et antibactériennes notables, avec des applications potentielles dans le domaine pharmaceutique et nutraceutique.

Dans ce contexte, le présent travail se concentre sur la valorisation des macroalgues brunes *Cystoseira stricta*, récoltés sur la côte ouest algérienne, par l'extraction de plusieurs polysaccharides : le fucoïdane, l'alginate de sodium, la cellulose et la cellulose microcristalline, avec l'évaluation de l'effet de la taille des particules, du rapport liquide/solide et de la variation de la période de récolte sur leur rendement d'extraction. Les résultats ont suggéré qu'une taille de particule de 150 µm, un rapport Solide/Liquide de 1:30 et une récolte en Février donnent les meilleurs résultats pour l'alginate et le fucoïdane. Contrairement à la cellulose, le meilleur rendement a été obtenu en Septembre. Les caractéristiques physico-chimiques des extraits ont été étudiées par les analyses FTIR, DRX, DSC/ATG et MEB et leur activité antibactérienne a également été évaluée. De plus, l'alginate de sodium a été fonctionnalisé avec de l'anhydride maléique dans le but de synthétiser un nouveau matériau aux propriétés modifiées, et une activité antioxydante améliorée où le degré de substitution a atteint 0,93, tandis que la concentration inhibitrice semi-maximale (IC_{50}) était 55,6 mg/ml. L'alginate de sodium estérifiée a également été utilisé dans la synthèse d'un revêtement comestible pour la conservation des fraises fraiches. La formulation a montré une taille de gouttelettes à l'échelle nanométrique avec une haute stabilité selon l'analyse DLS. De plus, L'enrobage a démontré une grande efficacité en tant que barrière protectrice contre l'oxydation et la déshydratation du fruit, contribuant ainsi à une prolongation notable de sa durée de conservation. En tant que troisième application de l'alginate de sodium, un hydrogel à base d'alginate pour l'encapsulation de la céphalexine par la technique de gélification ionotropique a également été développé. Les billes préparées étaient presque sphériques et leur taille moyenne a été estimée à 807±0,097 µm, avec une efficacité d'encapsulation de 51,45±0,83 %. L'étude du profil de libération de la céphalexine a prouvé que la cinétique du premier ordre était le meilleur modèle suivi. Il a été démontré, via des tests antibactériens, que la microencapsulation a maintenu la disponibilité et l'efficacité de l'agent actif.

Les résultats significatifs de cette initiative de recherche ouvrent la voie à plusieurs études concernant l'utilisation des polysaccharides d'algues dans d'autres applications telles que la fabrication des nanocomposites.

Mots-clés :

Algues, biomasse, extraction, matériaux biosourcés, encapsulation, revêtement comestible, activité antibactérienne, activité antioxydante.

Dedication

This peace of achievement is affectionally dedicated

To my Parents, Sisters, and Teachers

The pillars of my academic journey

To my Husband, Family, and Friends

For being source of support, guidance, and unwavering faith

To all those who believe in the virtues of effort, patience, determination and success.

Acknowledgments

First and foremost, praise and thanks to the Almighty **GOD** for His showers of blessing and granting me strength and patience throughout the completion of this work.

My appreciations go to my supervisor Mr. **Mahmoud BELALIA** for his constant guidance, valuable feedback, recognition of my efforts and trust he has always shown me. It was a great privilege to work and study under his supervision. I am equally thankful to my co-supervisor Mrs. **Louiza BELKACEMI** whose advice and assistance have been invaluable.

My gratitude extends to the Jury members for accepting to examine and evaluate this work:
Mr. **Aissa BELOUATEK**, Professor at UMAB, in recognition for his attendance to chair the jury; Mr. **Amine Harrane**, Professor at UMAB, and Mr. **Youcef BOUHADDA,** Professor at UMMS who took the time to attend and thoroughly evaluate this work.

I would like to give my warmest thanks to Messrs. **Abdelghani BOUCHAMA, Fouad MEKHALEF BEN HAFSA** and **Yacine LAICHI**, the technical staff of CRAPC, for their help, generosity and collaboration.

I wish to acknowledge the contributions of Pr. **Mostefa BELHAKEM**, the director of the laboratory Structure, Elaboration and Application of Molecular Materials and Pr. **Fadela NEMCHI** the former lab director. My acknowledgements also go to the laboratory stuff **Rabia, Hasna, Djahira, Toufik, Hmida** and **Touati** whose help ensure the execution of this research.

I am profoundly thankful to my **Teachers** who inspired my academic growth and intellectual curiosity.

A special thanks goes to my **Family** for their continuous support and understanding. Your love has been my greatest treasure.

I will not forget my **Colleagues** and **Friends** who stood by me throughout this challenging path, offering emotional support and intellectual stimulation.

Table of contents

ملخص……i

Abstract……ii

Resume……iii

Dedication……iv

Acknowledgments……v

List of tables……vi

List of figures……vii

List of abbreviations……viii

General Introduction……1

Chapter I Literature Review

I.1 Marine macroalgae……3

I.1.1 Brown algae……3

I.2 Polysaccharides……4

I.2.1 Algal polysaccharides……4

I.2.2 The advantages of using seaweeds for extracting polysaccharides……6

I.2.3 Brown algae polysaccharides……6

I.2.3.1 Laminaran……6

I.2.3.2 Fucoidan……7

I.2.3.3 Sodium alginate……7

I.2.3.4 Cellulose……8

I.3 Polysaccharide-based hydrogels……9

I.3.1 Advantages of using hydrogels as drug delivery system……10

I.4 Polysaccharide based-active coating……10

I.5 Antibacterial activity……11

I.6 Antioxidant activity……12

I.7 References……14

Chapter II Materials and Methods

Section 1: Extraction of Algal polysaccharides

II.1 Extraction of Algal polysaccharides……..…..**24**

II.1.1 Chemical products…….....**24**

II.1.2 Plant material presentation……...**24**

II.1.3 Plant material preparation……..……...**25**

II.1.4 Moisture content and ash determination……...**26**

II.1.5 Polysaccharides extraction process……..**27**

II.1.5.1 Pretreatment……**27**

II.1.5.2 Fucoidan extraction……**28**

II.1.5.3 Alginate extraction……..**28**

II.1.5.4 Cellulose extraction……**28**

II.1.5.5 Microcrystalline cellulose preparation……**29**

II.1.6 Extraction yield determination……**31**

II.1.7 Evaluation of the antibacterial activity of the products……**31**

II.1.7.1 Inoculum preparation……**31**

II.1.7.2 Agar plates inoculation……**31**

II.1.7.3 Disc deposition……**32**

II.1.7.4 Agar plates incubation……..**32**

Section 2: Elaboration of Alginate-Based Materials

II.2 Elaboration of alginate based-materials...……**34**

II.2.1 Chemical products……**34**

II.2.2 Sodium alginate modification……..**34**

II.2.2.1 Experimental procedure of the modification……**34**

II.2.2.2 Determination of the degree of substitution……**35**

II.2.2.3 Antioxidant activity evaluation……**36**

II.2.2.3.1 Preparation of DPPH solution……..**36**

II.2.2.3.2 Preparation of sample solutions……**36**

II.2.2.3.3 DPPH scavenging assay setup……..**36**

II.2.2.3.4 Data analysis……**37**

II.2.3 Preparation and application of maleated sodium alginate-date seed oil-based oil-in-water nanoemulsion……**37**

II.2.3.1 Synthesis procedure of the nanoemulsion……..…**37**
II.2.3.2 Protective effect evaluation of the nanoemulsion……**38**
II.2.4 Cephalexin-loaded hydrogel beads preparation……...**39**
II.2.4.1 Synthesis procedure of hydrogel beads……**39**
II.2.4.2 Quantification of the encapsulated active agent……**39**
II.2.4.2.1 Quantitative analysis of cephalexin……..…**39**
II.2.4.2.2 Encapsulation efficiency and loading capacity determination.....**40**
II.2.4.3 Swelling behaviour measurement……**41**
II.2.4.4 In vitro drug release study and kinetic modelling……**41**
II.2.4.5 Antibacterial activity evaluation……...**42**
II.3 Physicochemical characterizations……**42**
II.3.1 Ultraviolet-visible spectrophotometry (UV-Vis).……**42**
II.3.2 Fourier transform infrared analysis (FTIR).……...**43**
II.3.3 X-ray diffraction analysis (XRD) ……..……**44**
II.3.4 Thermal analysis (TGA/DSC) ……**44**
II.3.5 Optical microscopy……..**45**
II.3.6 Scanning electron microscopy (SEM) ……**45**
II.3.7 Dynamic light scattering analysis (DLS) ……...**46**
II.4 References……...**47**

Chapter III Results and Discussion

Section 1: Extraction of Algal polysaccharides

III.1 Extraction of algal polysaccharides……...**51**
III.1.1 Moisture content and ash determination……**51**
III.1.2 Extraction yield determination……...**52**
III.1.2.1 Influence of particle size on the yield of polysaccharides……..….**53**
III.1.2.2 Influence of the solid to liquid ratio on the yield of polysaccharides……....**53**
III.1.2.3 Influence of harvesting time on the yield of polysaccharides……....**54**
III.1.3 Characterization……**55**
III.1.3.1 FT-IR analysis……**55**
III.1.3.2 XRD analysis**……**……..**59**
III.1.3.3 TGA/DSC analysis……..**61**

III.1.3.4 SEM/EDX analysis……**64**
III.1.3.5 DLS analysis……..**69**
III.1.4 Antibacterial activity……..**71**
III.1.5 Conclusion……..**73**

Section 2: Elaboration of Alginate-Based Materials

III.2 Elaboration of Alginate-Based Materials……...**76**
III.2.1 Sodium alginate modification……**76**
III.2.1.1 Characterization……..**76**
III.2.1.1.1 FT-IR analysis……**76**
III.2.1.1.2 XRD analysis……..**77**
III.2.1.1.3 TGA/DSC analysis……..**78**
III.2.1.1.4 SEM/EDX analysis……..……...**79**
III.2.1.2 Determination of the degree of substitution……**80**
III.2.1.3 Antioxidant activity test……..**80**
III.2.2 Protective effect evaluation of maleated sodium alginate-date seed oil-based oil-in-water nanoemulsion……**81**
III.2.3 Cephalexin-loaded hydrogel beads preparation……**82**
III.2.3.1 Characterization ……**82**
III.2.3.1.1 Shape, morphology and size measurement……**82**
III.2.3.1.2 FT-IR analysis……**84**
III.2.3.1.3 DSC analysis……...**85**
III.2.3.2 Quantification of the encapsulated active agent……**86**
III.2.3.2.1 Quantitative analysis of cephalexin……**86**
III.2.3.2.2 Encapsulation efficiency and loading capacity determination……...**87**
III.2.3.3 Swelling behaviour measurement……..**87**
III.2.3.4 In vitro drug release study and kinetic modelling……..**88**
III.2.3.5 Antibacterial activity evaluation……**90**
III.2.4 Conclusion……..**91**
III.3 References ……**92**
General Conclusion……**101**
Appendix

List of tables

Table I.1 Polysaccharides of marine algae……..…….……**5**

Table I.2 Antibacterial sensitivity…….……..…**12**

Table III.1 Influence of particle size distribution on extraction yield of polysaccharides……..…**53**

Table III.2 Assignment and location of the main characteristic bands of extracted Fucoidan, alginate, cellulose and microcrystalline cellulose……...**55**

Table III.3 Alginate content and M/G ratio of different species……..…..**58**

Table III.4 Fucoidan content, sulfate content and sulfation degree of different species……...….**65**

Table III.5 Inhibition zone values of extracted polysaccharides……..……..**71**

Table III.6 Caracteristics of maleated sodium alginate-date seed oil-based nanoemulsion…....**81**

Table III.7 Release kinetic parameters of the mathematical models applied for cephalexin release mechanism study……**89**

Table III.8 Inhibition zone values of free and cephalexin-loaded hydrogel beads……....……**90**

List of figures

Figure I.1 Cell wall composition of brown algae adapted from Baghel et al., 2021……..…..**4**
Figure I.2 Classification of marine algae polysaccharides……..……..…..**5**
Figure I.3 Chemical structure of Laminaran based on structure from Liu et al…….**6**
Figure I.4 Chemical structure of Fucoidan based on structure from Jönsson et al……**7**
Figure I.5 Chemical structure of sodium alginate based on structure from Collado-González…....**8**
Figure I.6 Chemical structure of cellulose based on structure from Zanchetta et al…….……**9**
Figure I.7 Hydrogel beads formation……...**9**
Figure I.8 Application methods of edible coating on food products……..……**11**
Figure I.9 The main action mechanisms of antibacterial drugs……..**12**
Figure I.10 DPPH reaction mechanism…….....**13**

Figure II.1 *Cystoseira stricta* brown algae……..…….……**24**
Figure II.2 Geographical location of Stidia…….…..**26**
Figure II.3 Desiccation…….…**27**
Figure II.4 Remaining ash…….…....**27**
Figure II.5 Pretreatment process…….…..**28**
Figure II.6 Polysaccharides extraction setup…….....**29**
Figure II.7 Polysaccharides extraction process…….**30**
Figure II.8 Inoculum preparation……..**31**
Figure II.9 Agar plates inoculation……....**32**
Figure II.10 Disc deposition……..**32**
Figure II.11 Agar plates incubation……...**32**
Figure II.12 Schematic diagram of sodium alginate modification……...**35**
Figure II.13 Discoloration of DPPH under the influence of test samples…….**37**
Figure II.14 (a) Sodium alginate and **(b)** maleated sodium alginate-based Nanoemulsions…....**38**
Figure II.15 (a) uncoated strawberry and **(b)** coated strawberry……..**38**

Figure II.16 (a) Sodium alginate crosslinking, **(b)** Sodium alginate-based hydrogel beads before drying and **(c)** after drying……..**39**
Figure II.17 Swelling test……..**41**
Figure II.18 Laboratory UV-Visible spectrophotometer apparatus……...**43**
Figure II.19 Laboratory FTIR spectrophotometer apparatus……**43**
Figure II.20 Laboratory X-ray diffractometer apparatus……...**44**
Figure II.21 Laboratory TGA/DSC apparatus……...**45**
Figure II.22 Laboratory optical microscope……..**45**
Figure II.23 Laboratory SEM apparatus……....**46**
Figure II.24 Laboratory DLS apparatus……....**46**

Figure III.1 Proximate composition of WBA and SBA……....**51**
Figure III.2 FT-IR spectrum of fucoidan isolated from the Algerian Cystoseira stricta……..**56**
Figure III.3 FT-IR spectrum of sodium alginate isolated from the Algerian *Cystoseira stricta*….**57**
Figure III.4 FT-IR spectrum of cellulose and MCC isolated from the Algerian *Cystoseira*…..... *stricta*……..*59*
Figure III.5 XRD pattern of fucoidan isolated from the Algerian *Cystoseira stricta*……**60**
Figure III.6 XRD pattern of sodium alginate isolated from the Algerian *Cystoseira stricta*…...**60**
Figure III.7 XRD pattern of cellulose and MCC isolated from the Algerian *Cystoseira stricta*.....*61*
Figure III.8 TGA/DSC thermogram of fucoidan isolated from the Algerian Cystoseira stricta.....**62**
Figure III.9 TGA/DSC thermogram of sodium alginate isolated from the Algerian *Cystoseira stricta*…….....**63**
Figure III.10 TGA/DSC thermogram of cellulose and MCC isolated from the Algerian *Cystoseira stricta*……...**64**
Figure III.11 SEM images of fucoidan **(a-1)** at 30 µm and **(a-2)** 15µm magnifications, **(b)** Chemical composition……..……..**66**
Figure III.12 SEM images of sodium alginate **(a-1)** at 200 µm, **(a-2)** at 80 µm and **(a-3)** at 30 µm magnifications, **(b)** Chemical composition……...……**67**
Figure III.13 SEM images of cellulose **(a-1)** at 20 µm, **(a-2)** at 3 µm and MCC **(a'-1)** at 30 µm and **(a'-2)** 5µm magnification, **(b and b')** their chemical composition respectively. ……..…..**69**
Figure III.14 DLS analysis of 1% MCC suspension……**70**

Figure III.15 Antibacterial activity of fucoidan isolated from the Algerian *Cystoseira stricta*.....**72**
Figure III.16 Antibacterial activity of sodium alginate isolated from the Algerian *Cystoseira stricta*...……..**72**
Figure III.17 Antibacterial activity of cellulose and MCC isolated from the Algerian *Cystoseira stricta*…….....**73**
Figure III.18 Physical appearance of (a) crude and (b) modified sodium alginate…….…..**76**
Figure III.19 (a) FT-IR spectra of maleic anhydride, crude and maleated sodium alginate, **(b)** zoom of the 2000-500 cm^{-1} region……..**77**
Figure III.20 XRD patterns of native and modified sodium alginate……...……..**77**
Figure III.21 (a) TGA and **(b)** DSC curves of native and modified sodium alginate ….……**78**
Figure III.22 SEM images of modified alginate (NaMalg) **(a-1)** at 300 µm, **(a-2)** at 80 µm and **(a-3)** at 30 µm magnifications, **(b)** chemical composition……..…….……...**79**
Figure III.23 Antioxidant scavenging of **(a)** HO-alg and **(b)** NaMalg……..**80**
Figure III.24. Nanoemulsion coating effect on strawberries over the time at room temperature (**(a)** uncoated strawberries; **(b)** coated strawberries with sodium alginate-based nanoemulsion; **(c)** coated strawberries with maleated sodium alginate-based nanoemulsion)…….**82**
Figure III.25 (a) Digital images, **(b)** optical microscope images and **(c1-c3)** scanning electron microscope images of cephalexin loaded hydrogel beads at magnifications of ×340, ×1k and ×10k respectively……..…..**84**
Figure III.26 FT-IR spectra of CSSA and CSMS……...……**85**
Figure III.27 DSC curves of CSSA and CSMS……..**85**
Figure III.28 UV-Vis spectrum of cephalexin in a buffer solution of pH= 7.4 at T=37°C…..…..**86**
Figure III.29 Calibration curve of Cephalexin at pH 7.4, T=37°C……..….**86**
Figure III.30 Swelling behaviour of cephalexin loaded beads at pH 1.2 and 7.4…….....**87**
Figure III.31 (a) Release profile of cep from hydrogel beads in pH 7.4 at 37°C, **(b)** linear plot of first-order kinetic modal…….**89**
Figure III.32 Antibacterial activity of synthesized hydrogel beads……..….**91**

List of abbreviations

ATCC	American type culture collection
C. stricta	*Cystoseira stricta*
$CaCl_2$	Calcium chloride
CFR	Code for Federal Regulations
Chl	Chloroform
CL	Cephalexin
CO2	Carbon dioxide
CSBA	Cystoseira stricta brown algae
CSSA	Cystoseira stricta sodium alginate
CTAB	(1-Hexadecyl) trimethylammonium bromide
DLS	Dynamic light scattering
DPPH	2,2-diphenyl-1-picrylhydrazyl
DS	Degree of substitution
DSC	Differential scanning calorimetry
DSO	Date seed oil
DW	Distilled water
E.coli	*Escherichia coli*
EDX	Energy dispersive X-ray
EE	Entrapment efficiency
EtOH	Ethanol
F	Blank beads
FDA	Food and Drug Administration
FT-IR	Fourier-transform infrared spectroscopy
G	Guluronic acid
GRAS	Generally regarded as safe
h	Hours
HCl	Hydrochloric acid

HO-alg	Sodium alginate
IC_{50}	50% inhibition concentration
L	cephalexin-loaded bead
LC	Loading capacity
M	Mannuronic acid
MA	Maleic anhydride
MC	Moisture content
MC	Moisture content
MCC	Microcrystalline cellulose
min	Minute
NaMalg	Maleated sodium alginate
NCC	Nanocrystalline cellulose
OD	Optical density
r.t	Room temperature
R^2	Coefficient of determination
rpm	round per minute
S.a	*Staphylococcus aureus*
S/L	Solid to Liquid ratio
SBA	Brown algae harvested in summer
SD	Standard deviation
SEM	Scanning electron microscopy
SEM	Standard error of the mean
UV-Vis	Ultraviolet-visible
v	Volume
w	Weight
WBA	Brown algae harvested in winter
wt%	Weight percentage
XRD	X-ray diffraction
λ_{max}	Absorption maximum wavelength

General Introduction

General Introduction

In recent years, the concept of green chemistry has garnered widespread attention due to growing concerns about human health and environment. The desire to develop products based on natural components and adopt more eco-friendly methods for chemical synthesis is becoming more prevalent over time.

Biomass, that encompasses a wide range of sustainable and renewable materials derived from agricultural, forestry, animal wastes and aquatic sources, constitute a tremendous feedstock for the production of new bio-based materials.

Marine macroalgae, also known as seaweed, represent a sustained feedstock which can produce ten times more organic matter than the entire terrestrial vegetation. They are rich in bioactive nutraceuticals such as proteins, minerals, fatty acids, antioxidants, pigments and carbohydrates.

There was about 2040 identified species around the world and about 93 accepted mediterranean brown algal taxa were registered in Algeria until 2019 but unfortunately, they are not being well exploited which is actually problematic.

Polysaccharides are the most abundant renewable resource existed in the world. They are stored by algae as food storage and structural materials including cellulose, fucoidan and sodium alginate existing in brown seaweeds. Their unique properties for instance biocompatibility, biodegradability, safety and presence of reactive functions, particularly OH groups, in their molecular backbone structure, make them attractive for various applications in different areas such as medicine, food, and cosmetics, etc.

With increasing concerns about health and the environment, looking for greener materials as alternative of toxic materials has become an imperative. Regarding food packaging materials, they are disposed of in the environment and persist for years resulting in earth pollution. Moreover, packaging represents a hazard related to some harmful chemicals, such as phenols and phthalates, incorporated into these containers. The leaching of these chemicals resulting in human

consumption can provoke consequently serious diseases. The algae-based biopolymers are considered a brilliant material for the development of edible coating as a sustainable alternative of non-biodegradable packaging materials for food preservation, notably extremely perishable fruits, and shelf-life extension.

Some bioactive compounds are unstable when exposed to high temperature, high concentration of oxygen, pH, and incidence of light [1].

Encapsulation with natural biopolymers has gain much attention because it is an effective way to protect, control the release, enhance the availability, enhance the sensory quality, and increase the stability of therapeutic and food products.

In this thesis, we are specifically interested in the exploitation of marine macroalgae for the extraction of polysaccharides while expanding the knowledge of their diverse applications in addition the study of their biological activity.

The first chapter is a literature review on marine macroalgae, brown algae, their constitution in polysaccharides, their modification in addition to their application in hydrogel-forming and coating production. The biological potentials (antioxidative and antimicrobial) of brown algae polysaccharides are also investigated.

The second chapter is divided into two sections. The first one describes the materials and methods to the extraction of fucoidan, alginate cellulose and microcrystalline cellulose from local *Cystoseira stricta* brown algae with their characterization and study of their biological activity. The second section represents the exploitation of sodium alginate for various applications including the functionalization with maleic anhydride for the purpose of enhancing its antioxidant activity, production of edible coating for fruit preservation besides the production of hydrogel beads for drug encapsulation with conduction of different in-vitro tests.

The third chapter represents the results and discussion of all conducted experiments.

Finally, the general conclusion highlights the most brilliant findings and future perspectives.

Chapter I

Literature Review

I.1 Marine macroalgae

The marine environment represents a mine of useful products awaiting discovery for several reasons. They represent 71% of the globe but they are not greatly valorised [1]. In some countries, the term “Seaweeds” often invokes a negative image of smelly and rotting masses found on beaches, which are neglected or ignored [2]. In Asia, seaweeds have been used for direct human consumption and considered valuable from ancient time. Unlike consumers in other places, eating seaweed evoked memories of times of food shortage and famine [3].

In recent years, macroalgae constitution attract attention to be valorised and used in a wide range of ways. Their photosynthetic mechanism is similar to that of land-based plants. They are generally more efficient in converting solar energy into biomass, mainly because of their simple cellular structure and being submerged in an aqueous environment with access to water, CO2, and other nutrients [4]. This sustained feedstock can produce ten times more organic matter and release five times more oxygen compared to the entire terrestrial vegetation [5]. Seaweeds are rich in bioactive nutraceuticals such as carbohydrates, proteins, minerals, fatty acids, antioxidants, and pigments [6].

Traditionally, seaweeds are divided into three main groups: green, red and brown algae [7].

I.1.1 Brown algae

Brown algae (Phaeophyta) contain a pigment called fucoxanthin responsible for the brownish-yellow colour with only a little chlorophyll [7]. There was about 2040 identified species around the world [8]. About 93 accepted mediterranean brown algal taxa were registered in Algeria until 2019 [9]. Mehiaoui et al. were identified 162 species in western Algerian coast spread over three phyla among them 48 species Pheophyceae. It was found that *Cystoseira* species are one of the most dominant brown seaweeds in that region [10]. The presence of the *Cystoseira stricta* is a reliable indicator of a healthy marine environment [11].

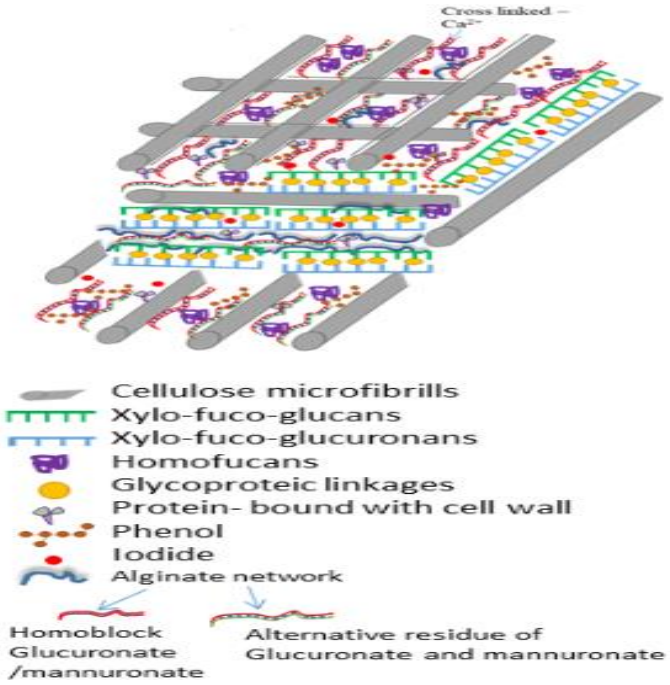


Figure I.1 Cell wall composition of brown algae adapted from Baghel et al., 2021 [12]

I.2 Polysaccharides

Polysaccharides are the most abundant renewable resource existed in the world [13]. They represent a group of monosaccharides linked together by glycosidic bonds as they can be covalently bonded to other moieties such as peptides, amino acids and lipids [14].

Polysaccharides can be classified based on different parameters:

- **Nature of monosaccharides components:** homopolysaccharides consisting of same monosaccharides and heteropolysaccharides which consist of different monosaccharides.
- **Nature of linkage:** Linear or branched polysaccharides.
- **Configuration:** Amorphous, semicrystalline or crystalline polymers.
- **Charge:** positively or negatively charged polysaccharides (polyelectrolytes).

I.2.1 Algal polysaccharides

Algal polysaccharides are used as an alternative renewable source for developing environmentally friendly materials [15]. This type of carbohydrates are stored by algae as food storage and structural materials, they differ in their composition and glycosidic bonding [16].

Species, harvesting period and geographical location of seaweeds dominate the structural features and bioactivities of polysaccharides [17]. Algal polysaccharides are safe, stable, economical, biocompatible, biodegradable and chemically modifiable to be applied for specific purposes [18].

Chemical modifications or also named derivatization reactions, are often used to confer or promote biological properties to biopolymers [19]. Esterification, amidation, ugi reaction of polysaccharides containing carboxylic acid (alginate), copolymerization reaction via oxidation, sulfonation and esterification for hydroxyl-containing polysaccharides.

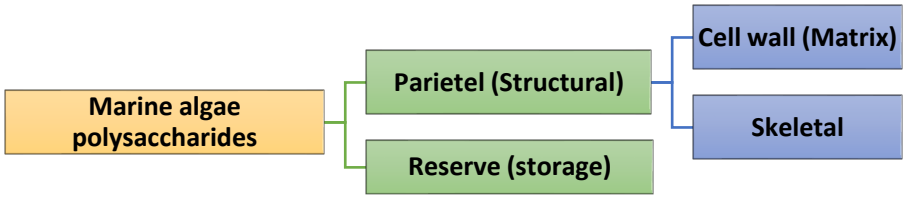


Figure I.2 Classification of marine algae polysaccharides.

Table I.1 Polysaccharides of marine algae [20]

Seaweed type	**Composition**		
	Reserve Polysaccharides	Skeletal Polysaccharides	Cell-wall Polysaccharides
Green (Chlorophyceae)	*Glucan: 1,4-ß-glucose *Starch	*Cellulose : (1,4)-β-glucopyranose *Xylans : β-(1,3)-D-xylose or β-(1,4)-D-xylose	*Ulvane *Galactan *Rhamnose *Other sulphated polymers
Brown (Phaeophyceae)	*Laminarine : 1,3-ß-glucopyranose		*Fucan *Alginate :β-D-mannuronic acid and α- L-guluronic acid, bonded in (1,4)
Red (Rhodophyceae)	*Floridean starch (Amylose free starch) : 1,4-α-glucose	*Mannans : β-(1,4)-D-mannose	*Carrageenan: D-galactopyranose β-(1,3) (G unit) or α-(1,4) or 3,6-anhydro-α-galactopyranose *Agars

I.2.2 The advantages of using seaweeds for extracting polysaccharides[21]

- Rapid growth rate and short harvesting time compared to terrestrial biomass.
- The presence of relatively higher yield of stored carbohydrates.
- The absence or lack of physicochemical barriers such as lignin and hemicellulose which makes the extraction of polysaccharides easier with low coast and low environmental impact.

I.2.3 Brown algae polysaccharides

Brown algae polysaccharide was firstly isolated in 1913. They are principally composed of Laminaran, fucoidan, sodium alginate and cellulose [22].

I.2.3.1 Laminaran

Laminaran is a water-soluble polysaccharide [23]. It is mainly found in some species such as Laminaria, Saccharina or Eisenia species [24]. It is consisted of a linear chain of D-glucose with β-(1,3) linkages and β-(1,6) intrachain branching **(Figure I.3)**. It exists two types of chain terminations, one with D-mannitol residues (M-series) and the other one with D-glucose residues (G-series) [25].

This polysaccharide can be used as dietary fiber, as a stimulant of the innate immune system of mammals, and as a plant pathogen defense stimulant for agriculture [26]. It has the ability to hold other properties including wound healing, drug delivery, anti-cancer, anti-inflammatory and anti-oxidative activities as it can be applied in the domain of tissue engineering [27].

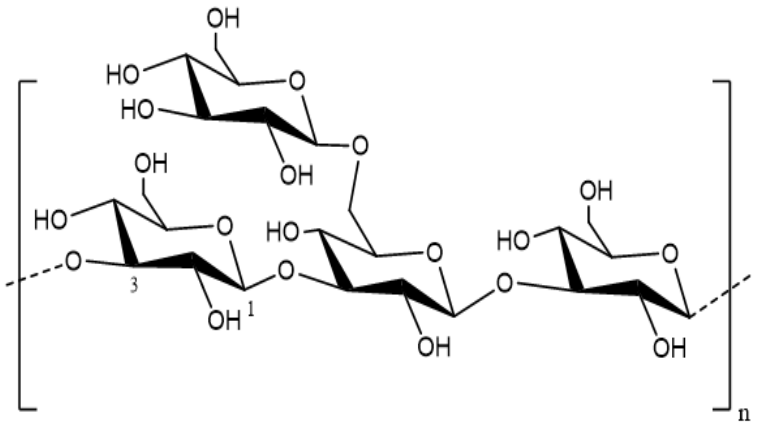


Figure I.3 Chemical structure of Laminaran based on structure from Liu et al. [22]

I.2.3.2 Fucoidan

Fucoidan is a water soluble sulphated hetero-polysaccharide from the class of fucans, found in brown algae and echinoderms [28]. It is essentially consisting of l-fucose etherified by residues of sulfuric acid with alternating (1→3) and (1→4) **(Figure I.4a)** or (1→3) **(Figure I.4b)** glycosidic linkages [29], [30]. The structure of fucoidan also contains additional monosaccharides such as glucose, galactose, mannose, xylose and uronic acids and yet acetyl groups [31].

Fucoidan is a candidate for the treatment of bleeding and immune disorders, inflammation and viral infections [32]. It can be also applied in food and cosmetics industries, drug delivery and tissue engineering [33].

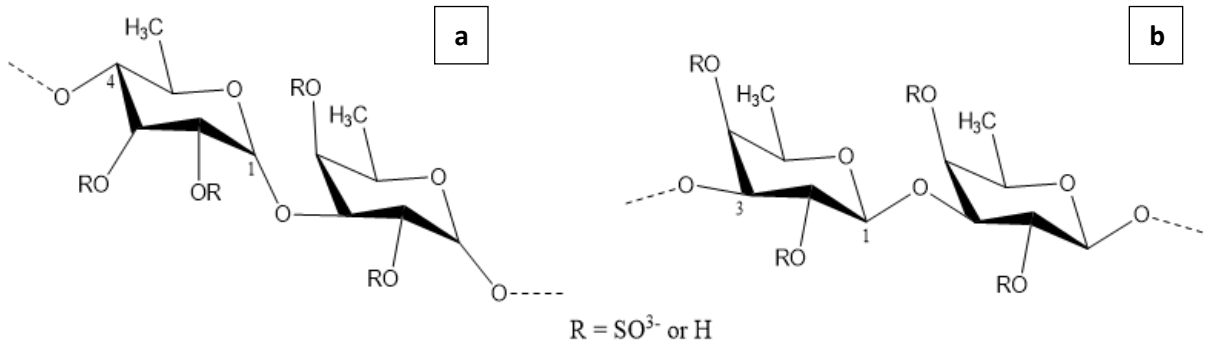


Figure I.4 Chemical structure of Fucoidan based on structure from Jönsson et al. [34]

I.2.3.3 Sodium alginate

Alginate is a water soluble non-sulphated polysaccharide extracted from brown algae and bacteria species. It is a linear block copolymer composed of α-L-guluronic acid (G) and β-D-mannuronic acid (M) with (1→4) linkages **(Figure I.5)** [35]. It is the only polysaccharide that naturally contains carboxyl groups in each constituent residue [36]. This feature enable sodium alginate to produce a gel through an ionic crosslinking in the presence of divalent cations [37]. The physicochemical properties of Alginate are dependent on the proportion and distribution pattern of M and G block. Alginate with high value of M/G ratio (>1) forms soft and elastic gels while a value of M/G less than the unit refers to the formation of mechanically stable, strong and brittle gel [38].

Brown seaweeds mainly from the genus *Ascophyllum*, *Alaria*, *Cystoseira*, *Ecklonia*, *Eisenia*, *Fucus*, *Laminaria*, *Lessonia*, *Macrocystis*, *Nereocystis*, *Sargassum* are the natural resources of alginates [39].

The U.S. Food and Drug Administration (FDA) classifies food grade sodium alginate as GRAS (generally regarded as safe) substance in Title 21 of the Code for Federal Regulations (CFR) and lists its usage as an emulsifier, stabilizer, thickener, and gelling agent [40]. Sodium alginate is a multifunctional material used in medicine, tissue engineering, wastewater treatment, pharmaceutical industry and fuel [41].

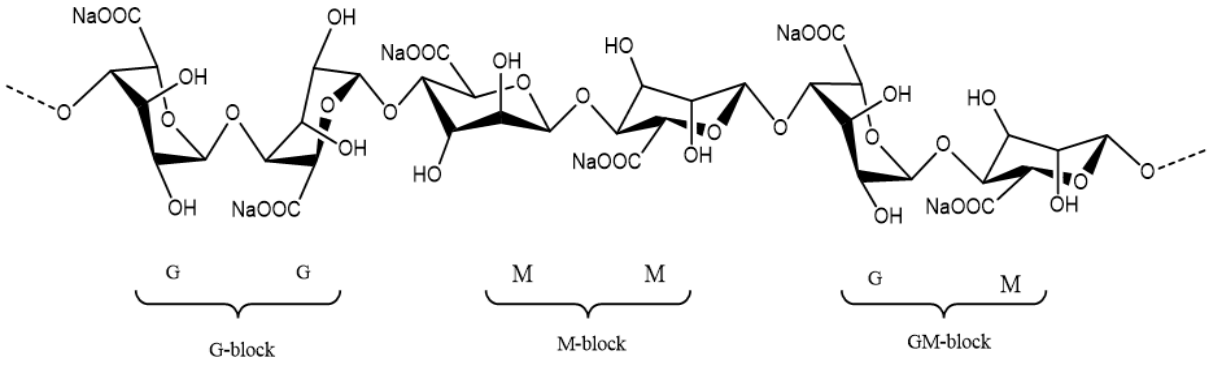


Figure I.5 Chemical structure of sodium alginate based on structure from Collado-González et al. [42]

I.2.3.4 Cellulose

Cellulose is a water-insoluble linear homopolymer extracted from terrestrial plants, seaweeds, microorganism and tunicate [43]. It is composed of amorphous and crystalline domains of anhydroglucose units **(Figure I.6)** [44]. It exists four polymorphs of cellulose: cellulose (I), (II), (III) and (IV) [45]. Several seaweed species were found to have significant cellulose content (9–34% dry weight) [46]. It can be used in paper production [47] even as food additive, dietary fibres or bio-based materials for packaging [48].

Two types of crystalline cellulosic derivatives could be extracted from cellulose: microcrystalline (MCC) and nanocrystalline cellulose (NCC) [49]. The lack of lignin in marine algae might be more suitable for high-quality MCC and NCC extraction with a broader range of applications than those extracted from lignocellulosic biomass [50].

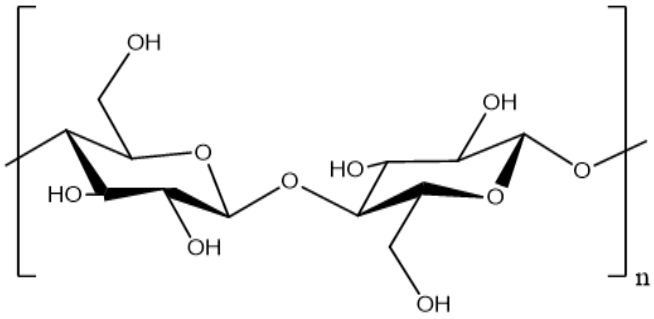


Figure I.6 Chemical structure of cellulose based on structure from Zanchetta et al. [45]

I.3 Polysaccharide-based hydrogels

Hydrogels are three-dimensional, insoluble, crosslinked network of polymers that can retain large amounts of water and biological fluids in their swollen state [51]. They can be made by physically and/or chemically crosslinking polysaccharide derivatives with various functional molecules **(Figure I.7)**, as a result of which porous network structures or nanofibrillar structures are formed [52]. Hydrogels can appeared as matrixes, films or microspheres depending on polymerization technique involved in their preparation process [53].

Hydrogels composed of polysaccharides can be fine-tuned to mimic various body tissues and organs as they are suitable for a variety of healthcare and biomedical applications such as drug delivery, wound healing, tissue engineering and fabricating and coating medical devices and implants [54].

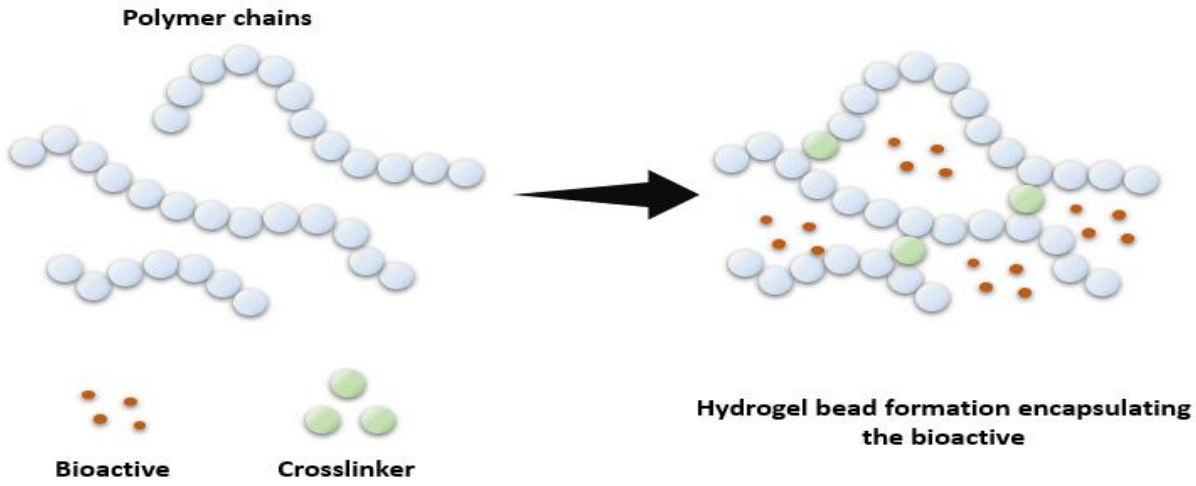


Figure I.7 Hydrogel beads formation.

I.3.1 Advantages of using hydrogels as drug delivery system [53]

- Possession of high degree of flexibility similar to natural tissues;
- Possibility of sustaining and prolonging drug action compared to conventional drug delivery systems;
- Decreasing the dose of administration;
- Decreasing drug side-effects;
- Drug targeting to specific site;
- Protection of mucosa from irritating drug.

I.4 Polysaccharide based-active coating

Food packaging is food protector against physical, chemical and biological influences. There is a great interest in the development of degradable packaging with environmentally friendly materials made from renewable natural polymers [55]. Such biopolymers include proteins, lipid derivatives and carbohydrates [56]. Thence, edible packaging was developed since polymers are excellent film-formers. However, edible coatings are mostly non-active, and therefore additives are used to bring functionality, such as antimicrobial and antioxidant activities [57]. Moreover, the combination of vegetable oils provide excellent resistibility against water-vapor migration when used in the composition of edible films and coatings [58]. Hammoudi et al.[59] prepared an active antimicrobial alginate-montmorillonite/lemon essential oil nanocomposite films which might be considered as promising active packaging materials. Santos et al.[60] developed a nanoscale system coating based on alginate and a blend of oils to extend the shelf-life of fruits and seeds.

The edible coating solutions can be applied to food, harvested fruits and vegetables using different methods as depicted in **Figure 8**.

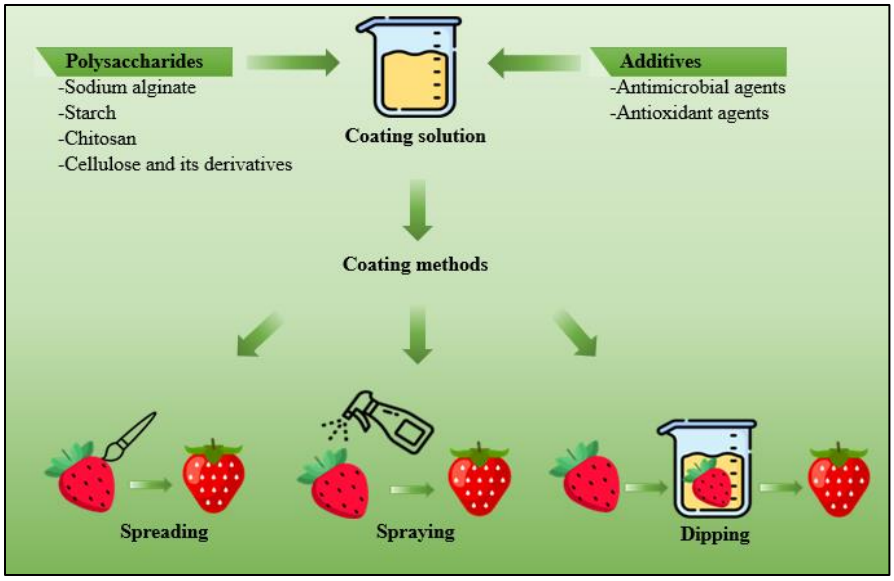


Figure I.8 Application methods of edible coating on food products

I.5 Antibacterial activity

Microbial infections cause a threat to a huge number of people over the world. To overcome this problem, many studies were conducted to develop new effective antimicrobial systems. Biopolymer antimicrobials are the most widely used materials owing to their cost-effectiveness and ease of modification. [61]. The antimicrobial macromolecular systems can be divided into three categories [62]:

- **Polymer biocides:** are macromolecules constituted of bioactive repeating units. They can be designed by synthetic routes. Literatures shows possibility to polymerize antibiotics maintaining their activity at the polymer backbone. Shi et al.[63] synthesized a Coumarin antimicrobial polymer fluorescent coating. It was shown that the polymer had a strong inhibitory effect on Staphylococcus aureus.
- **Biocidal polymers:** it was prepared by the inclusion of the active principle in the whole macromolecule. The gallic acid–polysaccharide (GA-g-PS) conjugate is one of the most studied conjugates, and its biological activities have been widely reported and have shown many potential applications [64].
- **Biocide-releasing polymers:** polymers represent a carrier for biocide that are transferred to the infected area. The antimicrobial agents can be introduced into polymer microparticles. Shi et al.[65] developed a polysaccharide-based hydrogel encapsulating

Tobramycin-loaded gelatine microspheres as an antibacterial system with good antibacterial activity and biocompatibility. The development of hydrogels containing antibiotics are also an alternative to overcome the bacterial resistance avoiding the systemic toxicity level [66].

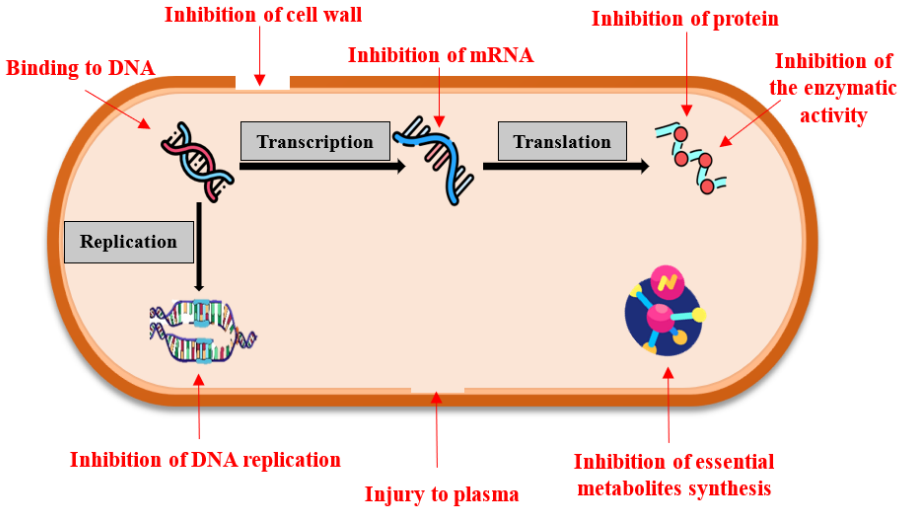


Figure I.9 The main action mechanisms of antibacterial drugs.

The antimicrobial susceptibility testing is conducted by "Kirby-Bauer test" also called "disc diffusion method" to observe the effect of antibiotics or formulations on the growth of pathogenic bacteria include *Bacillus*, *Staphylococcus*, *Escherichia coli*, etc. The zones of inhibition were observed and recorded with the following annotations [67]:

Table I.2 Antibacterial sensitivity.

Description	Significance	Sensitivity level
Absence of clear zone	No sensitivity	-
Clear zone 1-2mm diameter	Weak sensitivity	+
Clear zone 3-7mm diameter	Moderate sensitivity	++
Clear zone 8-11mm diameter	Quite sensitivity	+++
Clear zone 12-15mm diameter or above	High sensitivity	++++

I.6 Antioxidant activity

Antioxidants are used for their protective function in food items against oxidative deterioration and the organism body against oxidative stress-directed abnormal processes. These

potent natural antioxidants are in huge demand for pharmaceuticals/nutraceuticals and as food preservatives [68]. Many of the natural antioxidants of interest are of plant origin and belong to the phenolic and polyphenolic class of compounds as well as carotenoids and antioxidant vitamins, among others [69]. In recent years, polysaccharides were considered as an effective free radical scavengers and antioxidants [70]. Natural polysaccharides exert antioxidant effect by regulating signal transduction pathways, regulating the activity of enzymes or by scavenging free radicals or substances that easily form free radicals due to the presence of hydroxyl and side-chain glycosidic bonds in their structure [71].

Generally, antioxidant assays are conducted using appropriate traditional methodologies, collecting and processing the data in terms of % inhibition or the equivalent of standards, and finally, interpreting the results. Among the common methods used for measuring the in vitro antioxidant activity of polysaccharides is the 2,2-diphenyl-1-picrylhydrazyl (DPPH•) assay. The unpaired electron in DPPH• exhibits an intense deep purple colour charge-transfer band at 517 nm, however, while pairing up with another electron to form stable molecule (DPPH-H), a change in colour is observed resulting in pale yellow [72].

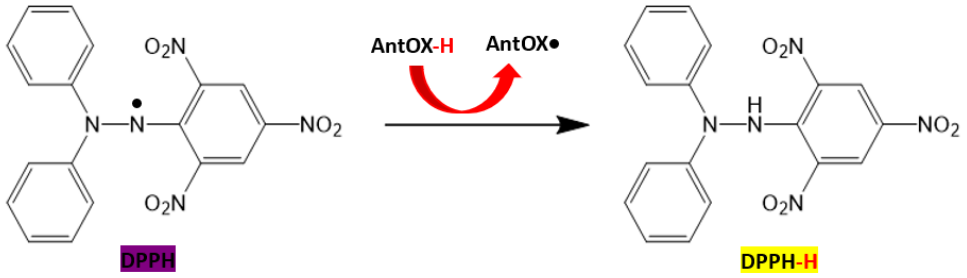


Figure I.10 DPPH reaction mechanism.

Reportedly brown algae have better antioxidant activity compared with green algae and red algae, [71]. It was shown in the study of Mohd fauziee et al. [73] that laminaran polysaccharides extracted from Sargassum polycystum have the highest superoxide anion scavenging ability, and alginate has high DPPH scavenging activity.

I.7 References

[1] S. kwon Kim, *Handbook of marine microalgae : biotechnology and applied phycology*. New Delhi: John Wiley & Sons, 2011.

[2] B. K. Tiwari and D. J. Troy, *Seaweed Sustainability: Food and Non-Food Applications*. London: Academic Press, 2015. doi: 10.1016/B978-0-12-418697-2.00006-4.

[3] O. G. Mouritsen, P. Rhatigan, and J. L. Pérez-lloréns, "World cuisine of seaweeds : Science meets gastronomy," *Int. J. Gastron. Food Sci.*, vol. 14, pp. 55–65, 2018, doi: 10.1016/j.ijgfs.2018.09.002.

[4] I. Muzzalupo, *Food Industry*. Rijeka: InTech, 2013. doi: http://dx.doi.org/10.5772/55834.

[5] C. A. M. Patrichi, D. R. Cioroiu Tirpan, A. A. A. Aljanabi, B. Trica, I. C. Gifu, and T. Dobre, "Extraction of cellulose from Ulva lactuca algae and its use for membrane synthesis," *Polymers (Basel).*, vol. 15, no. 24, p. 4673, 2023, doi: 10.3390/polym15244673.

[6] F. Menaa *et al.*, "Marine algae-derived bioactive compounds: A new wave of nanodrugs," *Mar. Drugs*, vol. 19, no. 9, p. 484, Aug. 2021, doi: 10.3390/md19090484.

[7] O. G. Mouristen, *Seaweeds: edible, available and sustainable*. London: University Of Chicago Press, 2013.

[8] M. M. Hakim and I. C. Patel, "A review on phytoconstituents of marine brown algae," *Futur. J. Pharm. Sci.*, vol. 6, no. 129, pp. 1–11, 2020, doi: 10.1186/s43094-020-00147-6.

[9] N. Ould-Ahmed, A. G. Garreta, and M. A. R. Siguan, "Checklist of the benthic marine macroalgae from Algeria, part II: Ulvophyceae," *An. del Jard. Bot. Madrid*, vol. 76, no. 2, pp. 1–7, 2019, doi: 10.3989/ajbm.2471.

[10] S. Mehiaoui, F. Nemchi, T. Bouzaza, T. Farah, and B. Bachir-Bouiadjra, "Algal diversity study in the western Algerian coast," *Ukr. J. Ecol.*, vol. 12, no. 5, pp. 1–11, 2022, doi: 10.15421/20.

[11] B. Y. S. Hellal and A. Ba, "Checklist of the marine macroalgae of Algerian west coast (Ain Témouchent site)," *Ukr. J. Ecol.*, vol. 11, no. 3, pp. 22–25, 2021, doi:

10.15421/2021.

[12] R. S. Baghel, C. Reddy, and R. P. Singh, "Seaweed-based cellulose: applications, and future perspectives," *Carbohydr. Polym.*, vol. 267, p. 118241, 2021, doi: 10.1016/j.carbpol.2021.118241.

[13] I. Benalaya, G. Alves, J. Lopes, and L. R. Silva, "A Review of natural polysaccharides: Sources, characteristics, properties, food, and pharmaceutical applications," *Int. J. Mol. Sci.*, vol. 25, no. 2, p. 1322, 2024, doi: 10.3390/ijms25021322.

[14] A. S. A. Mohammed, M. Naveed, and N. Jost, "Polysaccharides; classification, chemical properties, and future perspective applications in fields of pharmacology and biological medicine (a review of current applications and upcoming potentialities)," *J. Polym. Environ.*, vol. 29, no. 8, pp. 2359–2371, 2021, doi: 10.1007/s10924-021-02052-2.

[15] P. Thiviya *et al.*, "Algal polysaccharides: Structure, preparation and applications in food packaging," *Food Chem.*, vol. 405, p. 134903, 2023, doi: 10.1016/j.foodchem.2022.134903.

[16] A. K. Patel *et al.*, "Algal polysaccharides: current status and future prospects," *Phytochem. Rev.*, vol. 22, no. 4, pp. 1167–1196, 2023, doi: 10.1007/s11101-021-09799-5.

[17] Y. Fu *et al.*, "Structure-activity relationships of bioactive polysaccharides extracted from macroalgae towards biomedical application: A review," *Carbohydr. Polym.*, vol. 324, pp. 1–26, 2024, doi: 10.1016/j.carbpol.2023.121533.

[18] A. S. A. Mohammed, M. Naveed, and N. Jost, "Polysaccharides; classification, chemical properties, and future perspective applications in fields of pharmacology and biological medicine (a review of current applications and upcoming potentialities)," *J. Polym. Environ.*, vol. 29, no. 8, pp. 2359–2371, 2021, doi: 10.1007/s10924-021-02052-2.

[19] C. Santinon, D. Ochi, M. M. Beppu, and M. G. A. Vieira, "Chemical modifications in the structure of seaweed polysaccharides as a viable antimicrobial application: A current overview and future perspectives," *Algal Res.*, vol. 66, pp. 1–16, 2022, doi: 10.1016/j.algal.2022.102796.

[20] S. Peat and J. R. Turvey, "Polysaccharides of Marine Algae," in *Fortschritte der Chemie*

Organischer Naturstoffe / Progress in the Chemistry of Organic Natural Products, L. Zechmeister, Ed. Vienna: Springer Vienna, 1965, pp. 1–45. doi: 10.1007/978-3-7091-7139-4_1.

[21] Y. W. Chen, H. Voon Lee, J. Ching Juan, and S. Phang, "Production of new cellulose nanomaterial from red algae marine biomass Gelidium elegans," *Carbohydr. Polym.*, vol. 151, pp. 1210–1219, 2016, doi: 10.1016/j.carbpol.2016.06.083.

[22] Z. Liu, F. Niu, Y. Xie, S. Xie, Y. Liu, and Y. Yang, "A review : Natural polysaccharides from medicinal plants and microorganisms and their anti-herpetic mechanism," *Biomed. Pharmacother.*, vol. 129, pp. 1–21, 2020, doi: 10.1016/j.biopha.2020.110469.

[23] R. Anbuchezhian, V. Karuppiah, and Z. Li, "Prospect of marine algae for production of industrially important chemicals," in *Algal Biorefinery: An Integrated Approach*, Kharagpur: Capital Publishing Company, 2015, pp. 195–217. doi: 10.1007/978-3-319-22813-6.

[24] M. Zargarzadeh, A. J. R. Amaral, C. A. Custódio, and J. F. Mano, "Biomedical applications of laminarin," *Carbohydr. Polym.*, vol. 232, pp. 1–8, 2020, doi: https://doi.org/10.1016/j.carbpol.2019.115774.

[25] S. Sellimi *et al.*, "Antioxidant , antibacterial and in vivo wound healing properties of laminaran purified from Cystoseira barbata seaweed," *Int. J. Biol. Macromol.*, vol. 119, pp. 633–644, 2018.

[26] M. Sterner and F. Gröndahl, "Extraction of laminarin from Saccharina latissima seaweed using cross-flow filtration," *J. Appl. Phycol.*, vol. 33, pp. 1825–1844, 2021, doi: https://doi.org/10.1007/s10811-021-02398-z.

[27] S. Pramanik *et al.*, "From algae to advancements : laminarin in biomedicine," *R. Soc. Chem.*, vol. 14, pp. 3209–3231, 2024, doi: 10.1039/d3ra08161c.

[28] A. K. A. Silva *et al.*, "Anti-inflammatory activity of fucan from Spatoglossum schröederi in a murine model of generalized inflammation induced by zymosan," *Mar. Drugs*, vol. 21, no. 11, p. 557, 2023, doi: 10.3390/md21110557.

[29] A. V. Skriptsova, "Seasonal variations in the fucoidan content of brown algae from Peter

the Great Bay, Sea of Japan," *Russ. J. Mar. Biol.*, vol. 42, no. 4, pp. 351–356, 2016, doi: 10.1134/S1063074016040106.

[30] G. Kopplin, A. M. Rokstad, H. Mélida, V. Bulone, G. Skjåk-Bræk, and F. L. Aachmann, "Structural characterization of fucoidan from Laminaria hyperborea: Assessment of coagulation and inflammatory properties and their structure-function relationship," *ACS Appl. Bio Mater.*, vol. 1, no. 6, pp. 1880–1892, 2018, doi: 10.1021/acsabm.8b00436.

[31] L. Cunha and A. Grenha, "Sulfated seaweed polysaccharides as multifunctional materials in drug delivery applications," *Mar. Drugs*, vol. 14, no. 3, pp. 1–41, 2016, doi: 10.3390/md14030042.

[32] A. Zayed, M. El-Aasr, A. R. S. Ibrahim, and R. Ulber, "Fucoidan characterization: Determination of purity and physicochemical and chemical properties," *Mar. Drugs*, vol. 18, no. 11, pp. 1–31, 2020, doi: 10.3390/md18110571.

[33] S. H. Ptak, A. L. Hjuler, S. I. Ditlevsen, X. Fretté, M. Errico, and K. V. Christensen, "The effect of seasonality and geographic location on sulphated polysaccharides from brown algae," *Aquac. Res.*, vol. 52, no. 12, pp. 6235–6243, 2021, doi: 10.1111/are.15485.

[34] M. Jönsson, L. Allahgholi, R. R. R. Sardari, G. O. Hreggviosson, and E. N. Karlsson, "Extraction and modification of macroalgal polysaccharides for current and next-generation applications," *Molecules*, vol. 25, no. 4, 2020, doi: 10.3390/molecules25040930.

[35] S. Saji, A. Hebden, P. Goswami, and C. Du, "A brief review on the development of alginate extraction process and its sustainability," *Sustain.*, vol. 14, no. 9, pp. 1–20, 2022, doi: 10.3390/su14095181.

[36] X. Gao, Y. Zhang, and Y. Zhao, "Biosorption and reduction of Au (III) to gold nanoparticles by thiourea modified alginate," *Carbohydr. Polym.*, vol. 159, pp. 108–115, 2017, doi: 10.1016/j.carbpol.2016.11.095.

[37] S. Abang, E. S. Chan, and D. Poncelet, "Effects of process variables on the encapsulation of oil in ca-alginate capsules using an inverse gelation technique," *J. Microencapsul.*, vol. 29, no. 5, pp. 417–428, 2012, doi: 10.3109/02652048.2012.655331.

[38] N. A. R. Osman, T. O. Suliman, and K. A. Osman, "Characterization of native alginates of common alginophytes from the red sea coast of Sudan," *Int. J. Second. Metab.*, vol. 7, no. 4, pp. 266–274, 2020, doi: 10.21448/ijsm.685864.

[39] Ł. Magdalena, A. Jankowska, I. Michalak, and J. Detyna, "Applications of alginates in the biomedical field," in *Advances in biomedical research - from COVID to medical humanities*, 2020, p. 97.

[40] U.S. Food & Drug Administration, "CFR - Code of Federal Regulations Title 21 Part 184." https://www.accessdata.fda.gov/scripts/cdrh/cfdocs/cfcfr/CFRSearch.cfm?fr=184.1724 (accessed Jan. 02, 2023).

[41] W. Liu, H.-J. Li, and Y.-C. Wu, "Properties and applications of alginate," in *Properties and Applications of Alginates*, M. Y. Wilkerson, Ed. Nova, 2022, pp. 1–181. doi: 10.5772/intechopen.94635.

[42] M. Collado-González *et al.*, "Complex polysaccharide-based nanocomposites for oral insulin delivery," *Mar. Drugs*, vol. 18, no. 1, pp. 1–18, 2020, doi: 10.3390/md18010055.

[43] K. Dhali, M. Ghasemlou, F. Daver, P. Cass, and B. Adhikari, "A review of nanocellulose as a new material towards environmental sustainability," *Sci. Total Environ.*, vol. 775, p. 145871, 2021, doi: https://doi.org/10.1016/j.scitotenv.2021.145871.

[44] M. A. Jmel, N. Anders, G. Ben, M. N. Marzouki, A. Spiess, and I. Smaali, "The stranded macroalga Ulva lactuca as a new alternative source of cellulose : Extraction , physicochemical and rheological characterization," *J. Clean. Prod.*, vol. 234, pp. 1421–1427, 2019, doi: 10.1016/j.jclepro.2019.06.225.

[45] E. Zanchetta *et al.*, "Algal cellulose , production and potential use in plastics : Challenges and opportunities," *Algal Res.*, vol. 56, pp. 1–22, 2021, doi: https://doi.org/10.1016/j.algal.2021.102288.

[46] D. M. S. A. Salem and M. M. Ismail, "Characterization of cellulose and cellulose nanofibers isolated from various seaweed species," *Egypt. J. Aquat. Res.*, vol. 48, no. 4, pp. 307–313, 2022, doi: 10.1016/j.ejar.2021.11.001.

[47] A. Moral, R. Aguado, A. Tijero, and M. Ballesteros, "Potential Use of Green Alga Ulva sp. for Papermaking," *Bioresources*, vol. 14, no. 2004, pp. 6851–6862, 2019, doi: 10.15376/biores.14.3.6851-6862.

[48] L. Chávez-Guerrero, A. Toxqui-Terán, and O. Pérez-Camacho, "One-pot isolation of nanocellulose using pelagic Sargassum spp. from the Caribbean coastline," *J. Appl. Phycol.*, vol. 34, no. 1, pp. 637–645, 2022, doi: 10.1007/s10811-021-02643-5.

[49] D. Haldar and M. K. Purkait, "Micro and nanocrystalline cellulose derivatives of lignocellulosic biomass: A review on synthesis, applications and advancements," *Carbohydr. Polym.*, vol. 250, p. 116937, 2020, doi: 10.1016/j.carbpol.2020.116937.

[50] M. Zaki *et al.*, "Microbial treatment for nanocellulose extraction from marine algae and its applications as sustainable functional material," *Bioresour. Technol. Reports*, vol. 16, pp. 1–65, 2021, doi: 10.1016/j.biteb.2021.100811.

[51] M. Dattilo, F. Patitucci, S. Prete, O. I. Parisi, and F. Puoci, "Polysaccharide-based hydrogels and their application as drug delivery systems in cancer treatment: A review," *J. Funct. Biomater.*, vol. 14, no. 2, pp. 1–22, 2023, doi: 10.3390/jfb14020055.

[52] U. A. Dar, A. A. Tantary, and A. Ali, "Polysaccharide-based hydrogels: history and chronological developments," in *Polysaccharide-based hydrogels*, Elsevier, 2024, pp. 21–42. doi: https://doi.org/10.1016/B978-0-323-99341-8.00002-8.

[53] P. B. Mohite and S. S. Adhav, "A hydrogels: Methods of preparation and applications," *Int. J. Adv. Pharm.*, vol. 06, no. 03, pp. 79–85, 2017, doi: 10.7439/ijap.

[54] D. Sanjanwala *et al.*, "Polysaccharide-based hydrogels for medical devices, implants and tissue engineering: A review," *Int. J. Biol. Macromol.*, vol. 256, pp. 1–50, 2024, doi: 10.1016/j.ijbiomac.2023.128488.

[55] T. S. Parreidt, K. Müller, and M. Schmid, "Alginate-based edible films and coatings for food packaging applications," *Foods*, vol. 7, no. 10, pp. 1–38, 2018, doi: 10.3390/foods7100170.

[56] M. G. Kontominas, "Use of alginates as food packaging materials," *Foods*, vol. 9, no. 10, pp. 1–5, 2020, doi: 10.3390/foods9101440.

[57] A. A. P. Ribeiro, R. C. Sanfelice, G. R. P. Malpass, M. H. Okura, and A. C. G. Malpass, "Shelf life and sensory analysis comparison of alginate and chitosan edible coating incorporating avocado extract applied to minimally processed apples," *Food Mater. Res.*, vol. 3, no. 26, pp. 1–8, 2023, doi: 10.48130/FMR-2023-0026.

[58] B. Tirgarian, J. Farmani, and J. M. Milani, "Edible oleofilms with high vegetable oil content obtained from novel soy protein isolate/gelatin/chitosan nanofiber emulgels," *Food Hydrocoll.*, vol. 134, pp. 1–15, 2023, doi: 10.1016/j.foodhyd.2022.108082.

[59] N. Hammoudi, H. Z. Cherif, F. Borsali, and K. Benmansour, "Preparation of active antimicrobial and antifungal alginate-montmorillonite / lemon essential oil nanocomposite films," *Mater. Technol.*, vol. 35, no. 7, pp. 1–12, 2019, doi: 10.1080/10667857.2019.1685292.

[60] C. Santos *et al.*, "Green nanotechnology for the development of nanoparticles based on alginate associated with essential and vegetable oils for application in fruits and seeds protection," *Int. J. Biol. Macromol.*, vol. 232, p. 123351, 2023, doi: 10.1016/j.ijbiomac.2023.123351.

[61] F. Mohamed, A. Ahmed, and O. F. Abdel-Gawad, "Preparation and evaluation of the antimicrobial activity of sodium alginate-grafted diphenylamine embedded with silver nanoparticles," *Polym. Bull.*, vol. 80, no. 9, pp. 9797–9810, 2023, doi: 10.1007/s00289-022-04505-7.

[62] A. I. Barzic and S. Ioan, "Antibacterial Drugs — From Basic Concepts to Complex Therapeutic Mechanisms of Polymer Systems," in *Concepts, Compounds and the Alternatives of Antibacterials*, London: UK: IntechOpen, 2015. doi: 10.5772/60755.

[63] W. Q. Shi, J. Zhao, X. R. Liu, Y. Ming, and Y. M. Shen, "Synthesis and characterization of a coumarin antimicrobial polymer fluorescent coating," *Adv. Polym. Technol.*, vol. 2022, no. 1, p. 6213187, 2022, doi: 10.1155/2022/6213187.

[64] W. Zhang *et al.*, "Free radical-mediated grafting of natural polysaccharides such as chitosan, starch, inulin, and pectin with some polyphenols: synthesis, structural characterization, bioactivities, and applications—A review," *Foods*, vol. 12, no. 19, p.

3688, 2023, doi: 10.3390/foods12193688.

[65] M. Shi, Y. Xu, S. Li, L. Wang, J. Gu, and Y. X. Zhang, "The Development of a Polysaccharide-Based Hydrogel Encapsulating Tobramycin-Loaded Gelatine Microspheres as an Antibacterial System," *Gels*, vol. 9, no. 3, pp. 1–15, 2023, doi: 10.3390/gels9030219.

[66] R. Carpa, A. Remizovschi, C. A. Culda, and A. L. Butiuc-Keul, "Inherent and composite hydrogels as promising materials to limit antimicrobial resistance," *Gels*, vol. 8, no. 2, p. 70, 2022, doi: 10.3390/gels8020070.

[67] S. Arbab *et al.*, "Comparison of antibacterial activity of Ciprofloxacin and Cephalexin against Some common bacterial Species isolates from donkey wounds around the vicinity of Tandojam Sindh Pakistan," *Pure Appl. Biol.*, vol. 10, no. 4, pp. 1095–1103, 2021, doi: 10.19045/bspab.2021.100114.

[68] P. Chaudhary *et al.*, "Oxidative stress, free radicals and antioxidants: potential crosstalk in the pathophysiology of human diseases," *Front. Chem.*, vol. 11, pp. 1–24, 2023, doi: 10.3389/fchem.2023.1158198.

[69] F. Shahidi, "Antioxidants: Principles and applications," in *Handbook of Antioxidants for Food Preservation*, Woodhead Publishing, 2015, pp. 1–14. doi: 10.1016/B978-1-78242-089-7.00001-4.

[70] B. V. Nemzer, D. Kalita, A. Y. Yashin, N. E. Nifantiev, and Y. I. Yashin, "In vitro antioxidant activities of natural polysaccharides: An overview," *J. Food Res.*, vol. 8, no. 6, p. 78, 2019, doi: 10.5539/jfr.v8n6p78.

[71] L. Bai *et al.*, "Antioxidant activities of natural polysaccharides and their derivatives for biomedical and medicinal applications," *Antioxidants*, vol. 11, no. 12, p. 2491, 2022, doi: 10.3390/antiox11122491.

[72] N. B. Sadeer, D. Montesano, S. Albrizio, G. Zengin, and M. F. Mahomoodally, "The versatility of antioxidant assays in food science and safety—chemistry, applications, strengths, and limitations," *Antioxidants*, vol. 9, no. 8, p. 709, 2020, doi: 10.3390/antiox9080709.

[73] N. A. M. Fauziee, L. S. Chang, W. A. W. Mustapha, A. R. M. Nor, and S. J. Lim, "Functional polysaccharides of fucoidan, laminaran and alginate from Malaysian brown seaweeds (Sargassum polycystum, Turbinaria ornata and Padina boryana)," *Int. J. Biol. Macromol.*, vol. 167, pp. 1135–1145, 2020, doi: 10.1016/j.ijbiomac.2020.11.067.

Chapter II

Materials and Methods

Section 1

Extraction of Algal Polysaccharides

The present section aims to elucidate the protocols of the sequential extraction of fucoidan, sodium alginate, cellulose and microcellulose from the local macroalgal biomass "Cystoseira stricta".

Experiments of biological activity of all extracted materials as well as their characterization by different means such as infrared spectroscopy, X-ray diffraction, differential scanning calorimetry and scanning electron microscopy are presented.

II.1 Extraction of algal polysaccharides

This work was carried out at the Laboratory of Structure, Elaboration and Application of Molecular Materials (SEAMM), Department of Chemistry, Faculty of Exact Sciences and Computer Science, University of Mostaganem, Algeria. The antibacterial tests were conducted at the Laboratory of Beneficial Microorganisms, Functional Food and Health (LMBAFS), Faculty of Natural and Life Sciences, Abdelhamid Ibn Badis University, Mostaganem, Algeria.

II.1.1 Chemical products

Calcium Chloride dihydrat was purchased from (Merck), (1-Hexadecyl)trimethylammoniu bromide 98% (Alfa Aesar), Potassium Iodide, Sodium Carbonate, Sodium Hydroxide pellets >98% (Merck), Hydrogen Peroxide solution 34.5-36.5% (Sigma-Aldrich), Acetic Acid (Biochem), Acetone 99% (Organics), Chloroform (Biochem), Ethanol 96% (Specilab), Hydrochloric acid (Sigma-Aldrich), Mueller Hinton Agar (Realab). All reagents were used without further purification.

II.1.2 Plant material presentation



Figure II.1 *Cystoseira stricta* brown algae.

- ***Class:*** Phaeophyceae
- ***Family:*** Cystoseiraceae
- ***Order:*** Fucales
- ***Gender:*** *Cystoseira*
- ***Species:*** *Stricta*
- ***Characteristics:*** The Cystoseira stricta (*C. stricta*) is a brown macroalgae found in the western Mediterranean. It is a large photophyle, it is made up of one or more trunks carrying a lot of ramifications. It consists of [1]:

  Holdfast: root-like structure;

  Stipe: stalk-like structure**;**

  Blade: leaf-like structure**.**

  It colonizes the enlightened and beaten rocks of the infralittoral floor of the Mediterranean. It is very sensitive to water turbidity and pollution [2].

II.1.3 Plant material preparation

The brown seaweeds were collected at Stidia (35°49'N / 0°01'W) on the southwestern Algerian coast **(Figure I.2)** during February, 2022 (WBA) and September, 2022 (SBA) and the identification of the species was performed by Belkacemi. Thereafter, they were washed several times with tap water then with distilled water to eliminate any dirt then dried, grinded with an electric shredder, sifted into small particles using CISA BA200N compact digital electromagnetic sieve shaker. Finally, the powder was preserved at room temperature away from humidity and light for subsequent extraction and analysis[3].



Figure II.2 Geographical location of Stidia.

II.1.4 Moisture content and ash determination

Total solids and moisture content were determined by placing the samples WBA or SBA in dried crucibles and drying at 105±1°C until a constant weight was achieved. After this, the same crucibles were placed in a muffle furnace at 575±1°C for 4h for ash content determination. The samples were cooled in a desiccator and weighed **(Figure II.3)**. The process was repeated three times and the moisture and ash content were calculated according to Farzanah et al, [4] as follows:

$$\boldsymbol{MC}, \% = \left(\mathbf{1} - \frac{\boldsymbol{Wd}}{\boldsymbol{Wi}}\right) \times \mathbf{100} \quad \textbf{(II.1)}$$

$$\boldsymbol{Ash}, \% = \frac{\boldsymbol{Wr}}{\boldsymbol{Wd}} \times \mathbf{100} \quad \textbf{(II.2)}$$

Where W_i is the initial weight of sample, W_d is the weight of samples after drying at 105°C and W_r is the weight of residues after burning at 575°C. All measurements were conducted at a resolution of ±0.0001g



Figure II.3 Desiccation.



Figure II.4 Remaining ash.

II.1.5 Polysaccharides extraction process

The extraction process **(Figure II.7)** of four different algae polysaccharides was executed by adapting several methods used in the literature. The influence of harvesting period, particle size and solid to liquid ratio on the extraction yield was analysed.

The experiments were carried out for two different particle size distributions of the sample powder (150 and 400 µm), solid to solvent ratio of 1:10 and 1:30 and two different harvesting periods (February and September). All the other parameters such as reaction time and the extraction temperature remain unchanged for all set of experiments conducted. Each experiment was repeated in triplicate for reliable results. The extraction yield was calculated by dividing the weight of obtained polysaccharides per weight of dried biomass [5].

II.1.5.1 Pretreatment

Dried biomass was incubated in ethanol/chloroform/distilled water (4:2:1, v/v/v) for 15min under ultrasonic agitation then under simple magnetic stirring overnight at room temperature **(Figure II.5)**. This step is crucial in order to remove low molecular weight compounds such as pigments and proteins. The biomass was separated by filtration using Whatman filters, washed with acetone and finally ovendried at 30°C [6].

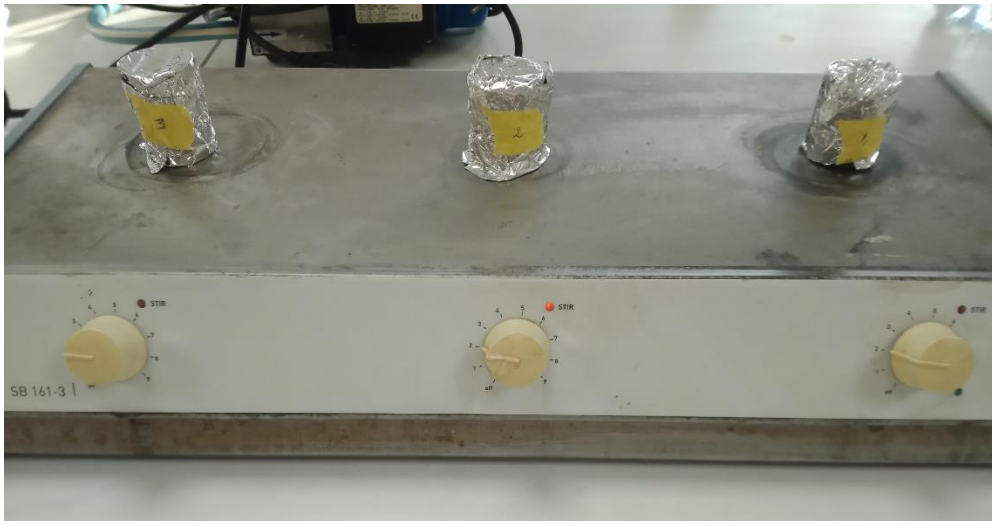


Figure II.5 Pretreatment process.

II.1.5.2 Fucoidan extraction

Pretreated sample was mixed with 2% $CaCl_2$ aqueous solution at 85°C with regular stirring for 5h. The supernatant was recovered by centrifugation and mixed with 10% hexadecyltrimethylammonium bromide and kept at 4°C overnight. Subsequently, the precipitate formed was centrifuged, rinsed abundantly with distilled water by vacuum filtration until CTAB excess removal, then stirred with 2% ethanolic sodium iodide solution. The excess of this later was washed away with ethanol and pure fucoidan was recovered by filtration and left to dry [7].

II.1.5.3 Alginate extraction

The calcium alginate remaining in the residual seaweed was converted to the water-soluble sodium alginate by 3% aqueous sodium carbonate solution at 70°C for 5h. Next, the mixture was cooled at room temperature and centrifuged for 10min and the recuperated supernatant was mixed with cold ethanol to precipitate Na-alginate. This later was dried and milled [8].

II.1.5.4 Cellulose extraction

The previous step was followed by the bleaching process using 32% hydrogen peroxide which was conducted and repeated twice on the residual powder at a temperature of 80°C for 4h. Some quantity of water was added if needed. Finally, the precipitate was collected and washed with distilled water until neutral pH to afford crude water insoluble polysaccharide[9] [10].

II.1.5.5 Microcrystalline cellulose preparation

The preparation of crystalline microcellulose (MCC) from isolated cellulose was conducted according to Bezzakhami et al.[11] with some modifications. 0.5g of isolated cellulose was mixed with 4mL of 2.2 N HCl and heated in a water bath at 40°C for 24h. After that, another 4mL of hydrochloride solution was added slowly and the reaction was continued for additional 48h. After that, the sample was centrifuged and rinsed abundantly with distilled water for excess acid elimination than with ethanol. MCC was ovendried at 60°C, milled and stocked for further uses.

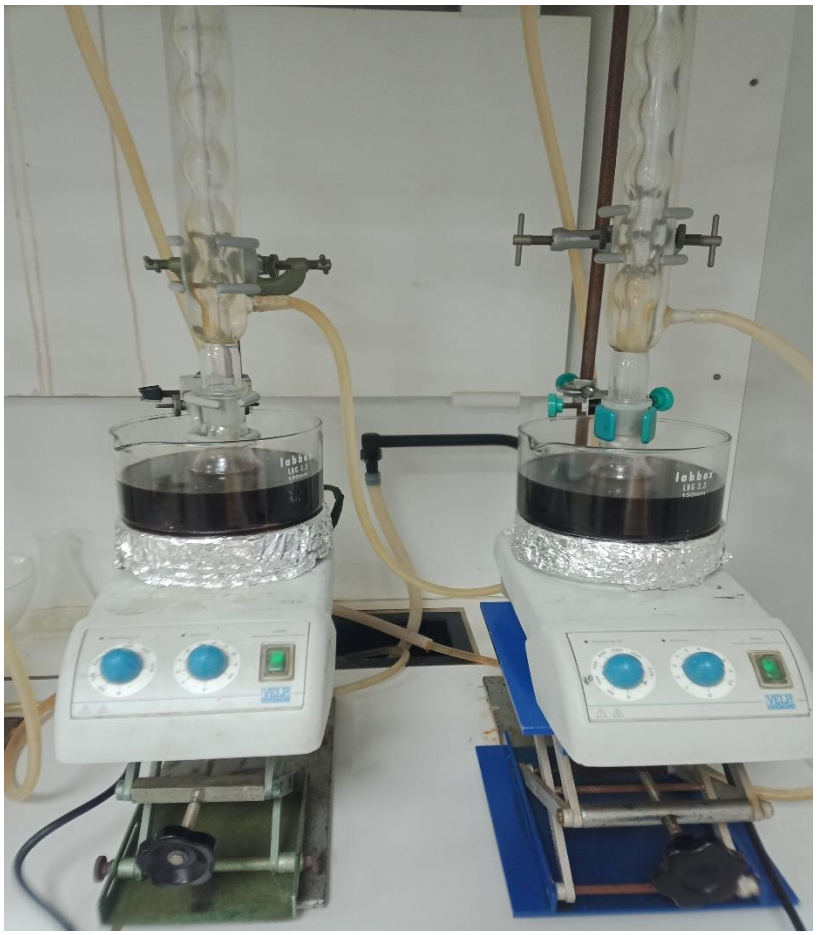


Figure II.6 Polysaccharides extraction setup.

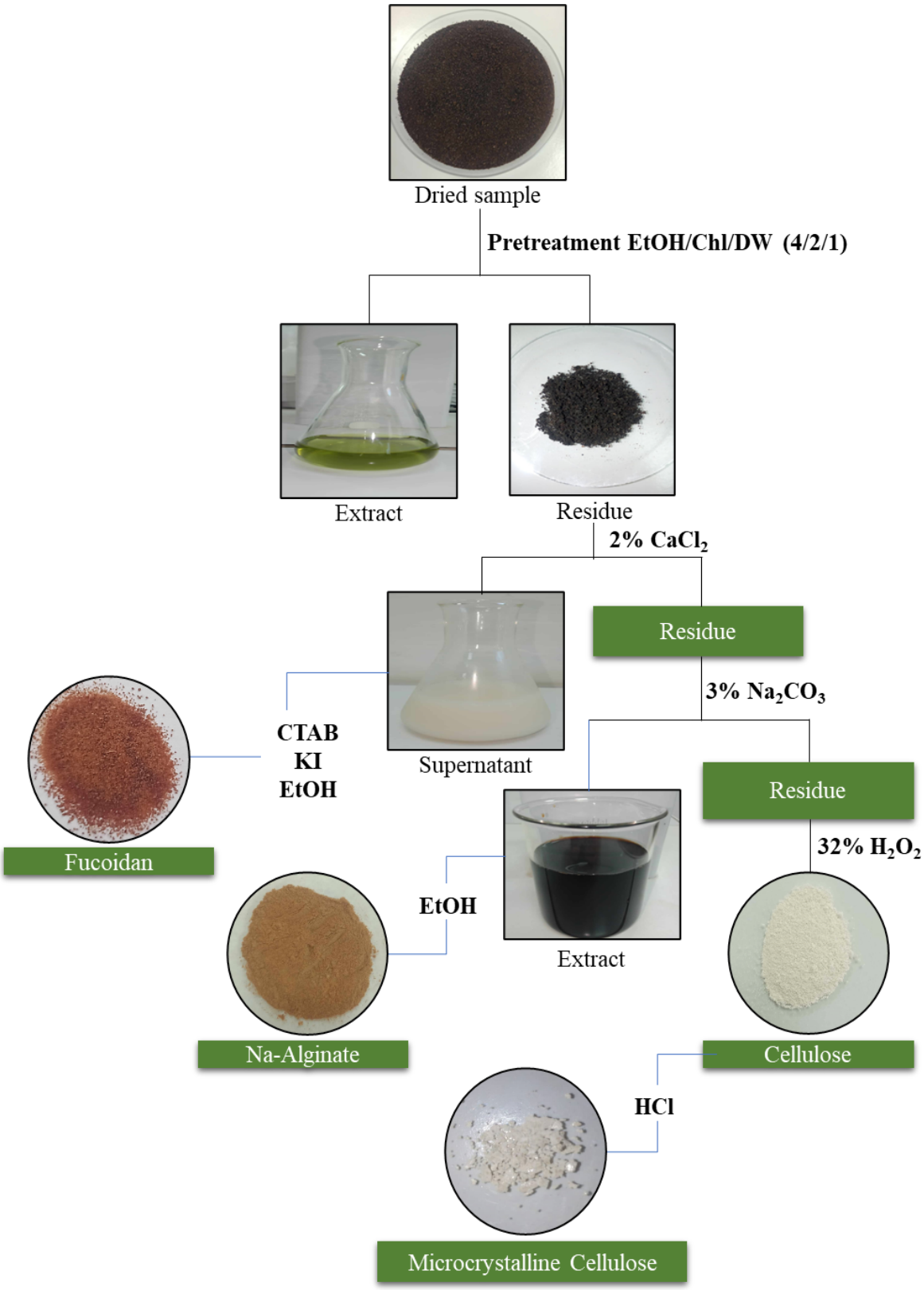


Figure II.7 Polysaccharides extraction process.

II.1.6 Extraction yield determination

The yield of polysaccharides were determined gravimetrically using the following equation [5]:

$$\boldsymbol{Yield, \%} = \frac{\boldsymbol{Wp}}{\boldsymbol{Wd}} \times \mathbf{100} \qquad \textbf{(II.3)}$$

Where W_p is the weight of obtained polysaccharide and W_d is the initial weight of the dried biomass.

II.1.7 Evaluation of the antibacterial activity of the products

The disc diffusion method [12] was used in order to investigate the antibacterial activity of the extracted polysaccharides against model gram negative (*Escherichia coli* (ATCC 25922)) and Gram positive (*Staphylococcus aureus* (ATCC 33862)) bacteria strains. So as to do this, a process involving four steps was followed:

II.1.7.1 Inoculum preparation

Initially, pure bacteria strains were revived in a nutrient broth and incubated at 37°C for 24 hours. After that, some quantity of the culture was mixed with sterile physiological water then thoroughly homogenized using a Vortex to prepare a suspension having a turbidity equivalent to the McFarland standard 0.5 which corresponds to 10^8 colony forming units per millilitre (CFU/ml) (OD= 0.08-0.13 / λ=625nm). Seeding must be done after 15 minutes following preparation of the inoculum.



Figure II.8 Inoculum preparation.

II.1.7.2 Agar plates inoculation

Muller Hinton agar was melted in a water bath then poured into Petri dishes (4mm thick) and left to dry in a sterile environment. Seeding was carried out using a sterile swab dipped in the standardized bacterial suspension, over the entire agar surface from top to bottom, in tight streaks. This operation must be repeated twice, each time rotating the petri dish by 60° and finished by passing the swab around the periphery of the agar.

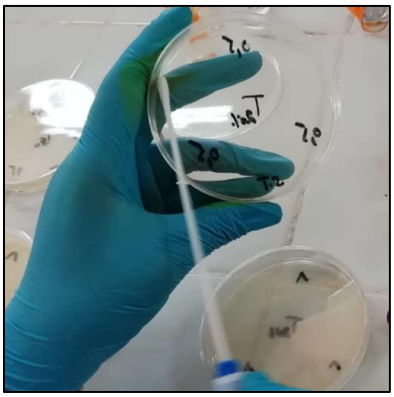


Figure II.9 Agar plates inoculation

II.1.7.3 Disc deposition

Sterilized Wattman paper disks of 6mm of diameter were soaked in the prepared extracts then delicately placed on the surface of the seeded medium in the presence of a control disk (CL). These discs are identified by marking their names on the underside of the dish. The tests were repeated three times for each strain. The operation must be carried out quickly in a sterile environment to avoid any kind of contamination.

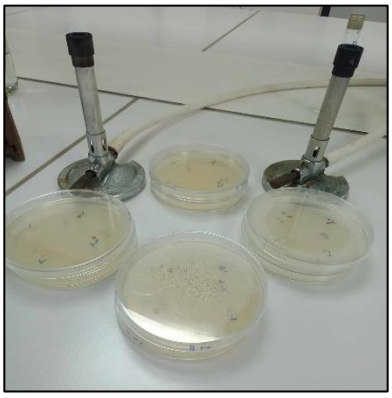


Figure II.10 Disc deposition

II.1.7.4 Agar plates incubation

The petri dishes were incubated at 37°C for 18-24 hours. The results were read after incubation by measuring the diameter of the transparent inhibition zone against the test microorganisms.

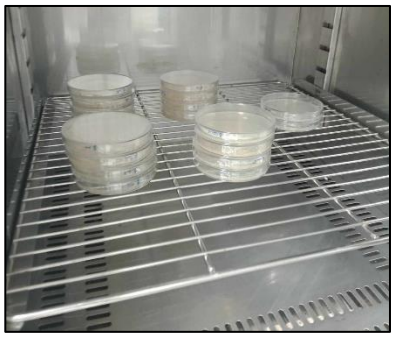


Figure II.11 Agar plates incubation

Section 2

Elaboration of Alginate-Based Materials

The functionalization of sodium alginate, the fabrication of alginate-based hydrogels and edible coating are detailed in this section. The antioxidant/antibacterial activity of the synthesised materials are also studied.

II.2 Elaboration of alginate-based materials

The experimental procedures and the antioxidant activity evaluation were carried out at the Laboratory of Structure, Elaboration and Application of Molecular Materials (SEAMM), Department of Chemistry, Faculty of Exact Sciences and Computer Science, University of Mostaganem, Algeria.

The antibacterial tests were conducted at the Laboratory of Beneficial Microorganisms, Functional Food and Health (LMBAFS), Faculty of Natural and Life Sciences, Abdelhamid Ibn Badis University, Mostaganem, Algeria.

II.2.1 Chemical products

Calcium Chloride.Dihydrat was purchased from (Merck), Sodium carbonate anhydre, Chloroform (Biochem), Acetone 99% (Organics), Ethanol 96% (Specilab), Maleic anhydride, Cephalexin (Gift simple).

II.2.2 Sodium alginate modification

II.2.2.1 Experimental procedure of the modification

The maleation of extracted sodium alginate was conducted according to a modified method [13]. 1g of sodium alginate (HO-alg) was mixed with 10mL of 20wt% NaOH aqueous solution and stirred at room temperature. After 4h, ethanol was added to crystallize the product. This later was filtered, washed with ethanol and dried overnight (NaO-alg). 1g of NaO-alg was added to a mixture of 10 mL of distilled water, 2.5mL of triethylamine and 1.5g of maleic anhydride (MA) and stirred for 90 min at 80°C. After cooling to room temperature, 10mL of 1M acetic acid solution was added and the mixture was stirred for further 2h. The resulting product (Malg) was recovered by recrystallization in ethanol, filtration and drying then subjected to an alkaline treatment with saturated sodium carbonate aqueous solution for 2h at r.t. The final product was recovered and finally dried (NaMalg). The whole chemical reaction processes are summarized in **Figure II.12**.

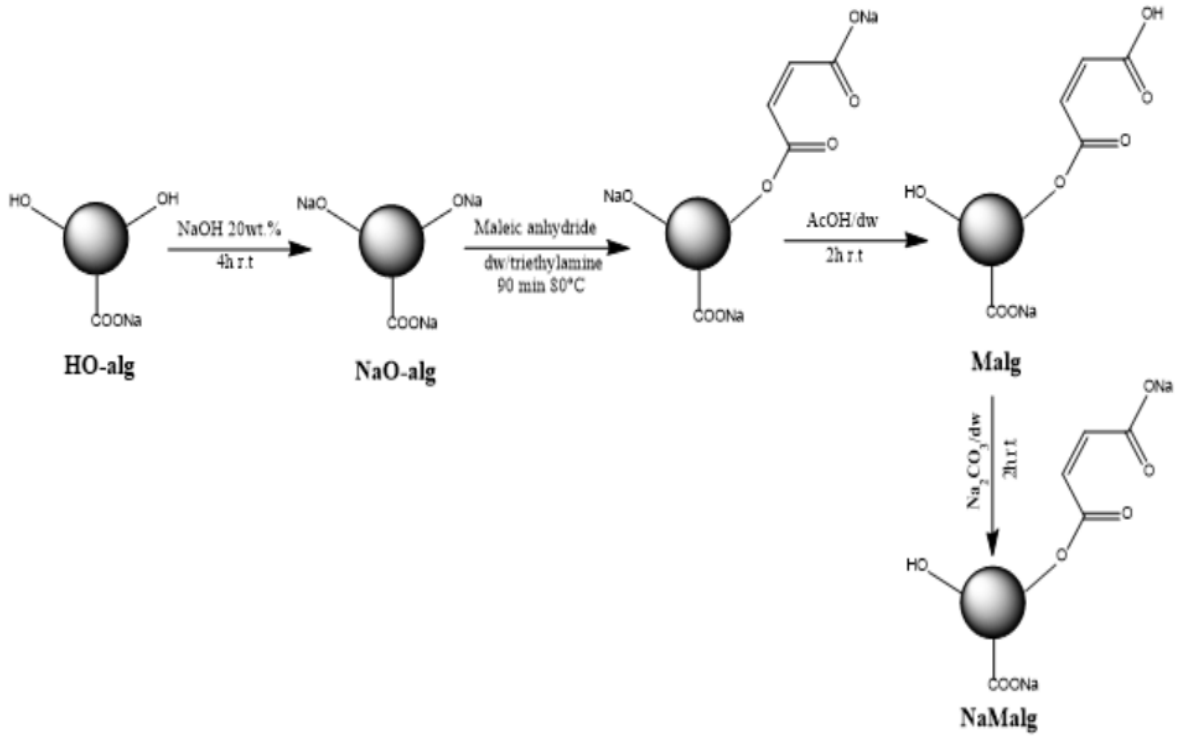


Figure II.12 Schematic diagram of sodium alginate modification.

II.2.2.2 Determination of the degree of substitution

The degree of maleation of sodium alginate was determined by titration method as reported by Pawar et al [14] with slight modifications. 0.05g of sodium alginate or maleated sodium alginate were reacted with excess NaOH (10 mL, 0.1N) overnight at room temperature to hydrolyze the ester groups. The remaining NaOH molecules were then back-titrated with 0.1N HCl solution using phenolphthalein as indicator. The degree of substitution was calculation using the following equation:

$$\boldsymbol{DS = \frac{M_a \times C(V_0 - V) \times 10^{-3}}{m - M_b \times C(V_0 - V)}} \quad \textbf{(II.4)}$$

Where m is the sample mass, M_a and M_b are the molecular weight of sodium alginate repeating unit (198) and acyl group respectively, V_0 and V are the titration consumed volumes of hydrogen chloride by native and modified sodium alginate respectively, C is the hydrogen chloride molar concentration.

II.2.2.3 Antioxidant activity evaluation

The 1,1-diphenyl-2-picrylhydrazine DPPH radical scavenging assay was conducted as described by Belkacemi et al [15] with slight modifications. A process involving four steps was followed:

II.2.2.3.1 Preparation of DPPH solution

An ethanolic solution of 0.08 mM of DPPH was prepared. The container was wrapped in aluminium foil, due to light sensitivity of DPPH. The absorbance of this solution was checked spectrophotometrically at 517 nm. Ideal value should be between 0.8 and 1.1. The solution was kept in dark for 2 hours before use.

II.2.2.3.2 Preparation of sample solutions

Aqueus solutions of HO-alg and NaMalg samples with varying concentrations (2-20 mg/L) were prepared. 50 µL of each test sample solution was placed using a micropipette into separate glass tubes. Ascorbic acid (31.25- 1000 µg/mL) was used as standard and manipulated with the same manner. Control reaction (without sample solution) and blanks (without DPPH solution) were also prepared.

II.2.2.3.3 DPPH scavenging assay setup

A volume of 1950 µL of the DPPH solution was added to each test tube. The tubes were mixed thoroughly by pipetting up or using a vortex. Color changing from purpule to yellow was observed by time **(Figure II.13)** indicating the neutralization of DPPH radical by receiving either an electron or a hydrogen from the antioxidant species. The absorbance was measured at 517nm after thirty minutes of incubation in dark at room temperature.

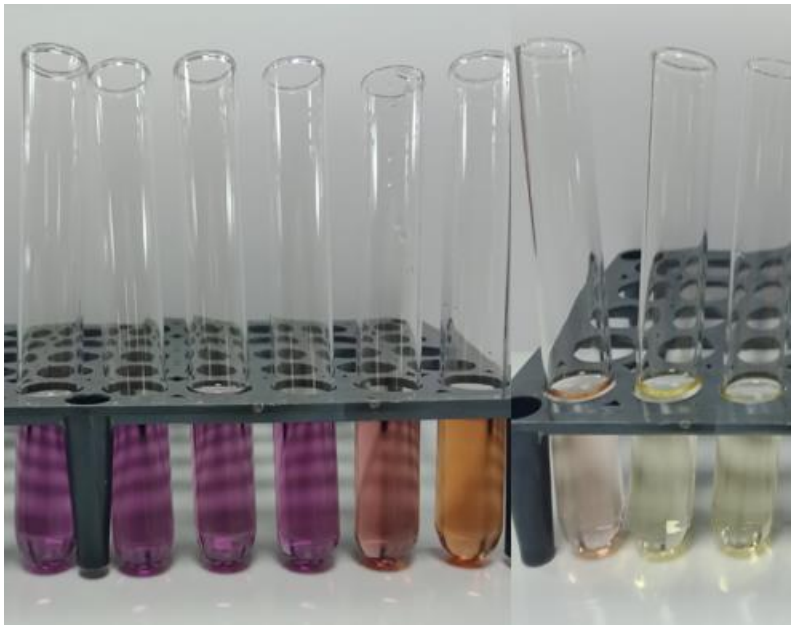


Figure II.13 Discoloration of DPPH under the influence of test samples.

II.2.2.3.4 Data analysis

The inhibition percentage of DPPH was calculated using the following equation:

$$\boldsymbol{Inhibition}\ (\%) = \frac{(A_C - A_S)}{A_C} \times \mathbf{100} \qquad \textbf{(II.5)}$$

Where A_c is the control reaction absorbance and A_s is the absorbance in presence of the sample or standard.

50% inhibition concentration (IC_{50}) was determined by linear regression analysis. The results are the mean of three repetitions.

II.2.3 Preparation and application of maleated sodium alginate date seed oil-based oil-in-water nanoemulsion

II.2.3.1 Synthesis procedure of the nanoemulsion

The nanoemulsion of maleated sodium alginate was prepared using date seed oil (DSO) purchased from Inovapalm company, Algeria. The DSO was extracted from date seeds of the *Phoenix dactylifera* species cultivated in Tolga, Biskra, Algeria. 300mg of date seed oil was dissolved in 150µl of ethanol for oil phase preparation. In parallel, the aqueous phase containing 300mg of NaMalg and 30mL of distilled water was prepared by stirring for 2h under slight heating.

0.3g of Tween80 was added and stirred more at room temperature. This later was poured slowly into the lipophilic organic phase under gentle stirring for 30 min. The nanoemulsion was stabilized by sonication for 15min. Finally, crosslinking was achieved by adding 10ml of 0.002 g/mL of $CaCl_2$ aqueous solution to obtain viscous solution [16]. The same steps were followed to prepare nanoemulsion (control) with sodium alginate and date seed oil.

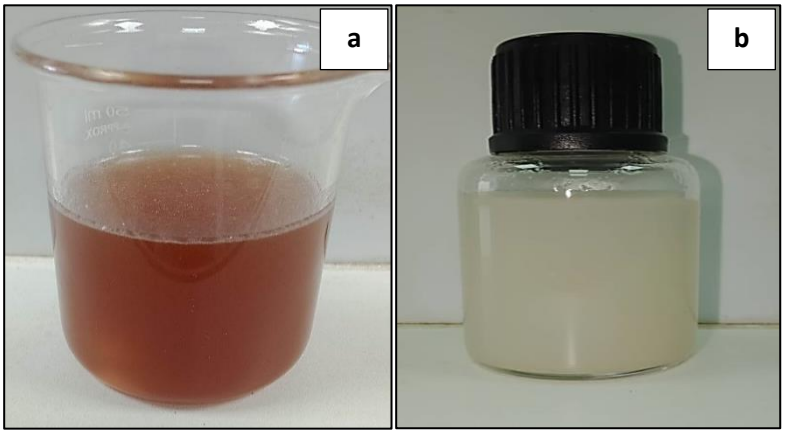


Figure II.14 (a) Sodium alginate and **(b)** maleated sodium alginate-based Nanoemulsions.

II.2.3.2 Protective effect evaluation of the nanoemulsion

The synthesized nanoemulsion was applied as an edible functional coating for strawberry protection from spoilage.. A thin layer of the nanocoating was applied by spreading on the entire surface of fresh strawberies, of comparable size, using a brush. Each sample was placed separately in a sterile container and kept over 14 days at room temperature. Uncoated samples were used as control for comparaison in the same conditions. All samples were imaged daily over the period of study.

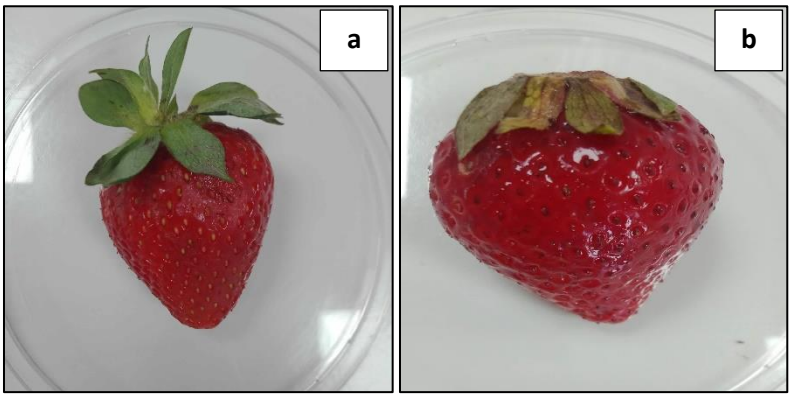


Figure II.15 (a) uncoated strawberry and **(b)** coated strawberry.

II.2.4 Cephalexin-loaded hydrogel beads preparation

II.2.4.1 Synthesis procedure of hydrogel beads

Hydrogel beads were synthesized by gelation technique according to the protocol of Aldawsari et al. [17]. First, alginate solution was prepared by dissolving 0.15 g extracted sodium alginate in 3 ml of distilled water under stirring at 40°C. After complete dissolution, 20 mg of cephalexin (CL) was added under same conditions. The mixture was slowly added dropwise to 20 ml of 6% calcium chloride solution prepared previously using a 10mL hypodermic syringe (1mm diameter) and kept under stirring at 200 rpm for 30min. The beads already formed (CSMS) were filtered and washed abundantly with distilled water then oven dried at 35°C. Cephalexin-free hydrogel beads were also prepared. For size measurement, 30 beads were randomly taken and their diameter was measured with an electronic digital calliper [18].

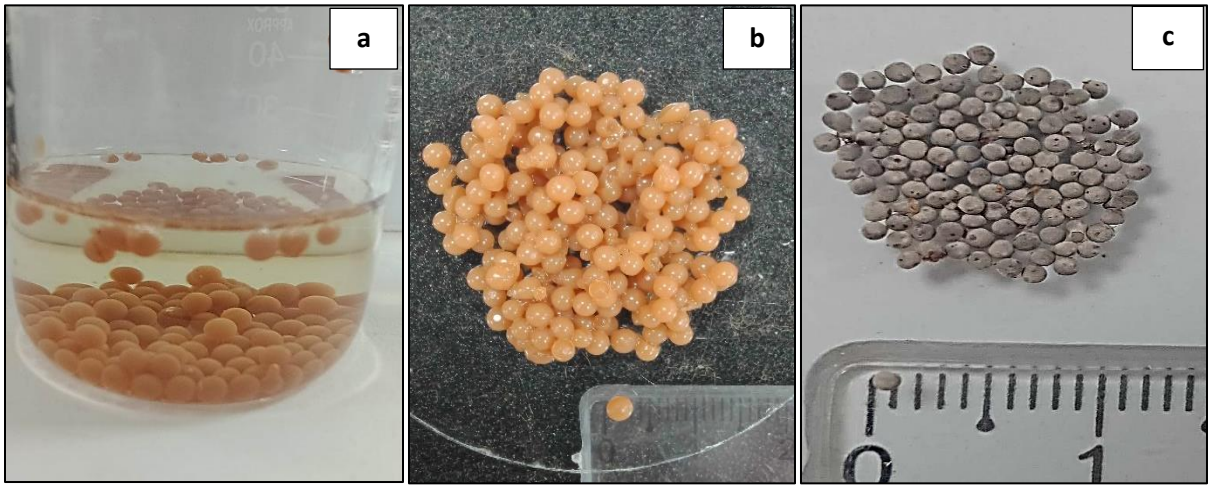


Figure II.16 (a) Sodium alginate crosslinking, **(b)** Sodium alginate-based hydrogel beads before drying and **(c)** after drying.

II.2.4.2 Quantification of the encapsulated active agent

II.2.4.2.1 Quantitative analysis of cephalexin

The absorption maximum wavelength (λ_{max}) of cephalexin was determined by plotting absorbance vs wavelength in graph (A=f (C)) through scanning a cephalexin solution prepared with buffer solution (pH 7.4) at T=37°C in the interval 180-600 nm using a spectrophotometer. Absorption cuvettes of 1 cm pathlength were used. The analysis was repeated for accuracy.

In order to determine the amount of the encapsulated active agent, a calibration curve was plotted by measuring the maximum absorbance of several standard solutions of known concentration (0.05-0.00625 mg/mL) that were prepared from a stock solution of CL at the determined λ_{max}. The coefficient ε is calculated by applying the Beer-Lamber law **(II.6)** relating the absorbance and the concentration of the species:

$$\boldsymbol{A = \varepsilon\, l\, C} \qquad \textbf{(II.6)}$$

Where A is the absorbance, ε is the molar absorption coefficient (L $mol^{-1}cm^{-1}$), l is optical path lengh (1cm) and C is the molar concentration (mol L^{-1}).

II.2.4.2.2 Encapsulation efficiency and loading capacity determination

The entrapment efficiency and drug loading capacity were calculated using **Equation II.7** and **II.8**. For this, 10 mg of CSMS were immersed in 10 ml of phosphate buffer solution in a container at 40°C under stirring. After centrifugation, a sample of the residue was analysed spectrophotometrically at the obtained λ_{max} (262 nm) using an optical cuvette made of quartz with 1cm optical path. The analysed sample is diluted, if necessary, with the same solvent of the medium. Drug concentration was calculated against calibration curve [19].

$$\boldsymbol{EE,\%} = \frac{\boldsymbol{Drug\ mass\ in\ beads}}{\boldsymbol{Initial\ drug\ mass}} \times \mathbf{100} \qquad \textbf{(II.7)}$$

$$\boldsymbol{LC, mg/g} = \frac{\boldsymbol{Drug\ mass\ in\ beads}}{\boldsymbol{g\ of\ dried\ beads}} \times \mathbf{100} \qquad \textbf{(II.8)}$$

The mass of the released drug (m_t) was calculated, which refers also to the experimental drug mass in beads in this case, following either equation **II.9** or **II.10**[20]:

Without dilution: $\boldsymbol{m_t, g} = \frac{(\boldsymbol{A \times V_c \times M})}{\boldsymbol{\varepsilon}}$ **(II.9)**

With dilution: $\boldsymbol{m_t, g} = \frac{(\boldsymbol{A \times V_s \times V_d \times M})}{\boldsymbol{\varepsilon \times V_c}}$ **(II.10)**

Where V_s is the volume of the sample to be diluted, V_d is the volume of dilution, V_c is the volume of the solution in the container and M is the molar weight of the drug (347.39 g/mol).

II.2.4.3 Swelling behaviour measurement

The swelling index was determined according to Öztürk et al. [21]. 10 mg of microspheres were immersed in 10 ml of 0.1 N HCl (pH 1.2) or phosphate buffer solution (pH 7.4) at 37°C with gentle stirring **(Figure II.17)**. The swelling percentage was calculated after 15, 30, 60 and 120 min via the equation:

$$\boldsymbol{Swelling}, \% = \frac{\boldsymbol{Ws - Wd}}{\boldsymbol{Wd}} \times \mathbf{100} \qquad \textbf{(II.11)}$$

Where W_d, W_s are the weight of beads in the dry and swollen state.

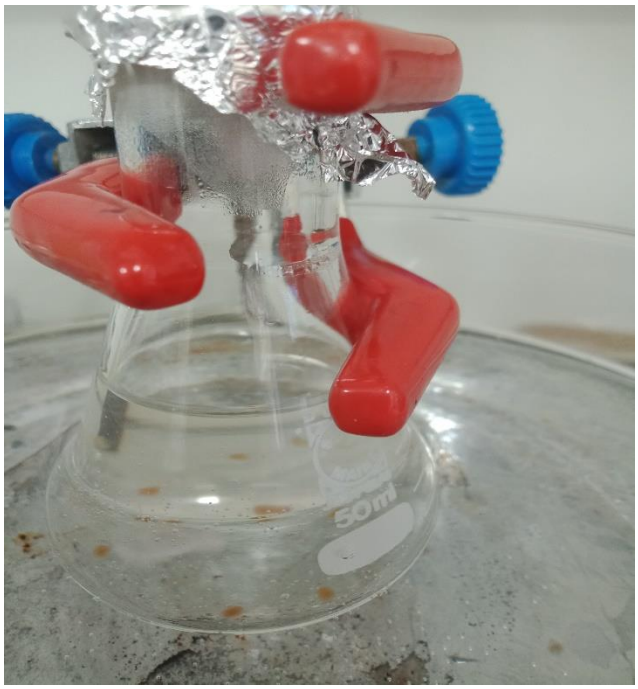


Figure II.17 Swelling test.

II.2.4.4 In vitro drug release study and kinetic modelling

The release profile study of beads was performed in phosphate buffer pH 7.4. First, 50 mg of CSMS were immersed in 50 ml of pH 7.4 phosphate buffer solution at 37°C under gentle stirring. 1mL aliquots were taken at chosen times for 24h, diluted with an appropriate factor and kept for absorbance spectroscopy measurement at λ_{max}= 262 nm. The experiment was performed in triplicate. Cumulative drug release percentages were calculated and plotted against time [19].

In order to determine the mechanism of cephalexin release from calcium alginate beads, different mathematical kinetics models **(Equations II.12-II.17)** were applied [22]. The most appropriate was the one which his plot has the high value of linear regression coefficient.

Zeroth-order model: $\mathbf{m_t = K_0 t}$ **(II.12)**

First-order model: $\mathbf{\ln(m_i - m_t) = -K_1 t + \ln m_i}$ **(II.13)**

Second-order model: $\frac{1}{m_i - m_t} = K_2 t + \frac{1}{m_i}$ **(II.14)**

Higuchi model: $m_t = K_H t^{1/2}$ **(II.15)**

Korsmeyer-Peppas model: $\log \frac{m_t}{m_\infty} = n \log t + \log K_{K-P}$ **(II.16)**

Hixson-Crowell method: $m_i^{1/3} - m_{left}^{1/3} = K_{H-C} t$ **(II.17)**

Where m_i, m_t, m_∞, and m_{left} are the initial amount of drug in beads, the amount of drug released in the medium at time t, the saturated drug content in the medium and the amount of drug left in the bead at time t respectively. K is the release rate constants for each model. n is the diffuse constant.

m_∞ is determined by plotting the curve **ln (m_t/m_i)=f (1/t) (Appendix)**, when **$t \rightsquigarrow \infty \Leftrightarrow 1/t = 0$,** The intersection of the line with the y-axis corresponds to the value of **ln (m_∞/m_i)** then m_∞ was calculated.

II.2.4.5 Antibacterial activity evaluation

The study of cephalexin effectiveness after encapsulation was investigated by agar diffusion method as described in section **II.1.7**. In brief, one cephalexin-loaded bead (L) was applied to Mueller-Hinton agar inoculated with *Escherichia. coli* or *Staphylococcus. aureus* suspension at a 10^8 CFU/mL concentration. The plates were incubated for 24 hours at 37 °C and the result was reported by the average inhibition zone diameters. Blank beads (F) were used for comparison.

II.3 Physicochemical characterizations

II.3.1 Ultraviolet-visible spectrophotometry (UV-Vis)

The samples concerned by uv-visible analysis were underwent this analytical precess using analytikjena SPECORD 210 PLUS spectrophotometer at the wavelength range of 180 to 1200nm using quartz cuvette. The analysis was conducted at the laboratory of SEAMM, University of Abdelhamid Ibn Badis, Mostaganem, Algeria.



Figure II.18 Laboratory UV-Visible spectrophotometer apparatus.

II.3.2 Fourier transform infrared analysis (FTIR)

The Samples were mixed and ground with KBr and pressed into fine pellets then analysed with Shimadzu-IRPrestige-21 spectrophotometer. The spectra were recorded in transmittance mode over the range of 500-4000 cm^{-1}. The analysis was conducted at the Laboratory of SEAMM, University of Abdelhamid Ibn Badis, Mostaganem, Algeria.



Figure II.19 Laboratory FTIR spectrophotometer apparatus.

II.3.3 X-ray diffraction analysis (XRD)

XRD analysis was conducted using Rigaku-MiniFlex 600 powder *X-ray diffractometer* equipped with Cu-Kα radiation (λ= 1.54186 Å) operating at the diffraction angle 2θ ranging from 4° to 70° with a 0.02° step with scanning rate 5°/min. The analysis was conducted at the Laboratory of Synthesis and Catalyst, University of Ibn Khaldoun, Tiaret, Algeria.



Figure II.20 Laboratory X-ray diffractometer apparatus.

II.3.4 Thermal analysis (TGA/DSC)

Simultaneous thermogravimetric analysis (TGA) and differential scanning calorimetry (DSC) were carried out with TA SDT650 analyser. Few milligrams of samples were put in crucibles and heated from ambient temperature to 1000°C at a ramping rate of 10 C°/min under N_2 flow of 50ml/min. The analysis was conducted at the Laboratory of SEAMM, University of Abdelhamid Ibn Badis, Mostaganem, Algeria.



Figure II.21 Laboratory TGA/DSC apparatus.

II.3.5 Optical microscopy

The shape of the dried beads was observed in OPTICA Axiom 7000 optical microscope equipped with a camera. The analysis was conducted at the Laboratory of Reproduction of Farm Animals, Institute of Veterinary Sciences, University of Tiaret, Algeria.



Figure II.22 Laboratory optical microscope.

II.3.6 Scanning electron microscopy (SEM)

The samples were coated with Gold-Palladium layer at current of 30mA for 30s then their surface morphology was observed by thermoscientific Phenom Pharos G2 Scanning Electron Microscope operating at high vacuum mode and acceleration voltage 5-10kV.

The analysis was conducted at the Technical Platform of Physico-Chemical Analysis, PTAPC-Mostaganem, Algeria.

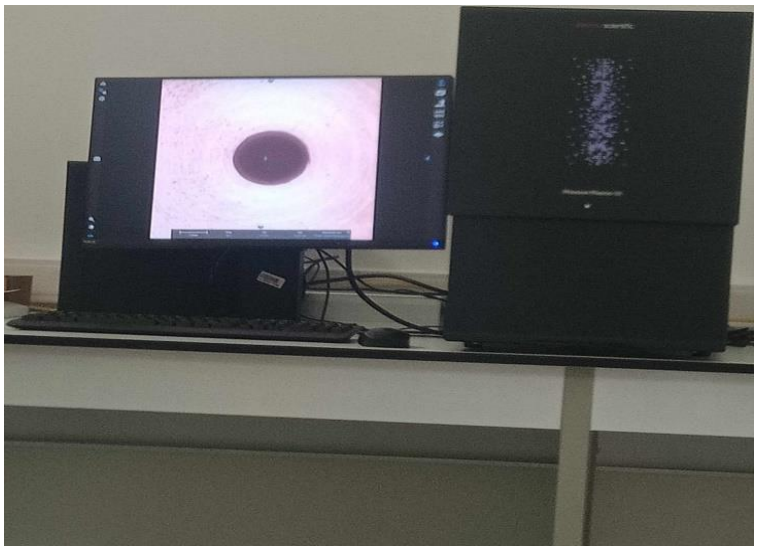


Figure II.23 Laboratory SEM apparatus.

II.3.7 Dynamic light scattering analysis (DLS)

The mean diameter size of particles and zeta potential of microsized or nanosized samples was analysed by Horiba nanoPartica SZ-100V2. 1% suspension of samples was prepared using ultrapure water then sonicated for at least 30min using an ultrasonic water bath. The analysis was conducted at the Laboratory of SEAMM, University of Abdelhamid Ibn Badis, Mostaganem, Algeria.



Figure II.24 Laboratory DLS apparatus.

II.4 References

[1] O. G. Mouristen, *Seaweeds: edible, available and sustainable*. London: University Of Chicago Press, 2013.

[2] T. Boukhatem, R. Chadli, and N. Berrahal, "Fatty acid profile and isolation of bioactive compounds from the acetone extract of Cystoseira stricta L., harvested from western Algeria," *Egypt. J. Microbiol.*, vol. 56, pp. 99–108, 2021, doi: 10.21608/ejm.2021.59732.1186.

[3] S. F. Mohamed, "Characterization of Sulphated Polysaccharide with Antiviral Activity from Marine Brown Alga Cystoseira myrica Collected from Jazan Coasts , KSA," *Int. J. PharmTech Res.*, vol. 8, no. 10, pp. 198–203, 2015.

[4] R. H. Farzanah, G. P. Brudecki, I. Cybulska, J.-R. Bastidas-Oyanedel, J. E. Schmidt, and M. H. Thomsen, "Screening and production of biogas from macro algae biomass of Padina boergesenii, Colpomenia sinuosa, and Ulva sp," in *Biorefinery*, Springer, 2019, pp. 727–740. doi: 10.1007/978-3-030-10961-5.

[5] V. Rani, R. J. Shakila, P. Jawahar, and A. Srinivasan, "Influence of species, geographic location, seasonal variation and extraction method on the fucoidan yield of the brown seaweeds of Gulf of Mannar, India," *Indian J. Pharm. Sci.*, vol. 79, no. 1, pp. 65–71, 2017, doi: 10.4172/pharmaceutical-sciences.1000202.

[6] S. Chen *et al.*, "Characterization of polysaccharides from different species of brown seaweed using saccharide mapping and chromatographic analysis," *BMC Chem.*, vol. 15, no. 1, pp. 1–11, 2021, doi: 10.1186/s13065-020-00727-w.

[7] G. G. January, R. K. Naidoo, B. Kirby-Mccullough, and R. Bauer, "Assessing methodologies for fucoidan extraction from South African brown algae," *Algal Res.*, vol. 40, pp. 1–10, 2019, doi: 10.1016/j.algal.2019.101517.

[8] N. A. M. Fauziee, L. S. Chang, W. A. W. Mustapha, A. R. M. Nor, and S. J. Lim, "Functional polysaccharides of fucoidan, laminaran and alginate from Malaysian brown seaweeds (Sargassum polycystum, Turbinaria ornata and Padina boryana)," *Int. J. Biol. Macromol.*, vol. 167, pp. 1135–1145, 2020, doi: 10.1016/j.ijbiomac.2020.11.067.

[9] Z. Z. Chowdhury and S. B. A. Hamid, "Preparation and characterization of nanocrystalline cellulose using ultrasonication combined with a microwave-assisted pretreatment process," *BioResources*, vol. 11, no. 2, pp. 3397–3415, 2016, doi: 10.15376/biores.11.2.3397-3415.

[10] H. Doh, M. Hyeock, and W. Scott, "Physicochemical characteristics of cellulose nanocrystals isolated from seaweed biomass," *Food Hydrocoll.*, vol. 102, p. 105542, 2020, doi: 10.1016/j.foodhyd.2019.105542.

[11] M. A. Bezzekhami, M. Belalia, D. Hamed, M. Bououdina, B. B. Berfai, and A. Harrane, "Nanoarchitectonics of starch nanoparticles rosin catalyzed by Algerian natural montmorillonite (maghnite-H+) for enhanced antimicrobial activity," *J. Inorg. Organomet. Polym. Mater.*, vol. 33, no. 1, pp. 193–206, 2023, doi: 10.1007/s10904-022-02490-y.

[12] J. Hudzicki, "Kirby-Bauer Disk Diffusion Susceptibility Test Protocol," *Am. Soc. Microbiol.*, vol. 15, no. 1, pp. 1–23, 2009.

[13] M. Belalia, M. Bendjelloul, A. Aziz, and E. H. Elandaloussi, "Surface modification of olive stone waste for enhanced sorption properties of cadmium and lead ions," *Acta Chem. Iasi*, vol. 26, no. 2, pp. 281–306, 2018, doi: 10.2478/achi-2018-0018.

[14] S. N. Pawar, "Chemical Modification of Alginates in Organic Media," Doctoral dissertation, Virginia Polytechnic Institute and State University, 2013.

[15] L. Belkacemi, M. Belalia, A. Djendara, and Y. Bouhadda, "Antioxidant and antibacterial activities and identification of bioactive compounds of various extracts of Caulerpa racemosa from Algerian coast," *Asian Pac. J. Trop. Biomed.*, vol. 10, no. 2, pp. 87–94, 2020, doi: 10.4103/2221-1691.275423.

[16] C. Santos *et al.*, "Green nanotechnology for the development of nanoparticles based on alginate associated with essential and vegetable oils for application in fruits and seeds protection," *Int. J. Biol. Macromol.*, vol. 232, p. 123351, 2023, doi: 10.1016/j.ijbiomac.2023.123351.

[17] M. F. Aldawsari, M. M. Ahmed, F. Fatima, M. K. Anwer, P. Katakam, and A. Khan,

"Development and characterization of calcium-alginate beads of apigenin: In vitro antitumor, antibacterial, and antioxidant activities," *Mar. Drugs*, vol. 19, no. 8, 2021, doi: 10.3390/md19080467.

[18] Z. Khoshdouni Farahani, M. Mousavi, S. M. Seyedain Ardebili, and H. Bakhoda, "Modification of sodium alginate by octenyl succinic anhydride to fabricate beads for encapsulating jujube extract," *Curr. Res. Food Sci.*, vol. 5, pp. 157–166, 2022, doi: 10.1016/j.crfs.2021.11.014.

[19] I. Abdelmalek, I. Svahn, S. Mesli, G. Simonneaux, and A. Mesli, "Formulation, evaluation and microbiological activity of ampicillin and amoxicillin microspheres," *J. Mater. Environ. Sci.*, vol. 5, no. 6, pp. 1799–1807, 2014.

[20] I. Boukhouya, "Elaboration de microparticules chargées d'Amoxicilline et de Théophylline à partir de polymères biodégradables ; Etude cinétique de leur libération," Doctoral dissertation Université Djillali Liabes, Sidi Bel-Abbes, 2019.

[21] K. Öztürk, "Development and in-vitro characterization of l-cysteine loaded alginate beads for oral delivery," *J. Res. Pharm.*, vol. 26, no. 1, pp. 210–218, 2022, doi: 10.29228/jrp.119.

[22] D. Wójcik-Pastuszka, J. Krzak, B. Macikowski, R. Berkowski, B. Osiński, and W. Musiał, "Evaluation of the release kinetics of a pharmacologically active substance from model intra-articular implants replacing the cruciate ligaments of the knee," *Materials (Basel).*, vol. 12, no. 8, 2019, doi: 10.3390/ma12081202.

Chapter III

Results and Discussion

Section 1

Extraction of Algal Polysaccharides

In this section, the outcomes of our study are presented, interpreted and discussed notably the determination of moisture content and ash in algae powder, parameters optimization toward the best extraction yield of fucoidan, sodium alginate and cellulose. The results of the antibacterial activity of the extracted polysaccharides and the prepared MCC are also detailed.

III.1 Extraction of algal polysaccharides

III.1.1 Moisture content and ash determination

Brown alga was selected as the raw material because it has not been exploited yet on a large-scale. Furthermore, this feedstock is characterized by its fast growing [1], cost-effective [2], and the inherent low lignin content [3] which make the extraction process easier and less costly. In the current research, *Cystoseira stricta* was the species of choice. Its presence in the sea is a reliable indicator of a healthy marine environment [4].

First of all, *C. stricta* seaweed was harvested, purified, dried and grounded then sieved to ensure the size uniformity and to increase the surface area of the seaweed to be exposed to the extraction solvent.

The proximate composition of the biomass studied regarding moisture and ash content was estimted gravimetrically **(Figure III.1)**. The average moisture content of the raw material WBA was estimated to be 6.69±0.06% and the ash content was 35.86±2.14%. for SBA, MC% was 6.52±0.68% and ash% was 58.21±2.63%. Highest level of ash content was measured during summer and the moisture content was almost equal between the two periods.

It was demonstrated by Schiener et al. 2015 [5] that the ash and moisture content can influence on the yield of targeted seaweed components where the maximum values of carbohydrates coincided with reduced concentrations of the component's protein, ash, polyphenols and moisture.

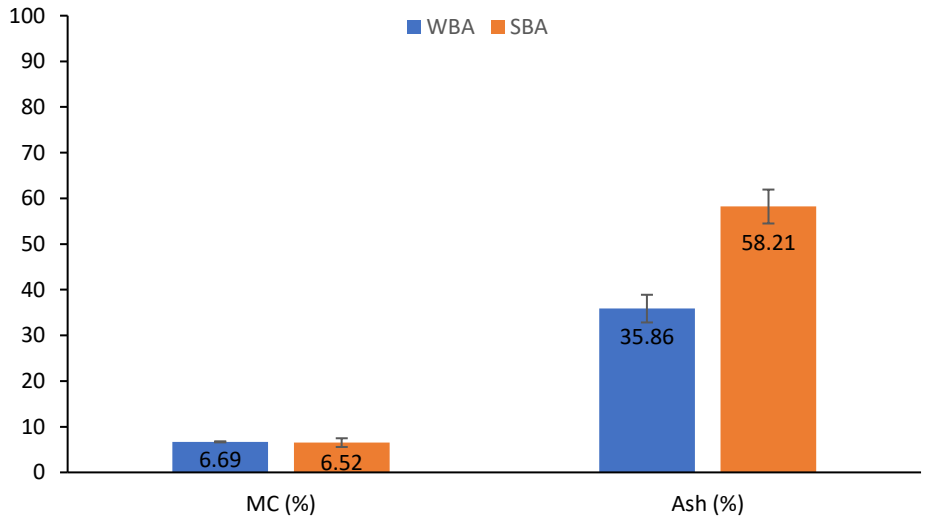


Figure III.1 Proximate composition of WBA and SBA.

III.1.2 Extraction yield determination

In this study, the extraction process of fucoidan, sodium alginate and cellulose including three variables: particle size, solid to liquid ratio, and harvesting period, was investigated. The preparation of microcrystalline cellulose was also done. Conventional extraction method was performed on account of simplicity, feasibility and industrialization.

The pretreatment process with organic solvents before extraction is crucial to eliminate undesired compounds E.g. chlorophyll and lipids. Ultrasonication is used to disrupt cell walls and enhance the mass transfer of bioactive compounds into extraction solvent to improve the quality and quantity of target compounds [6]. The pre-extraction step using acid, alkali or formalin can influence badly regarding the rheological and physicochemical properties of extracts [7]. The discolouration was not necessary in the early stage of extraction [8]. For this reason, this step was avoided in this study.

In the process to extract fucoidan from WBA and SBA, aqueous solution of $CaCl_2$ was used to convert cell wall sodium alginate into water insoluble calcium alginate which is removed together with solid seaweeds residues, leaving pure fucoidan in aqueous extract. This later is mixed with CTAB solution which is a cationic detergent, it forms with fucoidan, which is a polyanion, a water insoluble salt which precipitates and hence the other neutral polysaccharides remain soluble.

Sodium carbonate was then used to solubilize alginate into water soluble sodium salt form. The final product was purified by ethanol precipitation to remove low molecular weight impurities from the polysaccharide [9]. This step is considering also as an alkaline pre-treatment for the removal of undesirable components such as hemicellulose which made the cellulose extraction process sustainable and efficient [10].

Hydrogen peroxide is an environmentally friendly bleaching agent, was used in the final step to treat the residue, referred to as chlorine-free bleaching process, in order to produce cellulose [11]. Most commonly, bleaching of samples in order to get cellulose is carried out in a single stage. So, in this work, we have proposed to use two sages bleaching process in order to increase the effectiveness of H_2O_2 bleaching ability instead of using large quantity of H_2O_2 in one stage.

Cellulose derivatives were prepared by breaking down the glycosidic linkage between the amorphous and the crystallin regions of cellulose through a process called Acid hydrolysis. This later require the use of strong acids such as sulfuric and hydrochloride acid. The hydrolysis using H_2SO_4 has weaknesses including low yield, crystalline cellulose chain degradation and low thermal

stability of the product [12]. For this reason, we have chosen to use hydrochloric acid under hydrothermal conditions in this work to produce pure microcrystalline cellulose.

III.1.2.1 Influence of particle size on the yield of polysaccharides

To investigate the effect of particle size on the extraction efficiency from WBA, we have chosen two different sizes (150 and 400) and S/L ratio 1:10. From **Table III.1** it was observed that when the size of biomass powder decreased, the extraction yields increased which can be demonstrated by the increasing in the surface of contact between the powder and the extracting solvent making the extraction more effective. For this reason, the optimum sample particle size of 150µm is chosen for the rest of experiments.

Table III.1 Influence of particle size distribution on extraction yield of polysaccharides.

Polysaccharide / **Powder size (µm)**	**Extraction yield % (Mean±SEM)**	
	150	400
Fucoidan	5.65± 0.52	2.31±0.45
Alginate	15.89±0.41	12.41±0.28
Cellulose	15.27±2.56	12.68±3.31

III.1.2.2 Influence of the solid to liquid ratio on the yield of polysaccharides

The effect of dry weight biomass to extraction liquid ratio (S/L ratio) on the extraction yield was studied. The results show that when S/L proportion increased from 1:10 to 1:30 w/v, the extraction yield of sodium alginate has shown considerable increase from 15.89±0.29% to 37.52±1.22%. Only a slight decrease of 1% and 1.62% was recorded for fucoidan and cellulose yield respectively. As mentioned by [13], biomass loading ratio is one of the parameters that have a significant impact on the extraction yield with keeping the composition unchanged.

S/L ratio of 1:30 has led to significant higher percentage yield of sodium alginate. Further, the extraction yield of sodium alginate which was reached in this study is among the highest yield reported in the literature for Cystoseira species in the mediterranean coast. Our results are higher than those obtained for Tunisian *Cystoseira barbata*, 5.45% for fucans [14] and 9.9% (w/w) for sodium alginate [15]. Hadj Ammar et al.[16] also reported a value of 4.2% for fucoidans and 11%

for sodium alginate extracted from Tunisian *Cystoseira sedoides.* Besides, the average yield of sodium alginate extracted from Algerian *Cystoseira caespitosa* was 12% [17]. For Moroccan *Cystoseira myriophylloides*, alginate content was 31% and fucoidan was 0.87% of the dry weight of the algae [18]. On the other hand, the yield of crude cellulose obtained from Indian *Cystoseira indica* was 9% [19] which is less from that obtained in our work.

III.1.2.3 Influence of harvesting time on the yield of polysaccharides

For the purpose of this study, the solid to liquid proportion was maintained at 1:30 and the extraction was conducted on WBA and SBA samples. Compared to harvesting in February, the content in fucoidan extracted from algae harvested in September (SBA) has been decreased from 4.66±0.49% to 1.95±0.26%. Same fucoidan fluctuation was observed in the study of Benslima et al. [20]. where it has been suggested that winter is the best period to extract the highest yield of *Cystoseira schiffneri* fucoidan compared to summer. In contrast to other research, high content of fucoidan extracted from *Fucus* and *Ascophyllum* species was registered in September compared to February [21]. This may be return to the extraction process used, species and the geographical location of the algae.

Alginate content underwent a similar temporal variation to fucoidan. 37.52±1.22% was registered in February and dropped to 27.72%±4 in September. Same remark was noted in previous studies where the extraction yield of alginate from Tunisian *Cystoseira schiffneri* was variable across seasons, in September (21%) it was the lowest compared to that extracted in July (38.4%), April (28%) and December (25.1%) [22]. Similarly, The alginate content in February (~21%) was higher than in September (11,14%) in *Sargassum muticum* species harvested from the Atlantic coast of Morocco [23].

It has been extracted significantly more cellulose in September (31.78±7.72%) than February (13.65±3.27%). Contrary to the study of Schiener et al.[5] the cellulose content was not much variable across seasons (did not acceded 15%) for *Laminaria digitata*, *Laminaria hyperborea*, *Saccharina latissimi* and *Alaria esculenta* species.

The yield of MCC was approximately 31,44% from the dried cellulose which is lower than that of *Posidonia oceanica* brown algae reported by Tarchoun et al. [24].

In brief, the temporal fluctuation of polysaccharides yield would not follow similar trend in the same species even for all species.

III.1.3 Characterization

Products showing optimal results were selected for characterization and further uses.

III.1.3.1 FT-IR analysis

The absorption spectra produced after FT-IR analysis of the extracted *C. stricta* fucoidan **(Figure III.2)**, sodium alginate **(Figure III.3)**, cellulose and microcellulose **(Figure III.4)** showed multiple characteristic absorption bands providing insights into the tested sample's molecular structure and confirmed their successful extraction. Frequency assignments for major bands are summarized in **Table III.2**.

Broad bands of O-H and small band of C-H stretching vibrations related to hydroxyl and methyl groups (or covalent bound) of the main monosaccharides of each polymer were apparent in all spectra. As well as the intense absorptions in 1200–970 cm^{-1} of characteristic groups were common for all polysaccharides [25].

Table III.2 Assignment and location of the main characteristic bands of extracted Fucoidan, alginate, cellulose and microcrystalline cellulose.

Functional group	**Wavenumber (cm^{-1})**				**Ref**
	Fucoidan	Alginate	Cellulose	MCC	
υ(O-H)	3431	3454	3360-3415	3350-3415	[20][26][27]
υ(C-H)	2941	2926	2922-2855	2922-2855	
δ(O-H)			1645	1635	[28]
υ(C=O) (uronic acid residue)	1641				[29]
υ_{as}(COO-)		1631			[17]
υ_{s}(COO-)		1428			
δ(C-H)			1477	1431,1369	[27], [28]
υ_{as}(COO-) (uronic acid residue)	1391				[29]
υ(C-C) and υ(C-O) skeletal			1323	1323	[30]
υ_{as}(S=O)	1258				[20]
υ_{as}(C-O-C)			1163	1153	[31]
υ_{s}(C-O-C)	1051	1095 of M 1028 of G	1060	1063	[20][26] [30]
υ(C-O) (uronic acid residue)		947			[32]
δ(C-O-S) (C_4 axial sulfate ester group)	839				[33]

δ,υ, s and as symbols correspond to bending, stretching vibrations, symmetric and antisymmetric modes, respectively.

The distinctive bands of fucoidan were observed at 3431, 2941, 1641 cm^{-1} indicating the presence of hydroxide group, C-H bond and carbonyl group of uronic acids residues. In the fingerprint region, we observed a band at 1391 cm^{-1} corresponded to asymmetric stretching vibration of the carboxylic group of uronic acid residues. Sharp peak at 1258 cm^{-1} could be assigned to sulfate ester group, while the band at 1051 cm^{-1} is attributed to C-O-C glycosidic linkage. Finaly, the band at 839 cm^{-1} might indicate that the sulfate group is located at C-4 of the fucopyranose residues. The FT-IR spectra exhibited absorption bands typical of fucoidans showing a strong similarity to those obtained with *Cystoseira* species [20], *Sargassum* species [29] and *Laminaria japonica* [25] with differences in the content of chemical components such as sulfate group.

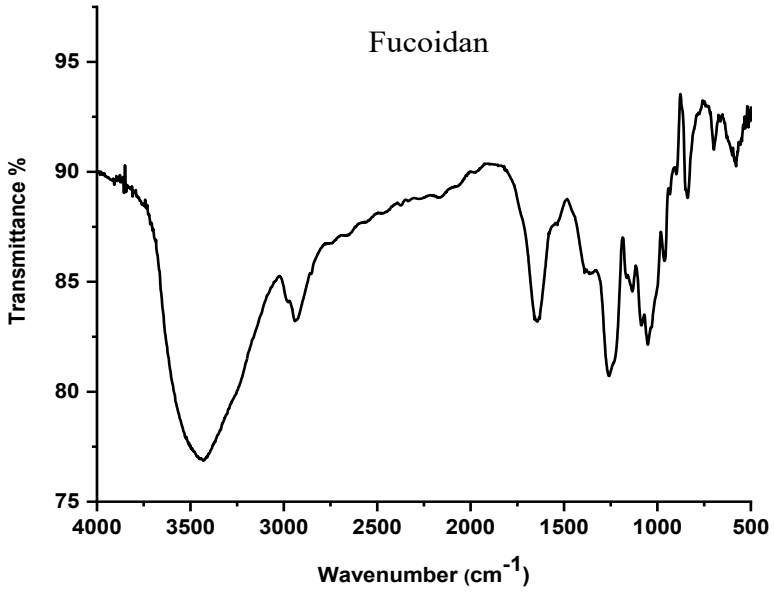


Figure III.2 FT-IR spectrum of fucoidan isolated from the Algerian *Cystoseira stricta*.

From the FT-IR spectrum of sodium alginate, bands around 3454, 2926, 1631, 1423, 1095, 1028 and 947 cm^{-1} were observed which are related to O-H bond stretching vibration, C-H bond stretching vibration, COO- asymmetric and symmetric stretching vibration, C-O-C stretching vibration of mannuronic and guluronic units and skeltal C–O stretching vibration of uronic acid residues respectively. The spectrum of extracted sodium alginate was not significantly different to that from the commercial one **(Figure in Appendix)** hence confirming the purity of the sample.

The proportion and distribution of mannuronic (M) and guluronic (G) units affect the physicochemical properties of sodium alginate solutions. M/G ratio is estimated by Sakugawa et al. [34] using FT-IR by calculating the ratio between the absorbance reading at the frequencies of M and G units. The M/G ratio of extracted Na-alg was given in **Table (III.3)** with comparison to other works.

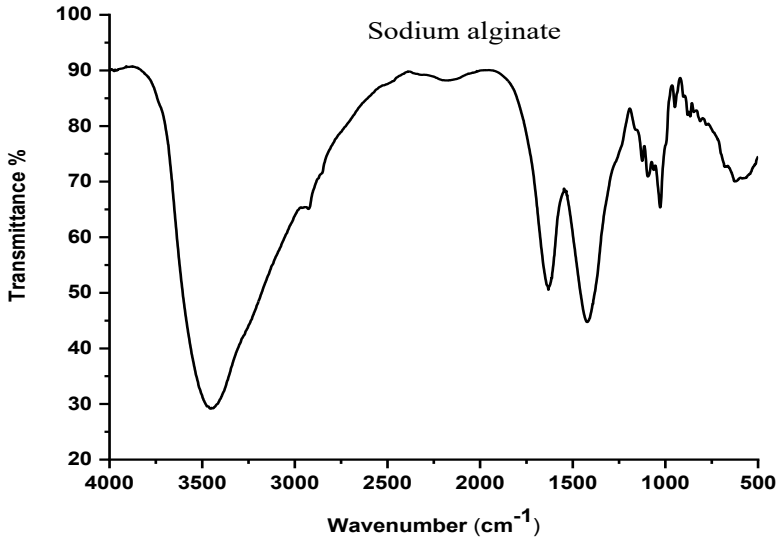


Figure III.3 FT-IR spectrum of sodium alginate isolated from the Algerian *Cystoseira stricta*.

The FTIR spectra of cellulose and MCC are shown in **Figure III.4**. Similarities can be observed between the two patterns. Vibrational frequencies between 3360 and 3415 cm^{-1} were attributed to inter/intramolecular stretching mode of O-H bond. The peaks between 2922-2855 cm^{-1} represented the symmetric and asymmetric C-H stretching vibrations. The absorption band around 1635 cm^{-1} in MCC spectra is assigned to O-H bending of bound water. The presence of water molecules in MCC prove the bond breaking in cellulose during acid hydrolysis process [35]. The peaks observed at 1431,1369 and 1477 cm^{-1} can be assigned to C-H bending and vibration of intramolecular hydrogen attractions. C-C and C-O skeletal vibration were indicated by the peak at 1323 cm^{-1}. C-O-C stretching vibration peaks of cellulose, pyranose ring and β-glycosidic linkage between sugar units are located at around 1163, 1060 and 898 cm^{-1} for cellulose and at 1153, 1063 and 900 cm^{-1} for MCC. Some peaks appeared clearly in MCC spectrum compared to cellulose owing to the reduction in amorphous zones by acid hydrolysis[36]. The intensity and the sharpness

of peak 1645, 1477 and 898 cm^{-1} were reduced probably due to cellulose order reorientation as

Species	Harvasting site	M/G ratio	Alginate content%	Reference
Dictyopteris polypodioides	El Jadida shoreline – Morocco	0.99	21,92	[38]
Dilophus ligulatus		0.99	8,8	
Halopteris scoparia		1.0	4,16	
Cystoseira barbata	Kerkennah island (Sfax, Tunisia)	0.59	9.9	[15]
Cystoseira sedoides	coastal region of Monastir (Tunisia)	1.67	11	[16]
Cystoseira caespitosa	Algerian Mediterranean coast	0.97	16 %	[17]
Dictyota dichotoma	Red Sea Coast of Sudan	0.92	8.8±2.12	[39]
Hormophysa cuneiformis		0.97	19.1±1.62	
Padina pavonica		0.93	7.99±2.60	
Turbinaria ornata		1.01	14.3±1.2	
Laminaria digitata	Isle of Seil, Scotland		34.6±3.1	[40]
Laminaria hyperborean			33.2±3.8	
Saccharina latissimi			28.5±3.9	
Alaria esculenta			37.4±4.0	
Laminaria ochroleuca (blade)	Atlantic Coast of Morocco		28.96 ± 0.20	[41]
Laminaria ochroleuca (stipe)		1.38	49.80 ± 2.40	
Saccorhiza polyschides (blade)		1.62	20.19 ± 2.00	
Saccorhiza polyschides (stipe)		2.14	26.28 ± 0.08	
Cystoseira stricta	Stidia Algerian coast	0.81	37.52±1.22	This work

cited in [37].

Table III.3 Alginate content and M/G ratio of different species.

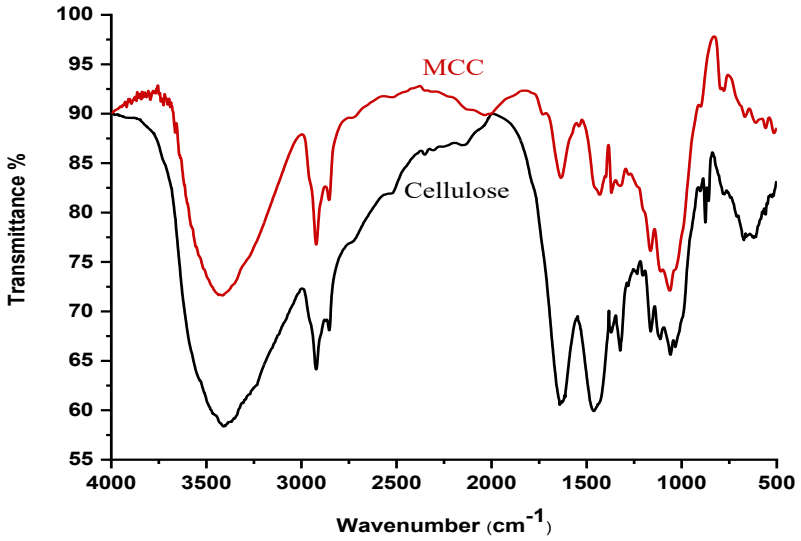


Figure III.4 FT-IR spectrum of cellulose and MCC isolated from the Algerian *Cystoseira stricta.*

III.1.3.2 XRD analysis

XRD diffractograms of extracted fucoidan is depicted in **Figure III.5**. Fucoidan showed a semi-crystalline structure represented by the peaks between 20 and 30°[42]. Whereas, the analysis of sodium alginate revealed a much higher crystallinity characterized by multiple peaks in the spectrum **(Figure III.6)**. The intense peak at around 32° was attributed to the plane (200)[43]. According to the report of Sayin et al. [44], our extracted sodium alginate has almost the same pattern as that obtained from *Sargassum vulgare.*

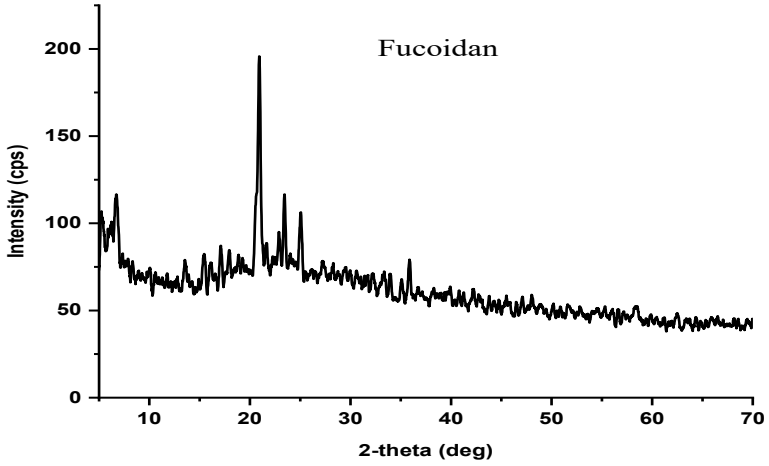


Figure III.5 XRD pattern of fucoidan isolated from the Algerian *Cystoseira stricta*.

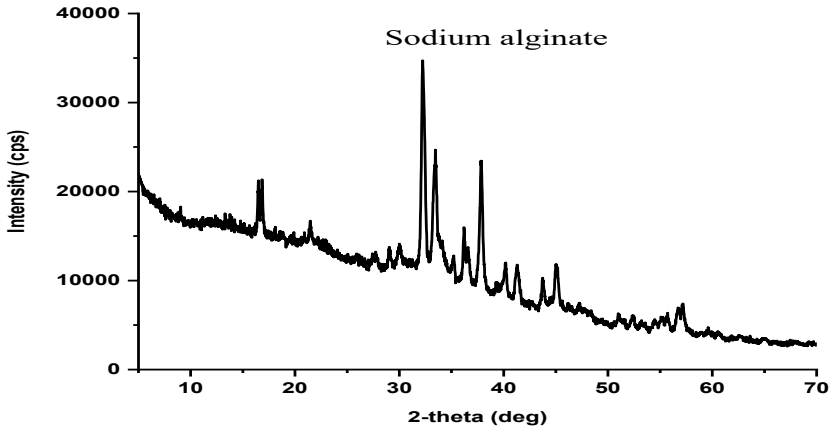


Figure III.6 XRD pattern of sodium alginate isolated from the Algerian Cystoseira stricta.

XRD patterns of extracted cellulose and MCC are depicted in **Figure III.7**. The effectiveness of acid hydrolysis is revealed by the intensity increase which clearly elucidated the decrease of crystallinity degree of cellulose [24]. Three main peaks were highlighted on each pattern: 14.33, 22.58. 32.29 of cellulose and 14.89, 22.42 and 36.55 of MCC attributed to the lattice planes (110), (002) and (004) respectively. According to previous study, this pattern represents the cellulose I allomorph [35]. The peaks at around 2θ = 26° and 29° are attributed to the presence of mineral impurities such as silica (SiO_2) and weddellite ($CaC_2O_4.2H_2O$) which are generally presented in sea biomass as cited in [45]. The XRD pattern of our extracted cellulose is similar to that reported in the work of Baghel et al. [46]. The XRD patterns of cellulose and MCC are similar to those extracted from kombu and sargassum brown seaweeds [36] and even from another source which is peanut shells as described by Terea et al. [30].

The crystallinity index (CrI) of microcrystalline cellulose was calculated using the equation developed by Segal et al. [47]

$$\boldsymbol{CrI}, \% = \frac{(\boldsymbol{I_{002}} - \boldsymbol{I_{am}})}{\boldsymbol{I_{002}}} \times \mathbf{100} \qquad \textbf{(III.1)}$$

Where I_{002} is the maximum intensity of the (002) lattice diffraction and I_{am} is the minimum intensity of the amorphous peak (2θ=17.84°), following a previous report written by French and Cintron [48].

The crystallinity index of the obtained MCC was 69.2%. This value aligns closely with some values previously reported in scientific literature. Perumal et al.[35] have extracted MCC from *Valoniopsis pachynema* green algae with crystallinity index 71.9%. MCC was extracted from *Posidonia oceanica* brown algae with crystallinity index 74.23% [24]. This may be return to the use of strong base (KOH) in the alkali treatment which eliminated more the amorphous regions of cellulose.

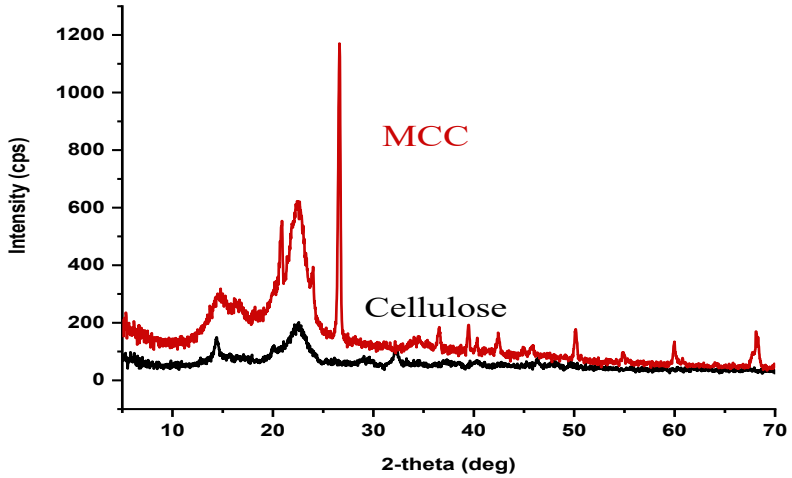


Figure III.7 XRD pattern of cellulose and MCC isolated from the Algerian *Cystoseira stricta*.

III.1.3.3 TGA/DSC analysis

Simultaneous thermogravimetric analysis and differential scanning calorimetry (TGA/ DSC) was performed on extracted fucoidan, sodium alginate, cellulose and microcellulose to evaluate their thermal stability under a constant heating rate.

From the TGA/DSC graphs of fucoidan **(Figure III.8)**, the first stage of weight loss described the evaporation of moisture noticed by an endothermic transition at a peak temperature of 60.7°C. The second stage consisted of devolatilization (removing of low molecular weight component and chemisorbed water) and pyrolysis (polymeric chain decomposition) which occurred till around 400°C with a weight loss of 46.6%. The next phase of degradation lasted until 1000°C with weight loss of 32.7% [49]. The same profile was obtained by Anastasakis et al. [50] from a commercial fucoidan. Our findings are very close to those reported in previous study [51] reflected that our extracted fucoidan from Cystoseira stricta has greater thermal stability compared to other sources.

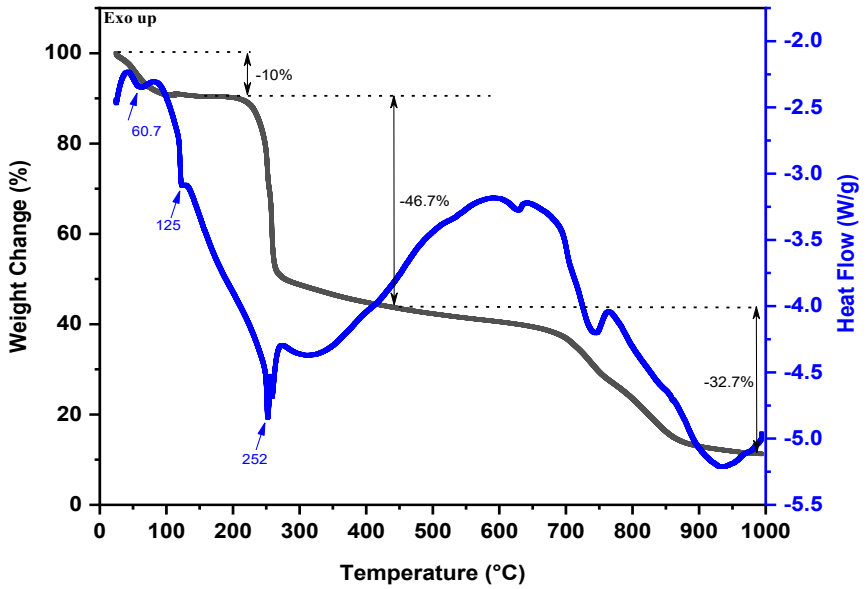


Figure III.8 TGA/DSC thermogram of fucoidan isolated from the Algerian Cystoseira stricta.

By plotting the TGA/DSC curves of sodium alginate **(Figure III.9)**, three regions of mass loss are noticed. The first one is between 50 and 170°C attributed to non-bonded then adsorbed water molecules evaporation confirming by the initial endothermic peak in the DSC plotting. The second endothermic peak that appeared at around 198°C is probably related to the transitions associated with the water loss of hydrophilic functional polymeric groups [52]. Subsequently, polymer chain degradation (pyrolysis process) was occurred describing by the exothermic peak at 245°C. This phase is accompanied with liberation of intermediates substance such as metal carbonates ($CaCO_3$) formed from the reaction between metal ions bound to the alginate and carbon dioxide released throughout the pyrolysis phase [53]. The last stage is attributed to the degradation of residues up to 1000°C.

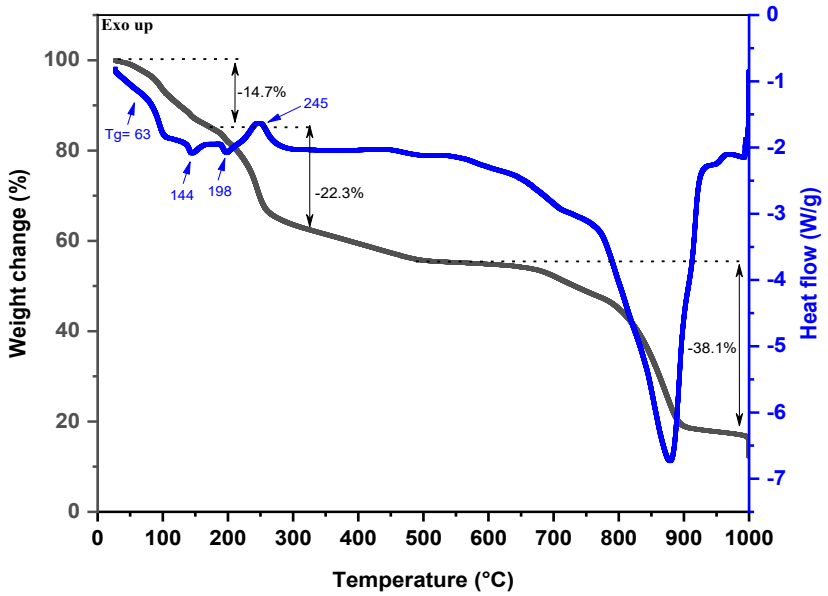


Figure III.9 TGA/DSC thermogram of sodium alginate isolated from the Algerian *Cystoseira stricta*.

As seen in the TGA/DSC thermogram of cellulose **(Figure III.10)**, the thermal decomposition of cellulose proceeded through two stages: the first stage characterised by loss of 2.7% of the total weight of the sample due to moisture evaporation. The second stage was occurred in two overlapping steps between 150 and 600°C. the temperature at which the maximum mass loss rate occurs during cellulose pyrolysis was 314°C. It was shown that the thermal stability of cellulose from seaweed varies between species and is usually in the range 250–300°C[54]. The small peak at higher temperature may be attributed to traces of non-cellulosic polysaccharides (hemicellulose) which are totally eliminated after acid hydrolysis confirmed by the disappearance of this peak in the thermogram of MCC.

MCC decomposition occurred at lower temperature (peak at 290°C) which is correlated with the reduction of cellulose molecular weight during hydrolysis [55]. In Addition, the increased surface area of particles came into direct contact with high temperatures resulted in thermal stability reduction. The maximum weight loss was reached at around 370°C and completely pyrolyzed at 900°C with a residual mass of 14.8 %. Additionally, the weight loss of cellulose is lower than that of MCC which is due to the high purity of MCC compared to cellulose [24]. Nevertheless, the thermal stability of our isolated MCC in this work was considerably great, which

may broaden their suitability to be used in biocomposites production with enhanced properties at high-temperature applications.

The observed thermal behaviours reflected the polysaccharide stability at room temperature, which will be suitable to be used as active agents and drug carriers.

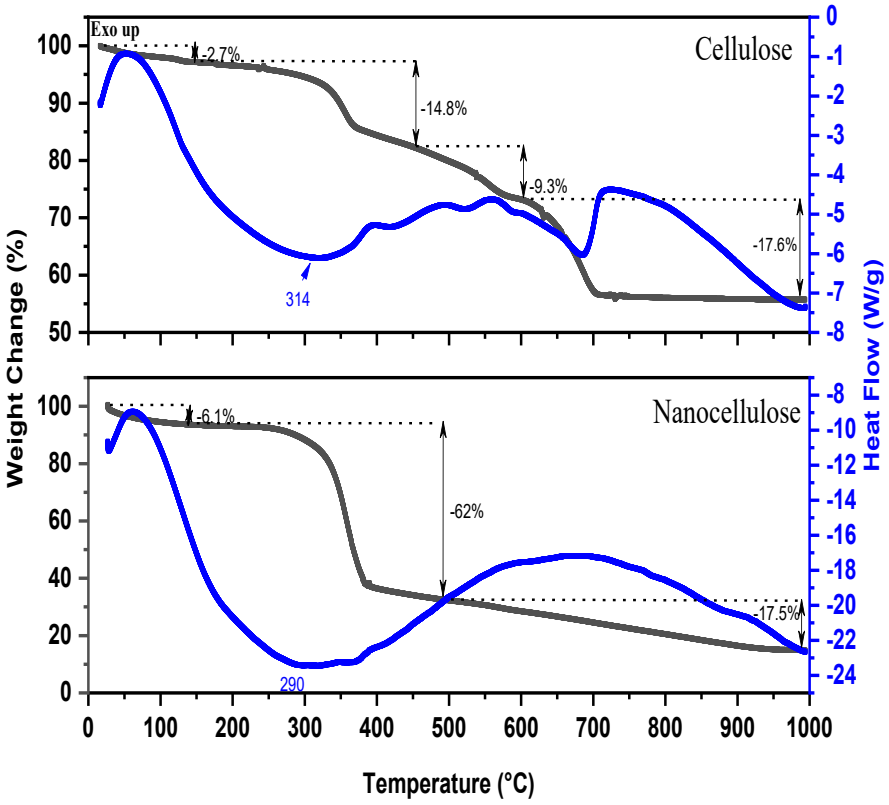


Figure III.10 TGA/DSC thermogram of cellulose and MCC isolated from the Algerian *Cystoseira stricta*.

III.1.3.4 SEM/EDX analysis

Micrographs of Cystoseira stricta extracted polysaccharides were captured using desktop SEM. The morphology of fucoidan **(Figure III-11 a)** was found to be further widespread smooth surface area overlapping with small irregular-shaped particles [56].

The elemental composition of fucoidan **(Figure III-11 b)** basically includes C (61.9%), O (27.8%) and S with a percentage weight of 6.9%. The presence of sulphur besides carbon and oxygen indicated the presence of sulphated groups that is also confirmed previously by FT-IR and

thereby revealed the success of the extraction of fucoidan. The appearance of traces of K element shall be return to the presence of residual salts ions of KI used for the elimination of CTAB. The absence of other elements such as Na is a strong indicator of the sample purity [20].

Ester sulfate content ($–SO_3^-Na+$) can be calculated on the basis of the percentage of S as follows [57]:

$$\boldsymbol{Sulfates, \% = S\% \times 3.22} \quad \textbf{(III.2)}$$

The sulfation degree (SD= moles of ($–SO_3^-Na+$) per mole of monosaccharide unit) as [58]:

$$\boldsymbol{NSS = \frac{C\%/12}{S\%/32}/6} \quad \textbf{(III.3)}$$

$$\boldsymbol{SD = 1/NSS} \quad \textbf{(III.4)}$$

Where NSS is the number of sulfate esters per monosaccharide, 12 and 32 are the atomic weights of carbon and sulfur, respectively, and 6 is the number of carbon atoms in a sugar monomer assuming that all monomers in the polymer are hexoses [59].

Our findings fell within the range of values reported in the literature which are summarized in **Table III.4**. The sulfate content and sulfation degree depend to the species, the seasonal variation, area of growth, harvesting period and the technique of extraction used [60].

Table III.4 Fucoidan content, sulfate content and sulfation degree of different species

Species	Harvesting site	Fucoidan content %	Sulfates %	SD	Reference
Cystoseira barbata	Kerkennah island (Sfax, Tunisia)	5.45±0.51	22.51	0.79	[14]
Cystoseira compressa	Kerkennah island (Sfax, Tunisia)	5.2±0.45	14.65		[33]
Cystoseira schiffneri	Kerkennah island (Sfax, Tunisia)	2.2±0.03	7.8		[20]
Saccharina latissimi	Seaweed Solutions farm (Frøya, Norway)		24.7	1.2	[61]
Alaria esculenta			8.3	0.6	
Fucus vesiculosus	Marinova Pty Ltd (Tasmania, Australia)		23.7	0.44	[60]
Cystoseira stricta	Stidia Algerian coast	4.66±0.49	22.2	0.25	This work

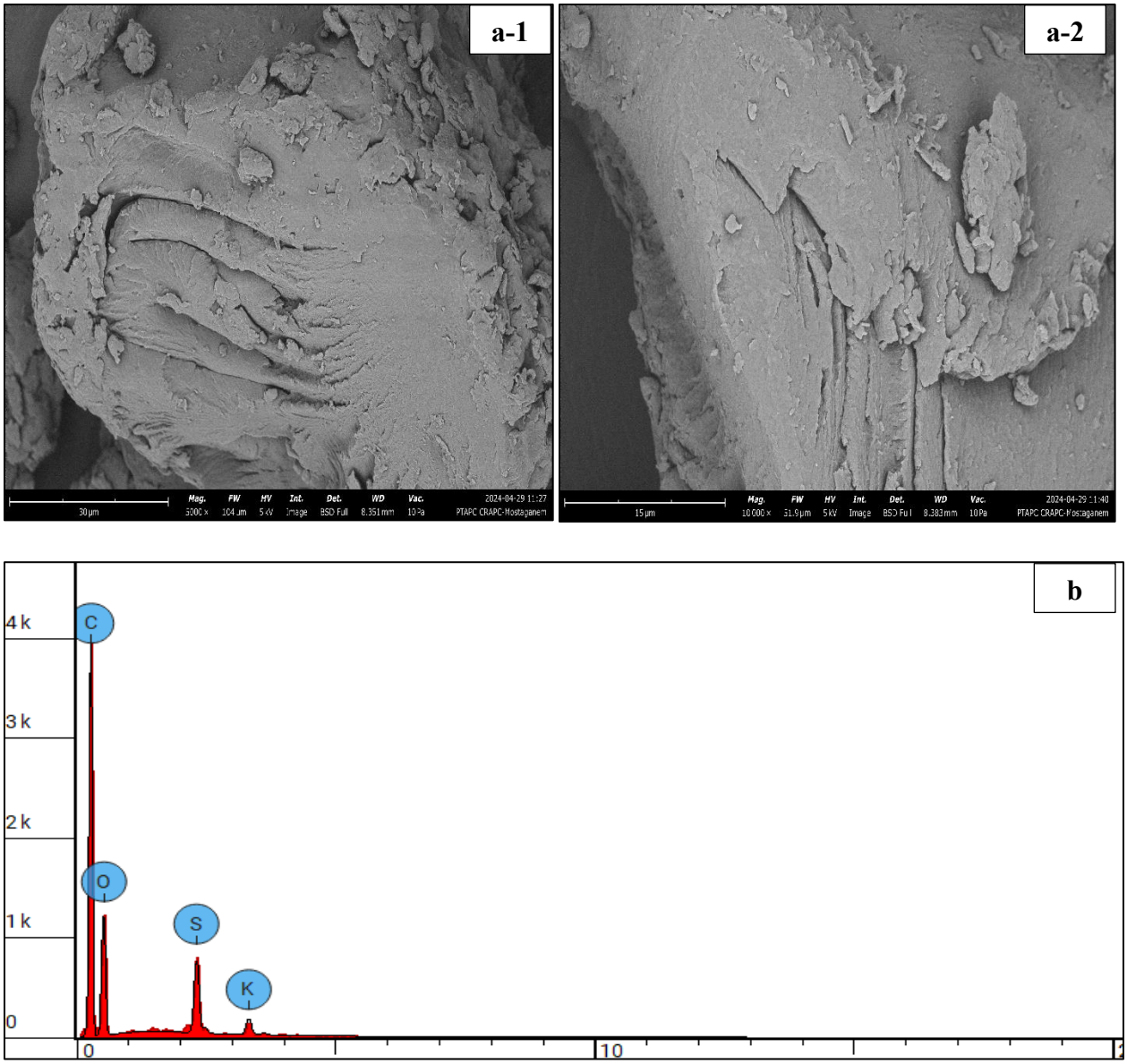


Figure III.11 SEM images of fucoidan **(a-1)** at 30 µm and **(a-2)** 15µm magnifications, **(b)** Chemical composition.

The SEM analysis of native alginate **(Figure III.12)** revealed a rough surface with visible voids. At higher magnifications, different alignments of thin and small-sized rods were observed distributed homogenously at the surface. The surface of sodium alginate (HO-alg) contained C, O and Na atoms in different proportions with no characteristic peaks of impurities.

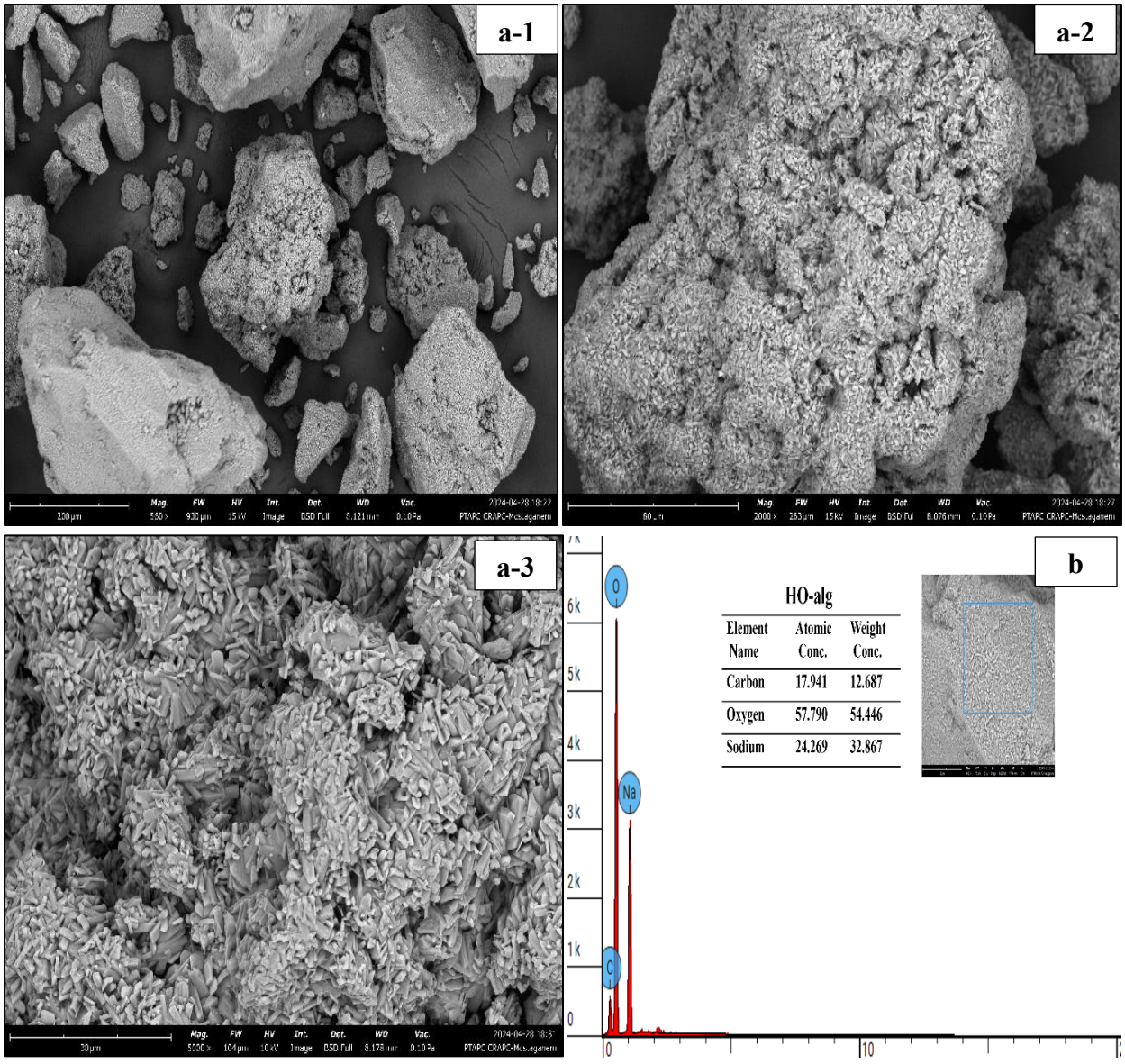


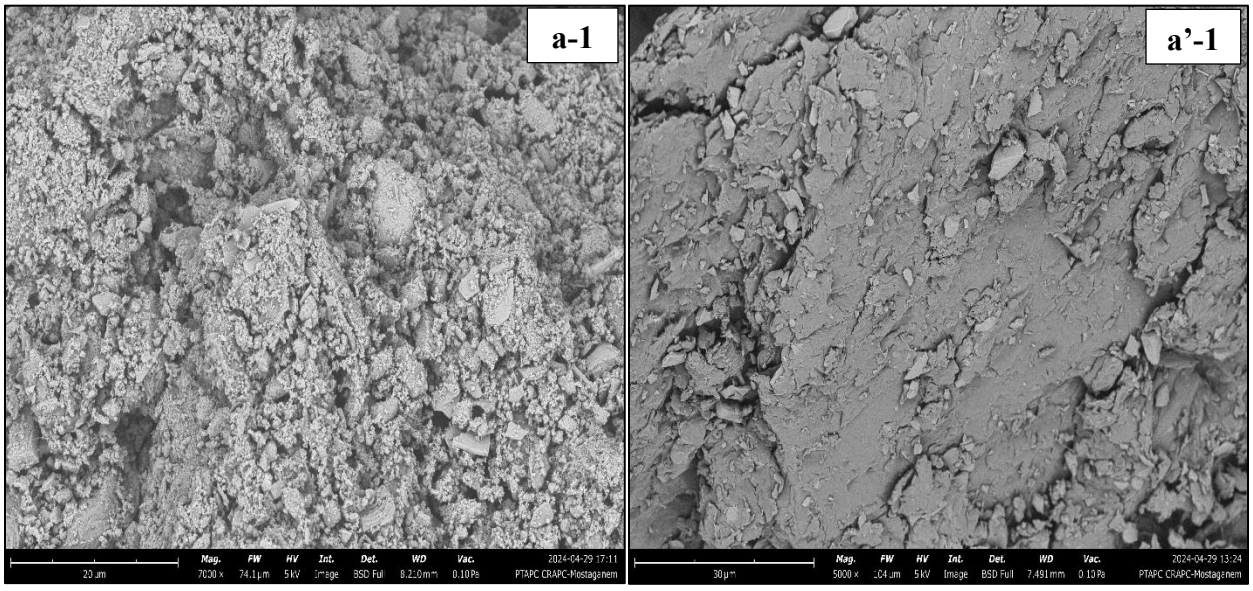
Figure III.12 SEM images of sodium alginate **(a-1)** at 200 µm, **(a-2)** at 80 µm and **(a-3)** at 30 µm magnifications, **(b)** Chemical composition.

The SEM images of cellulose are depicted in **Figure III.13 a**. Cellulosic fibres were detected distributing among the amorphous phase of cellulose and other residues (as demonstrated by EDX). During acidic hydrolysis process, hydronium ions penetrated the cellulose's internal structure. This led to the elimination of the weak amorphous region of cellulose. This latter underwent partial depolymerisation and subsequently the formation of fibril-like MCC which are marked with arrows in **Figure III.13 a'-2** [37]. Hamouda et al. [62] also found that MCC extracted

from *Ulva lactuca* comprises filaments. Slab-like patterns were also recognized which further reflected the aggregation of cellulose fibrils [63].

The microanalysis of cellulose showed that it was mainly composed of carbon (18.96%) and oxygen (39.62%) **(Figure III.13 b)**. the presence of Ca may return to the presence of residual salts ions of calcium chloride used for the precipitation of alginate in the first step of extraction process.

Few concentration of silicon, aluminium and magnesium were detected in cellulose which are left over from the algae as previously described in other papers [63], [64]. In counterpart, only carbon (54%) and oxygen (46%) have been detected in MCC **(Figure III.13 b')** which further confirms the purity of the sample. This outcome supported the results obtained by DSC where it was found that impurities were eliminated after acid hydrolysis. The difference in the amount of these two main elements between cellulose and MCC shall be attributed to the removal of amorphous residues [65].



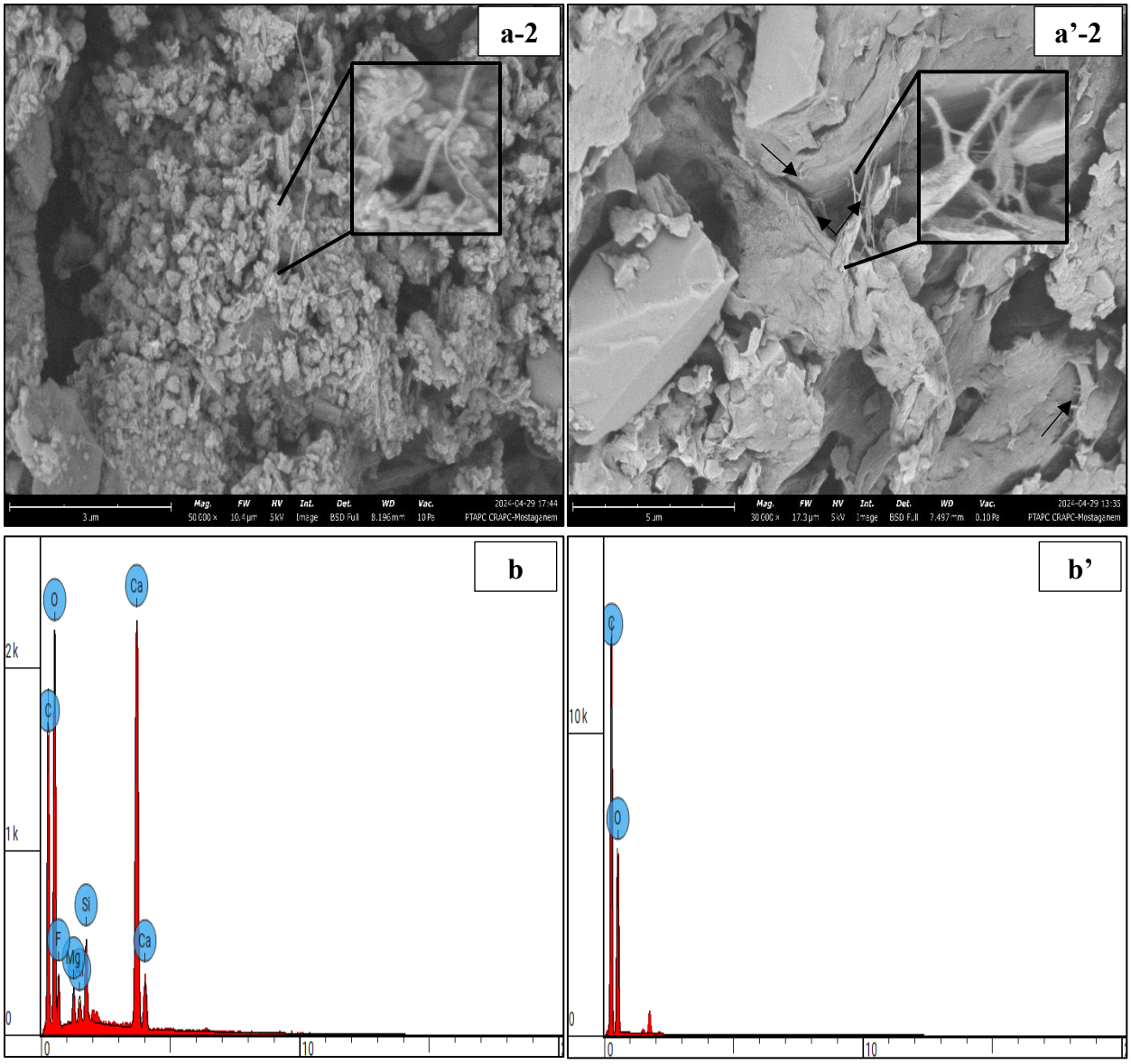
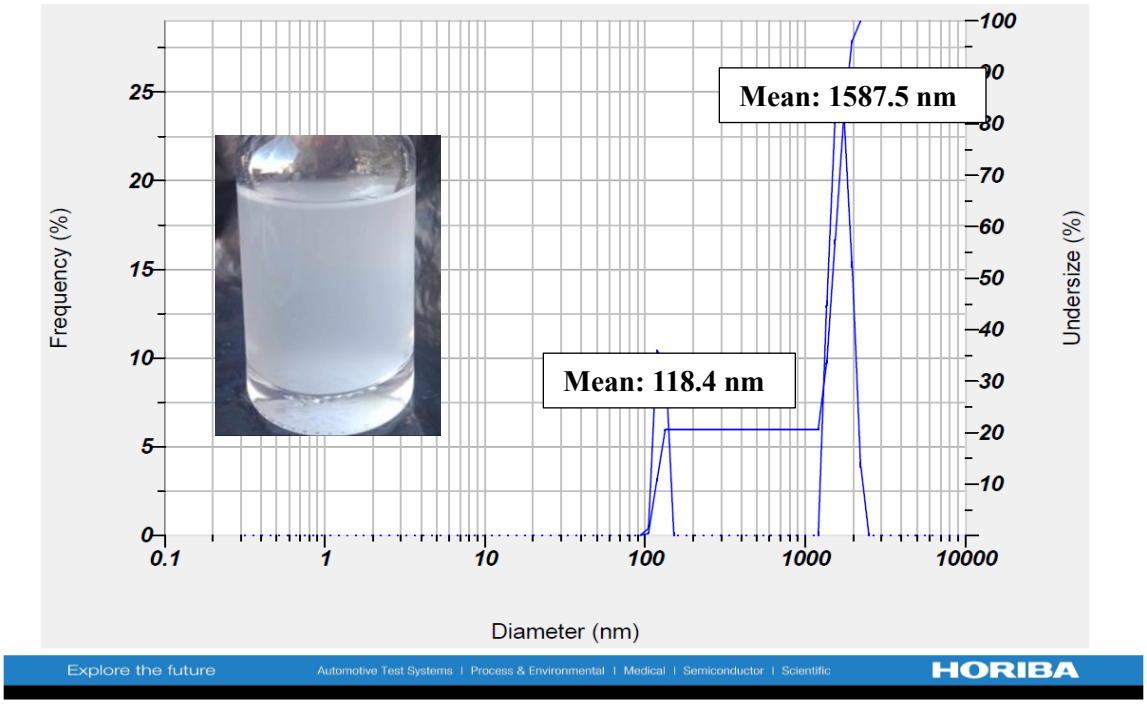


Figure III.13 SEM images of cellulose **(a-1)** at 20 µm, **(a-2)** at 3 µm and MCC **(a'-1)** at 30 µm and **(a'-2)** 5µm magnification, **(b and b')** their chemical composition respectively.

III.1.3.5 DLS analysis

The mean particle size and zeta potential of 1% MCC aqueous suspension were measured. A zeta potential higher than 30 mV or lower than -30mV is indicative of adequate stability of the system as mentioned in [66]. Hence, the sample has lower tendency to flocculation and aggregation. Z- average was 826.3 nm and the zeta potential was -40.7 mV indicating the stability of MCC particles.



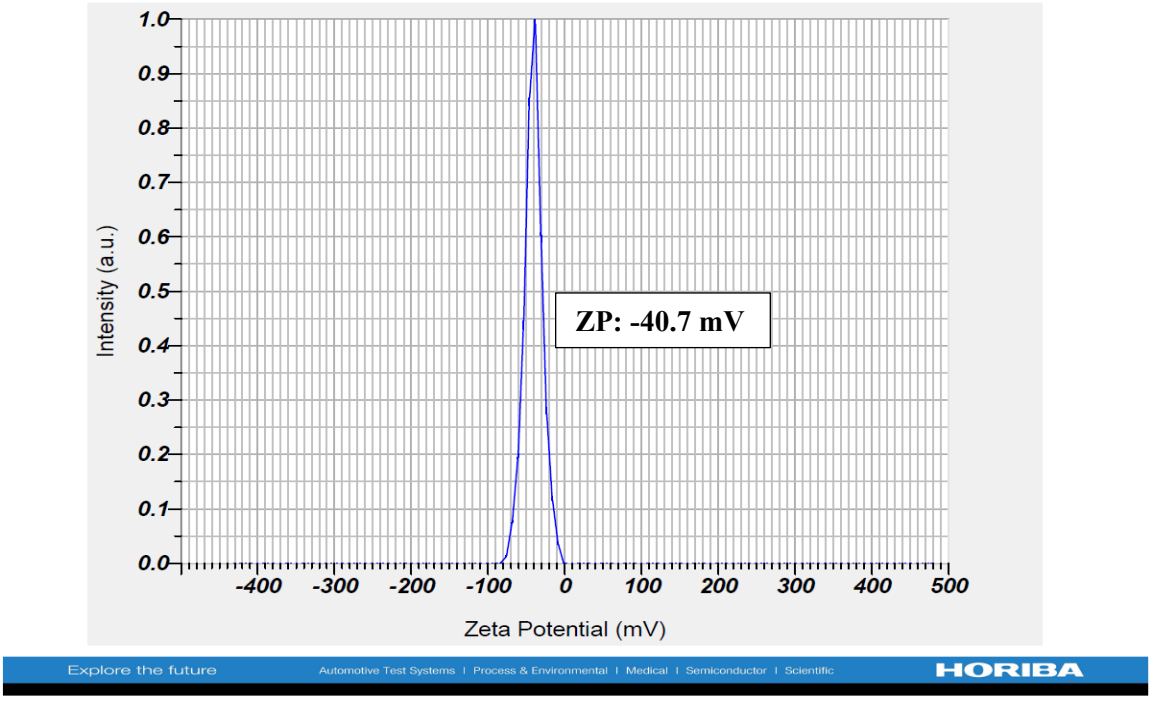


Figure III.14 DLS analysis of 1% MCC suspension.

III.1.4 Antibacterial activity

The screening of the antibacterial activity of the four extracts against Gram- bacteria (*Escherichia coli*) and Gram+ bacteria (*Staphylococcus aureus*) was carried out. The results were registered through zone of inhibition diameter on the plates and they are displayed in **Table III.5**.

Fucoidan (F) has shown a promising effect against *S.aureus* and *E.coli* **(Figure III.15)** where the maximum effect was registered at a concentration of 10 mg/mL and 20 mg/mL against *E.coli* and *S.aureus* respectively. It was demonstrated in the work of Yunhai et al. [67] that fucoidan extracted from *Ascophyllum nodosum* and *Laminaria digitata* cannot inhibit *E.coli* even at higher concentrations. But, fucoidan solutions at 25mg/mL has shown inhibitory effect against *S.aureus*. In contrast to the findings of Habibi et al. [25], important inhibitory effect of fucoidan from *Laminaria japonica* against *E.coli* was achieved at the concentration interval between 1.25 and 20 mg/ml while this latter has not shown any effect against *S.aureus*.

Sodium alginate (N) has shown a weak inherent antibacterial activity **(Figure III.16)**. This finding was in line with the literature [68].

High concentration of cellulose (C) suspension exhibited significant inhibition effects on both strains, and which were clearly inhibited by the MCC (MC) suspensions at all concentrations **(Figure III.17)**. This outcome supports the results obtained by El-Sheekh et al. [63] who found that cellulose and especially MCC obtained from the algal biomass *Ulva lactuca* showed great potential as antimicrobial which achieves tremendous challenges against Gram+ bacterium like *Staphylococcus aureus* (ATCC6538), and Gram-negative bacterium such as *Escherichia coli* (ATCC25922). Cellulose and MCC derived from macroalgae has gained more attention due to its many proposed advantages over cellulose derived from land-based biomass, which is more suited for biological applications [69].

Table III.5 Inhibition zone values of extracted polysaccharides.

Sample	Code	Diameters of inhibition zones (mm)	
		Staphylococcus aureus	***Escherichia coli***
Fucoidan	F_1	7	-
	F_{10}	9	16
	F_{20}	11	-
Sodium alginate	N_1	-	-
	N_{10}	6	-
	N_{20}	7	-
Cellulose	C_1	-	10
	C_5	-	13

	C_{10}	8	15
MCC	MC_1	11	6
	MC_5	10	6
	MC_{10}	9	6
Positive control	CL 30µg	6	6
	GEN 10µg	22	33

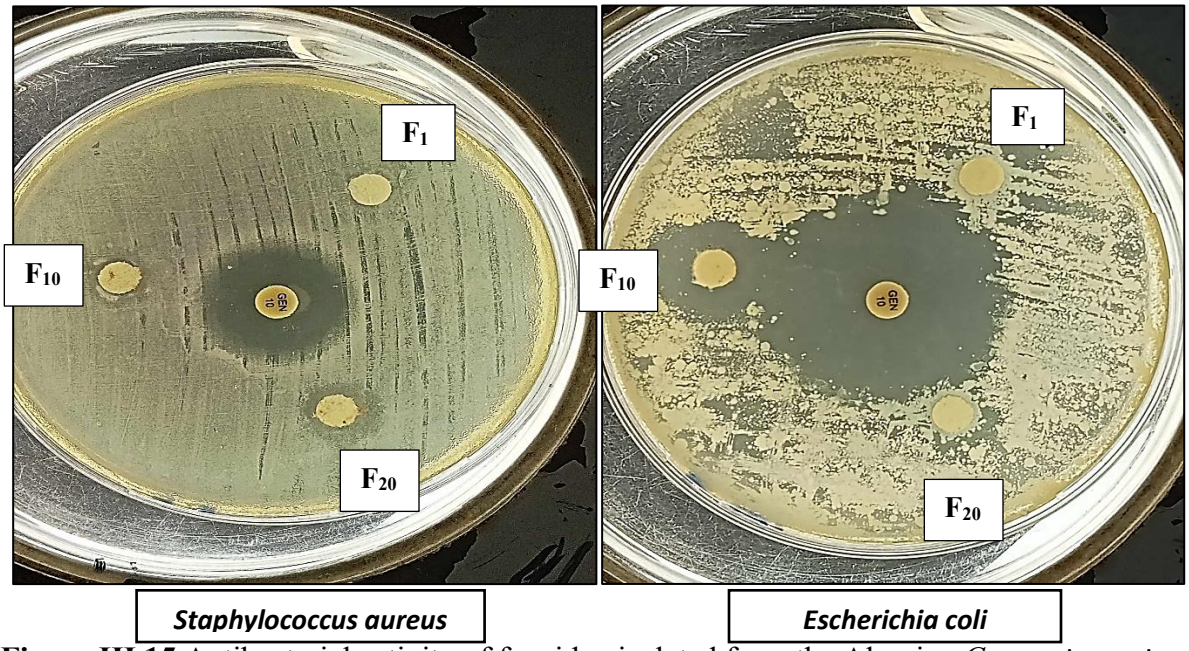


Figure III.15 Antibacterial activity of fucoidan isolated from the Algerian *Cystoseira stricta*.

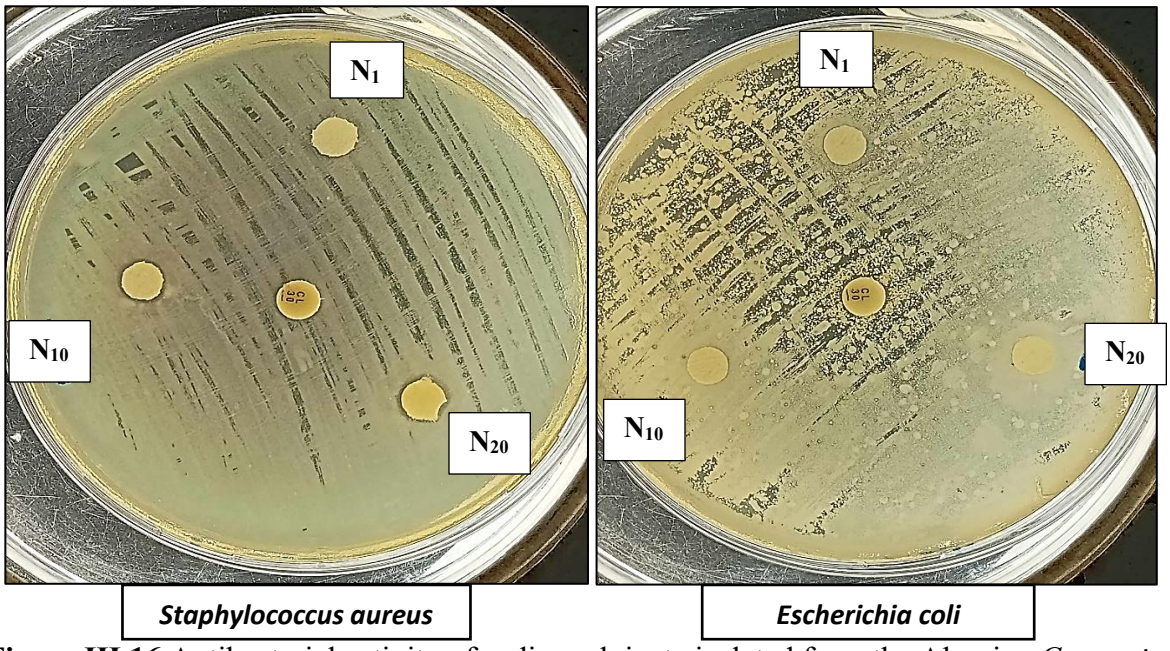


Figure III.16 Antibacterial activity of sodium alginate isolated from the Algerian *Cystoseira stricta.*

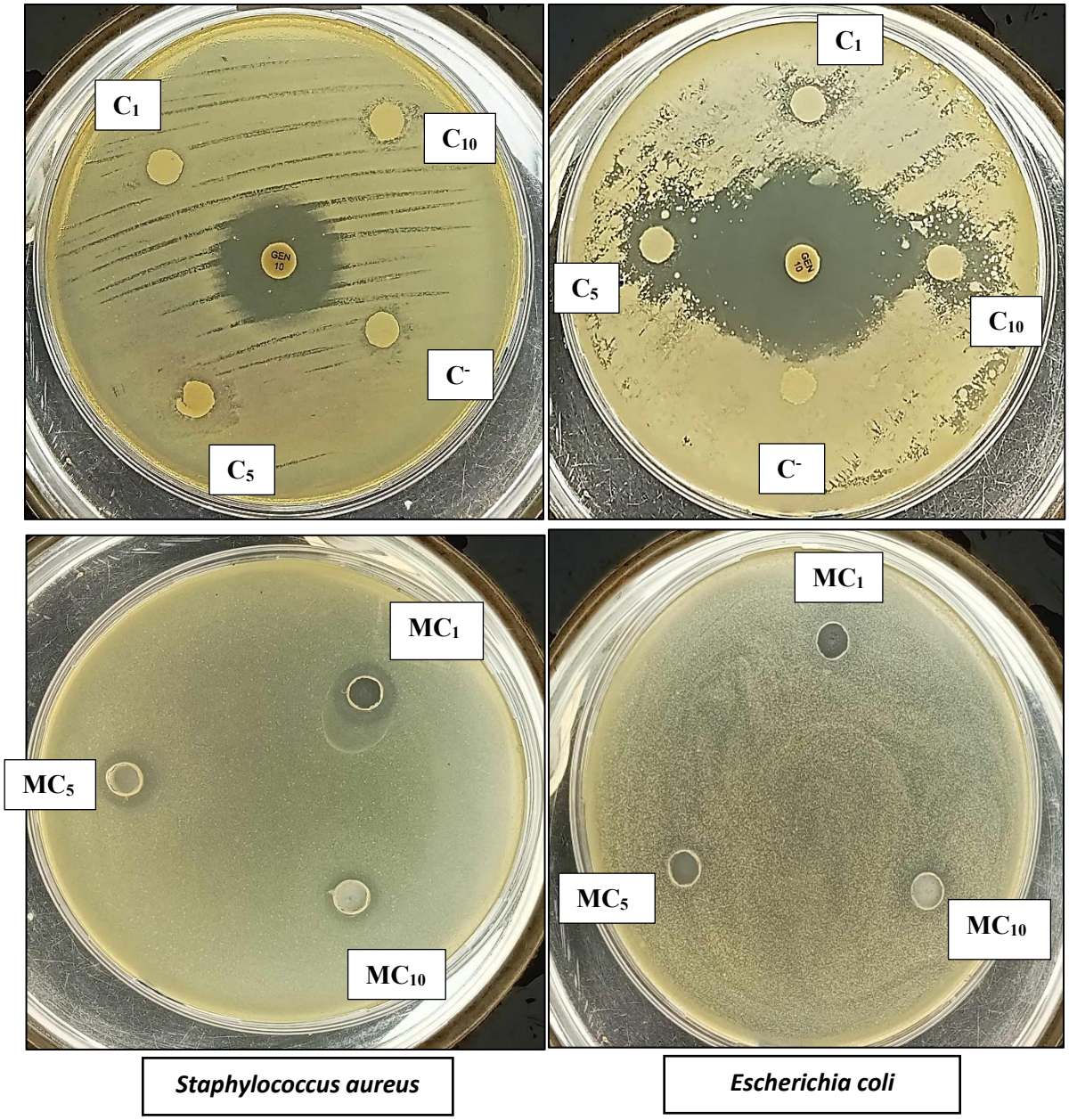


Figure III.17 Antibacterial activity of cellulose and MCC isolated from the Algerian *Cystoseira stricta.*

III.1.5 Conclusion

The content of ash, moisture and polysaccharides extracted from Cystoseira stricta species has been discussed for the first time. It was found that higher content of ash was measured during Summer and the moisture content was almost equal between Summer and Winter. The optimum sample particle size was found to be 150µm. S/L ratio of 1:30 has led to significant higher

percentage yield of sodium alginate. Further, the extraction yield of sodium alginate and fucoidan with sulphate content that have found in this study were among the highest values reported in the literature for Cystoseira species in the mediterranean coast. For fucoidan and cellulose, the change of S/L doesn't affect remarkably the extraction yield. Compared to harvesting in February, the content in fucoidan and alginate extracted from algae harvested in September have been decreased. Contrary to cellulose, it has been extracted significantly more cellulose in September than February. The characterization by FT-IR, XRD, TGA, DSC, SEM/EDX and DLS confirmed the identity and properties of the obtained products. Fucoidan, cellulose and MCC have given a promising antibacterial effect against *S. aureus* and *E. coli* whereas, sodium alginate has shown a weak inherent antibacterial activity.

Section 2

Elaboration of Alginate-Based Materials

The outcomes concerning the chemical modification of sodium alginate, preparation of alginate-based hydrogel and coating with their characterization and study of their biological activities are discussed in this section.

III.2 Elaboration of Alginate-Based Materials

III.2.1 Sodium alginate modification

The extracted sodium alginate has been chemically modified by maleic anhydride to get new product with enhanced properties. As the final colour of extracted sodium alginate is brown, it was found the maleation can noticeably improve the product aesthetic **(Figure III.18)**. This allows avoiding the utilization of toxic reagents, such as formaldehyde, in bleaching step during the extraction process which can influence badly regarding the rheological and physicochemical properties of alginate [15].



Figure III.18 Physical appearance of (a) crude and (b) modified sodium alginate.

III.2.1.1 Characterization

III.2.1.1.1 FT-IR analysis

Figure III.19 show that the characteristic absorption peaks of sodium alginate still exist after modification, with the appearance of new band at 1560 cm^{-1} assigned to maleic anhydride (MA) double bond. Two stretching vibration bands of ester carbonyl appeared near 1686 cm^{-1} and maleic carboxyl C=O bond at 1626 cm^{-1} overlapped with C=O stretching band of alginate. This is an indication of the successful MA grafting into sodium alginate chains.

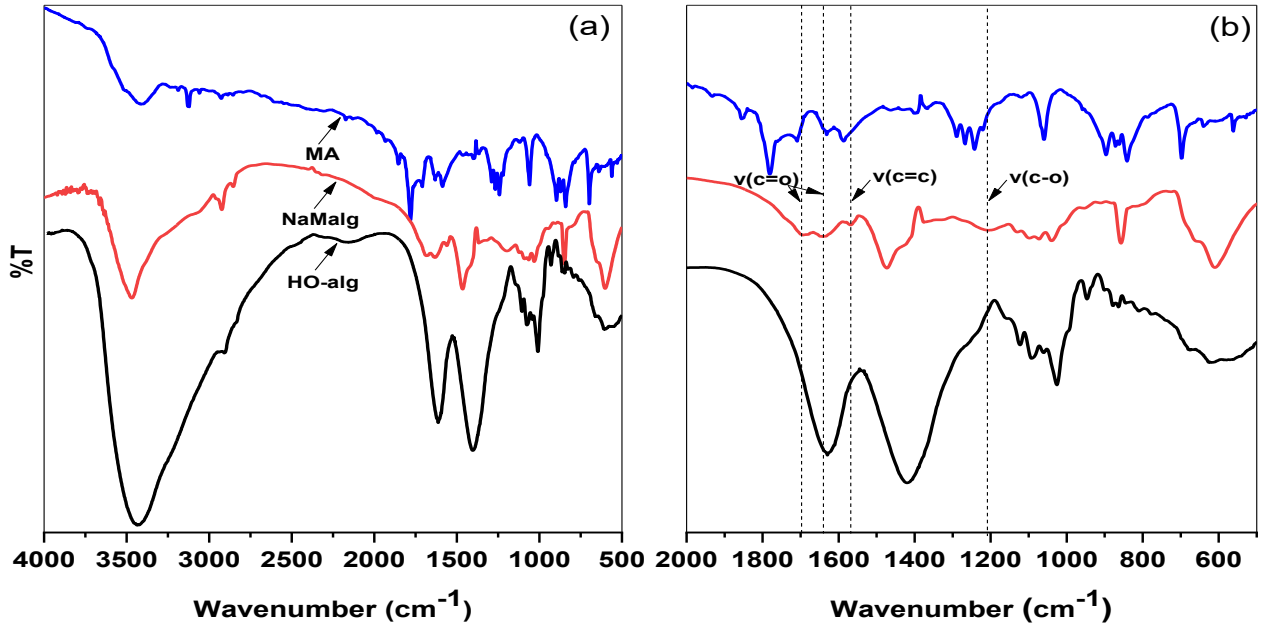


Figure III.19 (a) FT-IR spectra of maleic anhydride, crude and maleated sodium alginate, **(b)** zoom of the 2000-500 cm^{-1} region**.**

III.2.1.1.2 XRD analysis

The chemical modification induced a slight increase in the intensity of the characteristic peaks and they became slightly broader with maintaining the general pattern of pure alginate **(Figure III.20)**. Similar remarks were derived by Chen et al. [70] about crystal structures of alginate derivatives obtained through esterification modification.

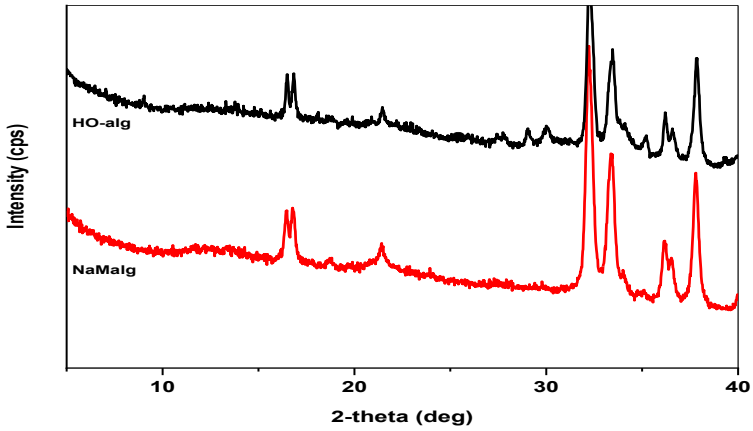


Figure III.20 XRD patterns of native and modified sodium alginate.

III.2.1.1.3 TGA/DSC analysis

The TGA and DSC thermograms of modified and unmodified extracted sodium alginate are depicted in **Figure III.21**. By plotting the differentiate of TGA curves, we noticed three stages. The first one is between 50 and 170°C attributed to non-bonded then adsorbed water molecules evaporation. The second stage corresponded to polymer chain degradation at 254 °C (modified) and 245°C (native) and liberation of intermediates substances. The later showed degradation curves from 300 up to 1000°C. The temperatures of 50% weight loss were 417°C (modified) and 732°C (native). These findings corresponded well with the values ranges previously mentioned in the work of Benslima et al. [22]. The DSC curves revealed clearly the thermal phase transitions occurring within samples. The first endothermic peak in the HO-alg curve is mainly caused by water evaporation overlapping with the glass transition phase (around 100°C). A second endothermic peak followed by an exothermic peak at 245°C, indicated a thermal decomposition process of native alginate [71]. Concerning the NaMalg curve, there is an increasing in the glass transition temperature with no obvious endothermic peak around 140°C, indicating the improvement of the thermal stability of alginate within this stage after modification [72]. The exothermic peak was shifted to a higher temperature after modification with MA.

This temperature increasing confirmed the sodium alginate chain modification. Madhusudana Rao et al.[73] also demonstrated that the exothermic peak temperature increased after grafting poly(vinyl caprolactam) onto sodium alginate chains.

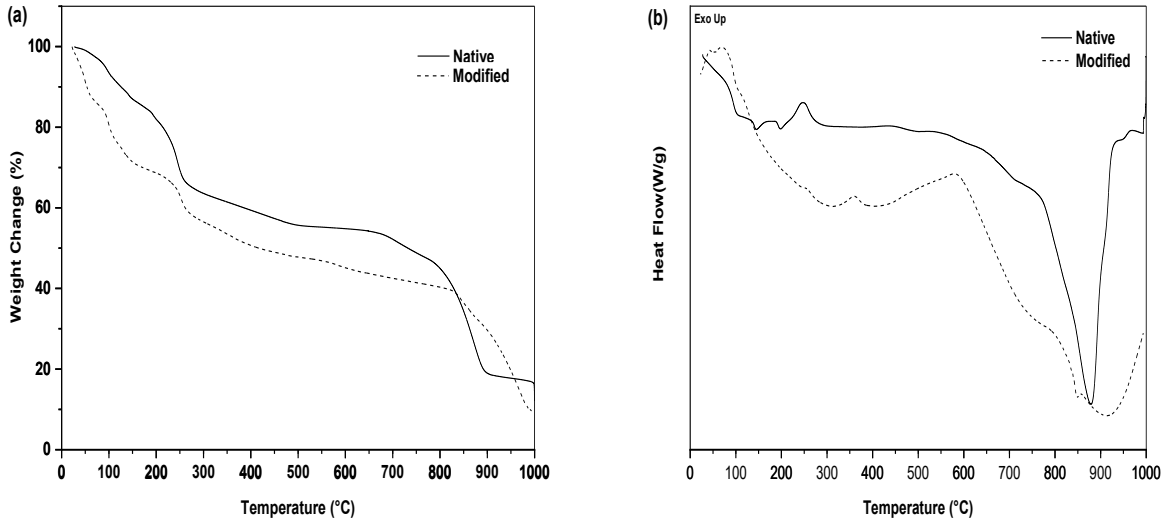


Figure III.21 (a) TGA and **(b)** DSC curves of native and modified sodium alginate.

III.2.1.1.4 SEM/EDX analysis

Functionalization of alginate with MA resulted in a morphology change characterized by the presence of several bundles of parallel rods **(Figure III.22 a)**. These later became thicker and greater, compared to HO-alg, which can be attributed to the covalent bonding of maleic anhydride resulting in the modification of internal polymeric chain order of sodium alginate. The surface of NaMalg **(Figure III.22 b)** contained C, O and Na atoms in different proportions with no characteristic peaks of impurities such as heavy metals (Arsenic, lead).

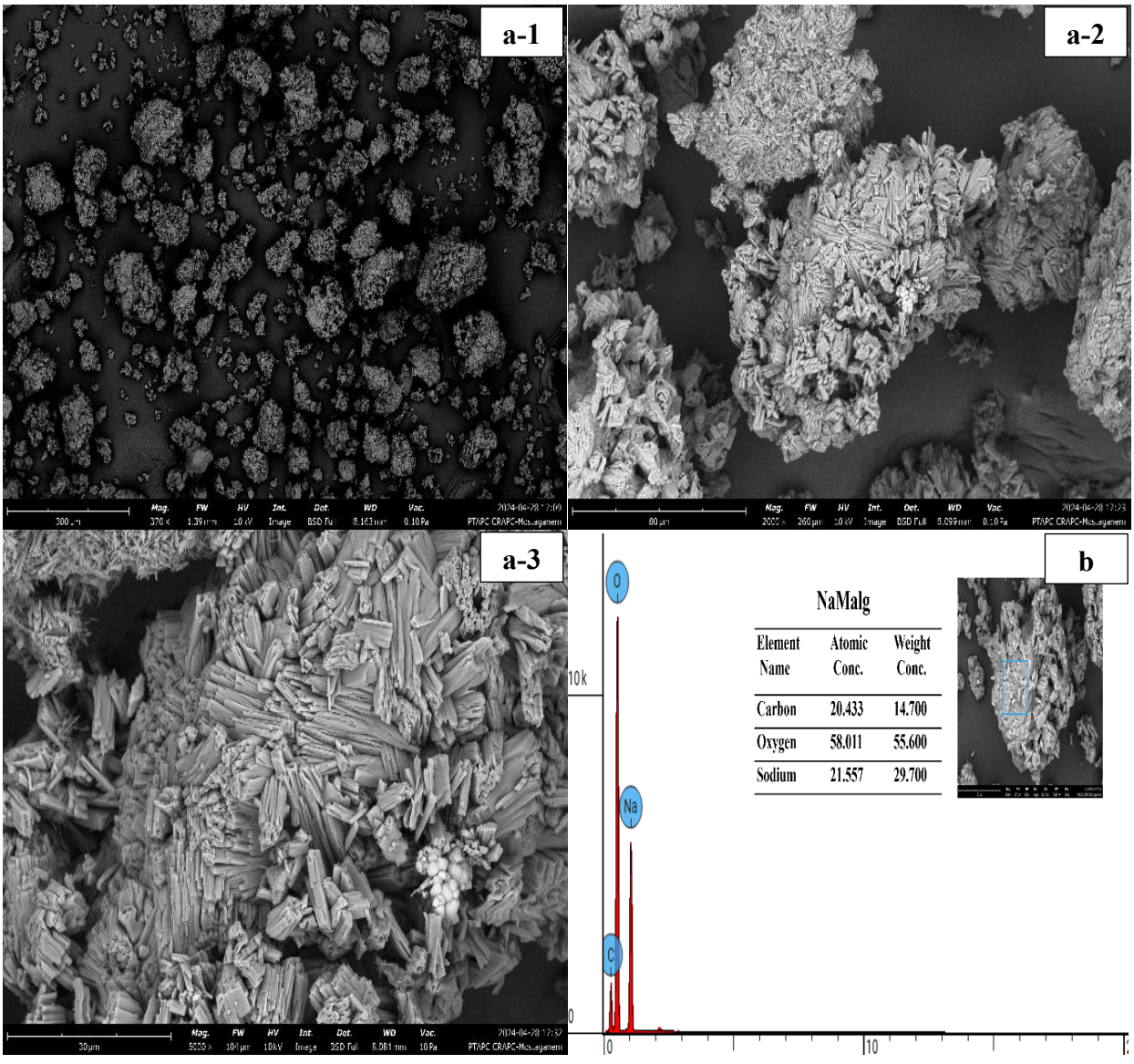


Figure III.22 SEM images of modified alginate (NaMalg) **(a-1)** at 300 µm, **(a-2)** at 80 µm and **(a-3)** at 30 µm magnifications, **(b)** chemical composition.

III.2.1.2 Determination of the degree of substitution

The DS value of the maleated alginate was found to be 0.9297±0.33. This implies that almost 93% of the hydroxyl groups present in the polysaccharide have undergone esterification reaction with maleic anhydride. The synthesis of maleic anhydride esterified sodium alginate has not been previously reported prior to this work. However, maleic anhydride was used for the modification of other polysaccharides such as corn starch [74], cellulose [75], pectin [76] and κ-Carrageenan [77]. The DS has reached 0.3386, 0.38, 0.6657 and 0.032, respectively.

III.2.1.3 Antioxidant activity test

The scavenging activity of DPPH radical is among the frequent methods used for the first screen of the antioxidant properties of polysaccharides because of its simplicity, low cost, and rapid outcomes [78]. In the present study, both native and modified sodium alginate were assessed for their DPPH scavenging ability. **Figure III.23** represents optical images of DPPH solutions showing colour graduation change with the increasing of the sample concentration. The native sodium alginate recorded a very high IC_{50} value (223.95 mg/ml) indicating its very weak DPPH antioxidant activity. The low M/G ratio (0.80) of the unmodified sodium alginate could influence negatively the DPPH antioxidant activity. As reported by Bai et al. [79], the antioxidant properties of polysaccharides are significantly affected by their proportion of monosaccharide components. The fraction with higher M/G has more potent antioxidant activity [80]. Maleic anhydride esterification of sodium alginate significantly reduced the IC_{50} to 55.6 mg/ml ($p < 0.001$), confirming its favourable effect on increasing the DPPH antioxidant activity of the NaMalg polymer. Similarly, Xiong et al. [81] found that grafting maleic anhydride onto xanthan oligosaccharides enhanced their DPPH radical-scavenging activity.

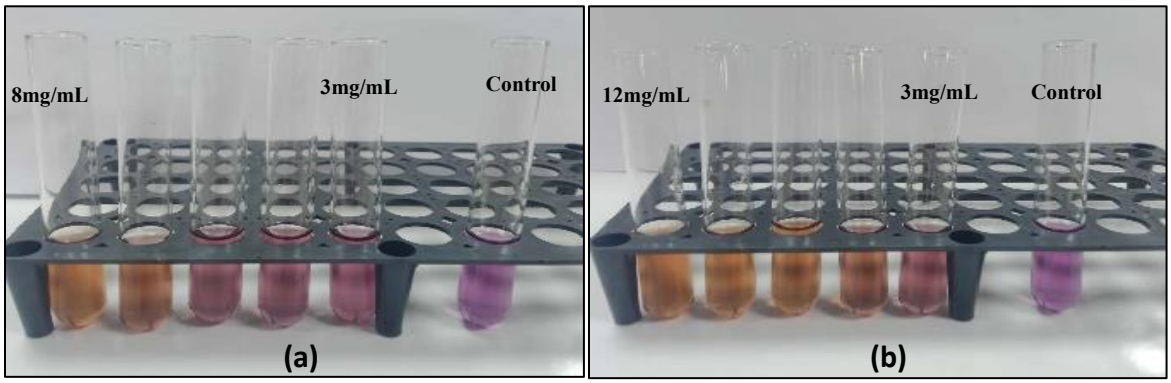


Figure III.23 Antioxidant scavenging of **(a)** HO-alg and **(b)** NaMalg.

III.2.2 Protective effect evaluation of maleated sodium alginate-date seed oil-based oil-in-water nanoemulsion

Nowadays, edible coatings are used as a strategy to preserve the postharvest quality of many fresh fruits and vegetables and extend their shelf life [82]. Polysaccharides are among the biomolecules being recently used as a sustainable material in coatings [83]. As polysaccharides, the alginate has good gas and mechanical barrier properties, however, its hydrophilic nature makes it a poor moisture barrier [84]. The objective was to assess the effect of grafting sodium alginate with maleic anhydride on the efficiency of nanoemulsion on strawberry preservation. The nanoemulsion was assessed for its dimensions and physical stability using DLS. The outcomes are reported in **Table III.6**. The zeta potential of about ±30 mV is indicative of adequate stability of the system as mentioned by Honary and Zahir [66].

Table III.6 Characteristics of maleated sodium alginate-date seed oil-based nanoemulsion.

Peak no.	S.P. area ratio	Mean particle diameter (nm)	S.D	Z average (nm)	PI	Mean zeta potential (mV) at 25°C
1	0.51	191	37.9	461.8	0.546	-29.9
2	0.49	1413.7	286.4			

PI: polydispersity index, SD: standard deviation.

The results of nanoemulsion protective effect on strawberries are shown in **Figure III.24**. The uncoated samples developed spoilage on their surface within only 5 days, and lost water as were totally covered by mold at the sixth day of storage at room temperature. Meanwhile, there was no change of the texture of the coated samples with the maleated sodium alginate-date seed oil nanoemulsion till the 11th day, whereas, the sample coated with sodium alginate-date seed oil nanoemulsion displayed a noticeable deterioration starting already at the fifth day. The incorporation of maleic anhydride as hydrophobic group contributed to the delaying of strawberries' spoilage. In this regard, Sousa et al. [85] reported that incorporating anhydrides in the molecular chain of chitosan has been shown to provide better antimicrobial properties. Besides, the nano-sized oil droplets dispersed in the alginate network provided a hydrophobic barrier that reduces moisture loss from the fruit surface. This kept fruit freshness, reduced textural changes and expended shelf- life. Those results are in agreement with the results of Santos et al.[86] which

indicated that the coating of fruits and seeds with a system of nanoparticles based on alginate associated with essential and vegetable oils inhibited the growth of microorganisms and delayed the fruit maturation.

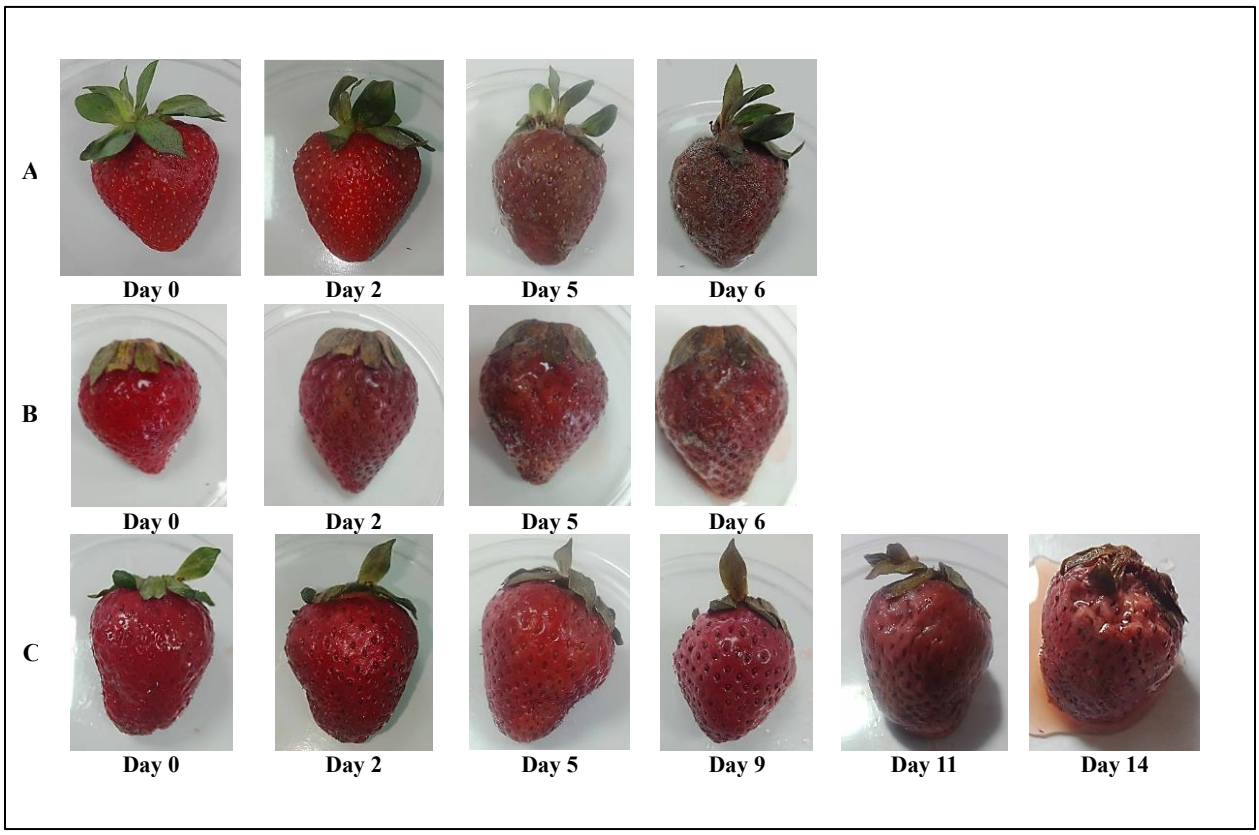


Figure III.24. Nanoemulsion coating effect on strawberries over the time at room temperature (**(a)** uncoated strawberries; **(b)** coated strawberries with sodium alginate-based nanoemulsion; **(c)** coated strawberries with maleated sodium alginate-based nanoemulsion).

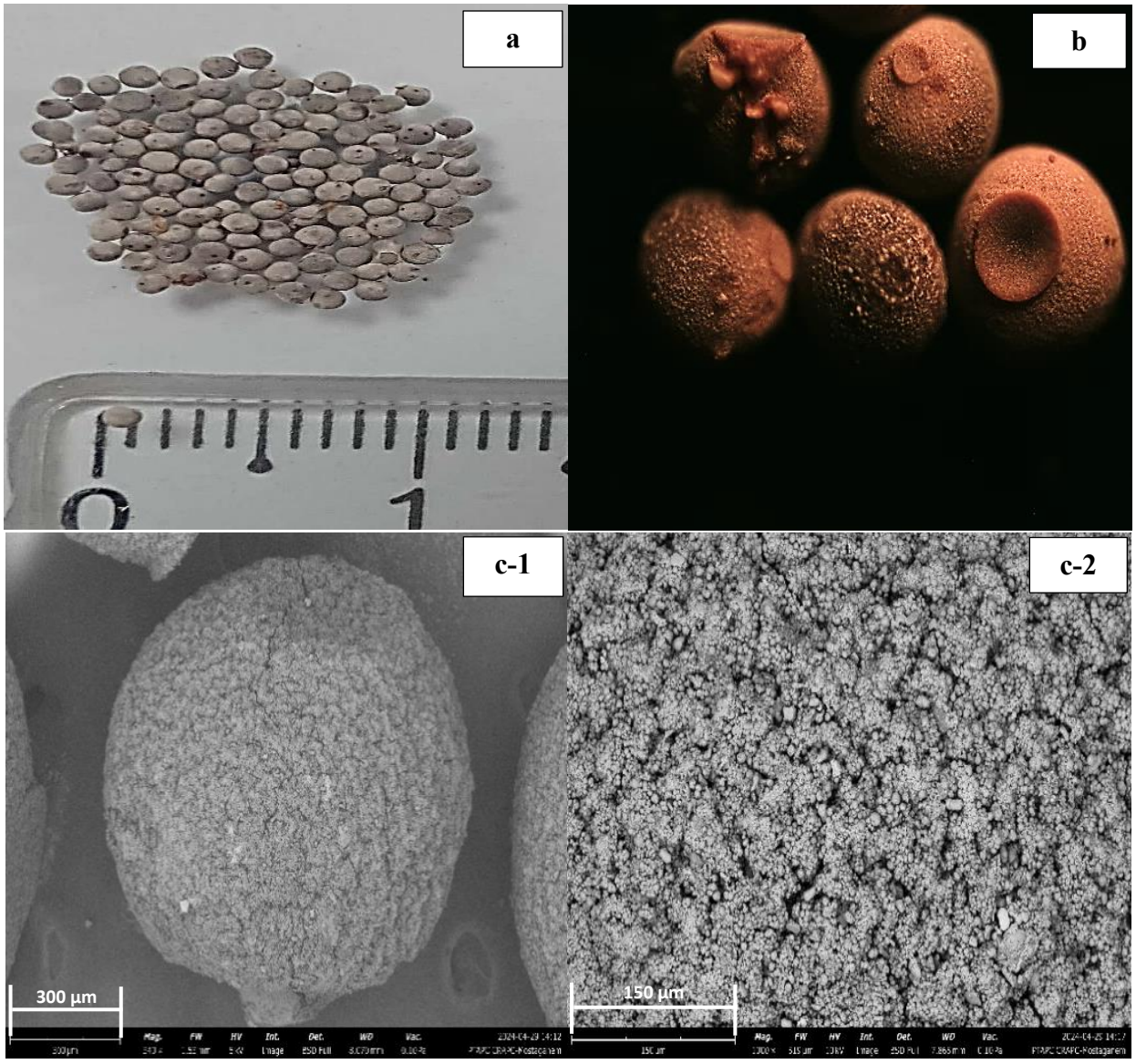
III.2.3 Cephalexin-loaded hydrogel beads preparation

III.2.3.1 Characterization

III.2.3.1.1 Shape, morphology and size measurement

Digital photos and images of dry cephalexin loaded alginate beads under optical microscope and scanning electron microscope are depicted in **Figure III.25 a,b and c**. The synthesized beads are nearly spherical in shape with slight distortions. This was suggested to be due to the pressure caused by the other beads during crosslinking stage [87]. At higher magnifications, the surface

seemed to be uneven and lumpy with some cavities created during water evaporation but no drug crystals were observed, indicating their well dispersion in the alginate matrix [88]. The mean size of free cephalexin hydrogel beads was estimated to be 1.015±0.06 mm and it decreased in the presence of cephalexin to 0.807±0.097 mm. This decrease might occur because of the junctions established between the coating materials and the drug [89].



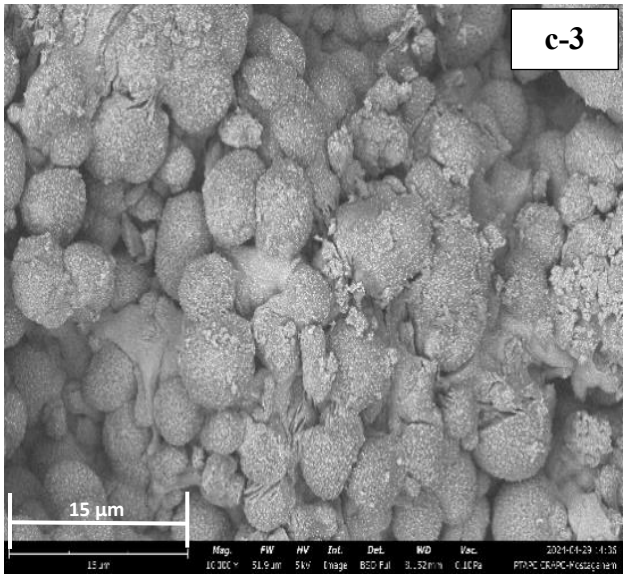


Figure III.25 (a) Digital images, **(b)** optical microscope images and **(c1-c3)** scanning electron microscope images of cephalexin loaded hydrogel beads at magnifications of ×340, ×1k and ×10k respectively.

III.2.3.1.2 FT-IR analysis

The FTIR spectra of extracted sodium alginate, cephalexin, cephalexin-loaded alginate beads and cephalexin-free alginate beads are shown in **Figure III.26**.

The CSMS's spectrum shows new bands in comparison with the spectra of CSSA and blank beads. Bands are observed at 3501cm^{-1}, 3368 cm^{-1}, 2515 cm^{-1}, 1728 cm^{-1} and 874 cm^{-1} which could be attributed to hydroxyl, aromatic C-H, β lactam C=O stretch and C-S stretching of cephalexin respectively. The symmetric and asymmetric stretching bands of carboxylate (COO-) have shifted to 1429 cm^{-1} and 1623 cm^{-1}. The shifting of absorbance bands is indicator of crosslinking reaction produced by ionic interaction between -COO^{-} groups and divalent calcium ions Ca^{2+}.[22] This interaction affects the electron distribution of polymer's group so the molecular environment changed. As consequence, the vibrational energy levels changed [90]. This indicate the successful cephalexin entrapment into the calcium alginate beads.

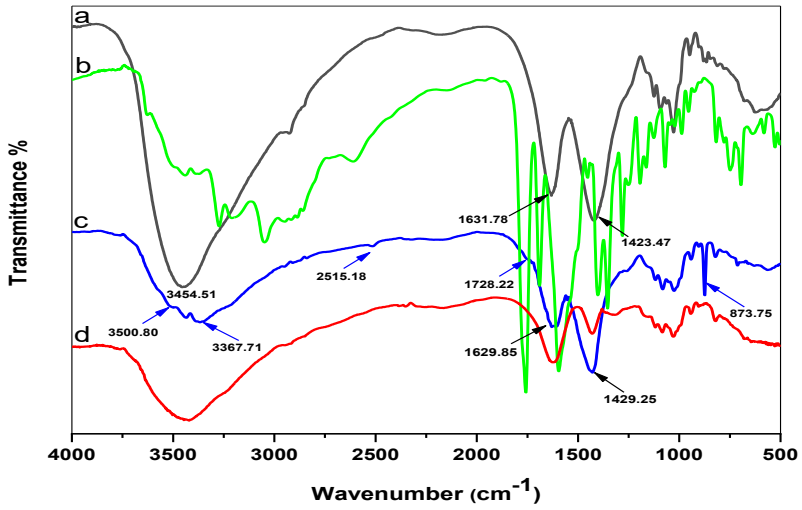


Figure III.26 FT-IR spectra of (a) sodium alginate, (b) cephalexin, (c) cephalexin loaded beads, (d) cephalexin-free beads.

III.2.3.1.3 DSC analysis

The DSC thermograms of pure sodium alginate and encapsulated cephalexin are provided in **Figure III.27**. The curve of CSSA show an endothermic peak at around 103°C can be attributed to the evaporation of entrapped water molecules. The exothermic peak at around 247°C was related to sodium alginate decomposition. This peak was shifted to 296°C in the thermogram of crosslinked alginate beads which tended to be more thermally stable than sodium alginate polymer [87]. The appearance of a small endotherm around 196°C reflects the presence of cephalexin in the beads with no sharp melting peak confirmed the efficient drug loading inside the matrix. Thus, confirmed the chemical compatibility of all component as cited in [91].

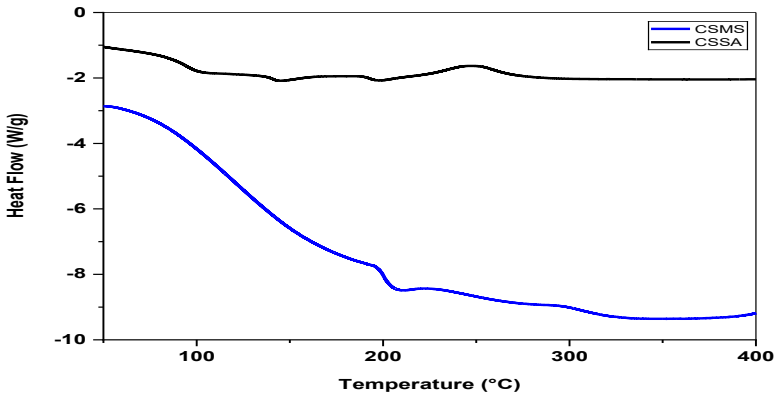


Figure III.27 DSC curves of CSSA and CSMS.

III.2.3.2 Quantification of the encapsulated active agent

III.2.3.2.1 Quantitative analysis of cephalexin

The figure bellow represents the absorption spectrum of a diluted solution of cephalexin in pH 7.4 at 37°C. It shows the change in its absorbance as a function of the wavelength of the incident light. We have noticed the maximum absorption wavelength λ_{max} at 262nm.

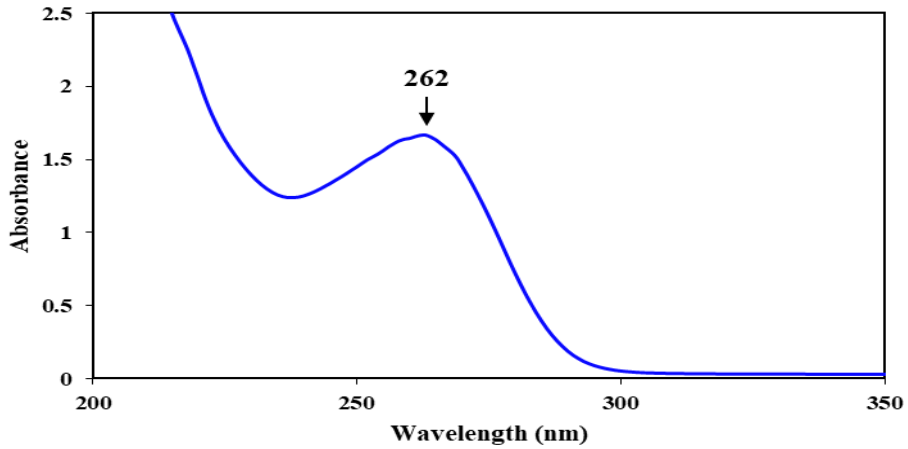


Figure III.28 UV-Vis spectrum of cephalexin in a buffer solution of pH= 7.4 at T=37°C.

The calibration curve has been drawn from the variation of absorbance as a function of the variation of the concentration of different cephalexin solutions **(Figure III.29)**. It allows the determination of the equation slope which represents the molar absorption coefficient ε according to Beer-Lambert's low. As a result, the value of ε is 5762.1 L $mol^{-1}cm^{-1}$.

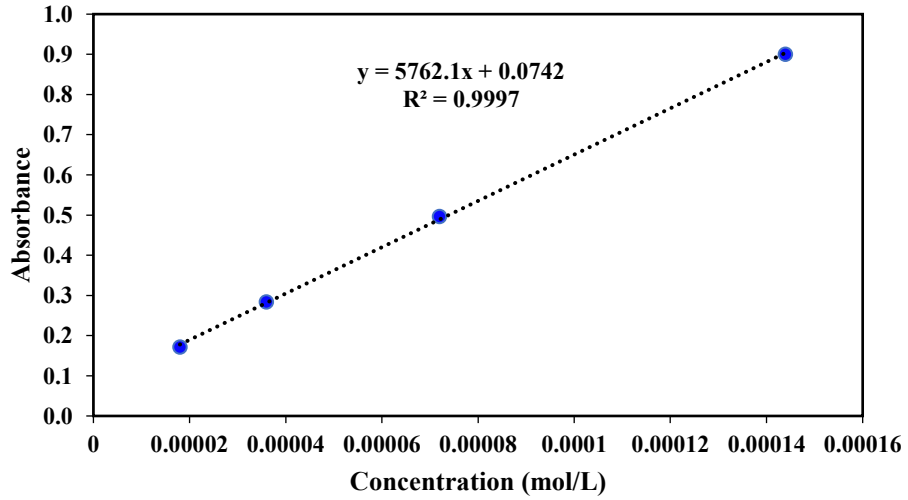


Figure III.29 Calibration curve of Cephalexin at pH 7.4, T=37°C.

III.2.3.2.2 Encapsulation efficiency and loading capacity determination

The outcomes of the estimation of the encapsulation efficiency and loading capacity verified the success of cephalexin encapsulation in alginate beads. The encapsulation efficiency was estimated to be 51.45±0.83% and CL loading in CSMS was 74.58±2.28 mg/g. The outcomes obtained in our work were found to be greater than the values declared in some papers. Khoshdouni et al.[89] encapsulated jujube extract in native and modified sodium alginate beads and the encapsulation efficiency didn't acceded 35.21%. The entrapment efficiency of CL was previously reported as only 18% in PLGA beads [92] and loading of 61mg/g in carboxymethyl cellulose beads capsulated layered double hydroxides/cephalexin nanohybrids [93].

III.2.3.3 Swelling behaviour measurement

The swelling ratio in different pH solutions indicates the hydrogel's response to external stimuli which is critical for applications like drug delivery. At pH 1.2, the swelling percentage of calcium ion-crosslinked beads remains unchanged over time **(Figure III.30)**. Low swelling is due to the protonation of matrix moieties resulting in hydrogen bond formation which negates the electrostatic repulsion[93]. This improves cephalexin retention and premature degradation reduction. However, calcium alginate beads exhibited nearly 300% of swelling in phosphate buffer solution at pH 7.4, and subsequently dissolved. High swelling causes high CL diffusion into the media[94].

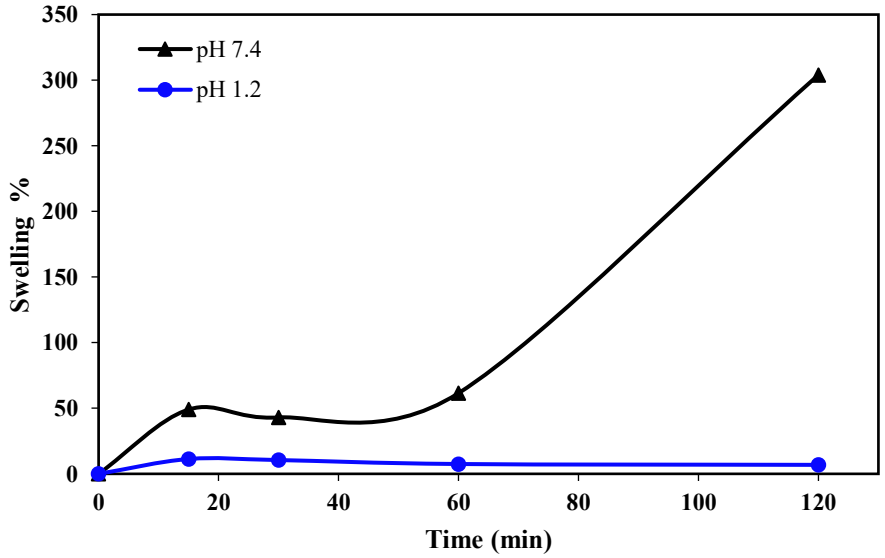


Figure III.30 Swelling behaviour of cephalexin loaded beads at pH 1.2 and 7.4.

III.2.3.4 In vitro drug release study and kinetic modelling

The cumulative release study was conducted at pH 7.4, T=37°C and plotted against time **Figure III.31a**. It has shown that cephalexin was completely released from CSMS within 7h. From the literature, CL powder dissolves only in 10min. Also compared to CL released from poly(L-lactic acid) microspheres for at least 4h[95], our results indicate the effectiveness of our extracted sodium alginate based hydrogels as good cephalexin carrier with sustained release appropriate for certain infection treatment.

In order to determine a reaction order to the kinetics of release, the release profile of the drug was tested with classic models (order 0,1 and 2), Higuchi, Korsmeyer-Peppas and Hixson-Crowel models. For instance, the zero-order reflects an ideal controlled release. In this case, the drug dissolved from dosage forms that do not disaggregate and release the drug slowly. First order model described water-soluble drugs dissolution in porous matrices [96]. At the beginning of the release, the speed is fast then it slows down exponentially as a function of time until the active agent is exhausted. The initial rapid release in large quantities is a case called "Brust effect". This phenomenon is generally observed in the case of drug adsorbed on the surface of microparticles, in the case of a non-homogeneous distribution of the active agent or in the case of a porous matrix [97]. Higuchi model could explain the mechanism of drug release through matrix system. Korsmeyer-Peppas is applied to the study of drug release from polymeric systems. Hixson-Crowell model describes the release happening in planes that are parallel to the drug surface [96].

The results showed that the release of CL from calcium alginate hydrogel beads in pH= 7.4 medium was in accordance with the first-order model (Highest R^2= 0.97) **(Figure III.31 b)**. It means that the drug release process is linear with its concentration in the system [98]. The other models **(Figures in Appendix)** showed lowest values of correlation coefficient **(Table III.7)** so they were unsuitable to describe the release profile in this case. The “n” value extracted from Korsmeyer-Peppas equation was 0.35 indicated that CL release is governed by Fickian diffusion mechanism as reported in [90]. Our finding also supports the research done by Sipos et al.[99] showing that metformin-hydrochloride (MET) would follow first-order kinetics from sodium alginate bead system. However, the study of Armutcu and Piskin [100] showed that the controlled hydroxychloroquine releasing from calcium-alginate beads fitted well with Korsmeyer-Peppas modal.

Table III.7 Release kinetic parameters of the mathematical models applied for cephalexin release mechanism study.

Kinetic modal	Correlation coefficient (R^2)	Rate constant (K)
Zero-order	0.815	7.4×10^{-3}
First-order	0.970	5.8×10^{-3}
Second-order	0.936	2.27×10^{-2}
Higuchi	0.636	1.49×10^{-1}
Korsmeyer-Peppas	0.515	9.3×10^{-3}, n=0.35
Hixson-Crowel	0.925	1.9×10^{-3}

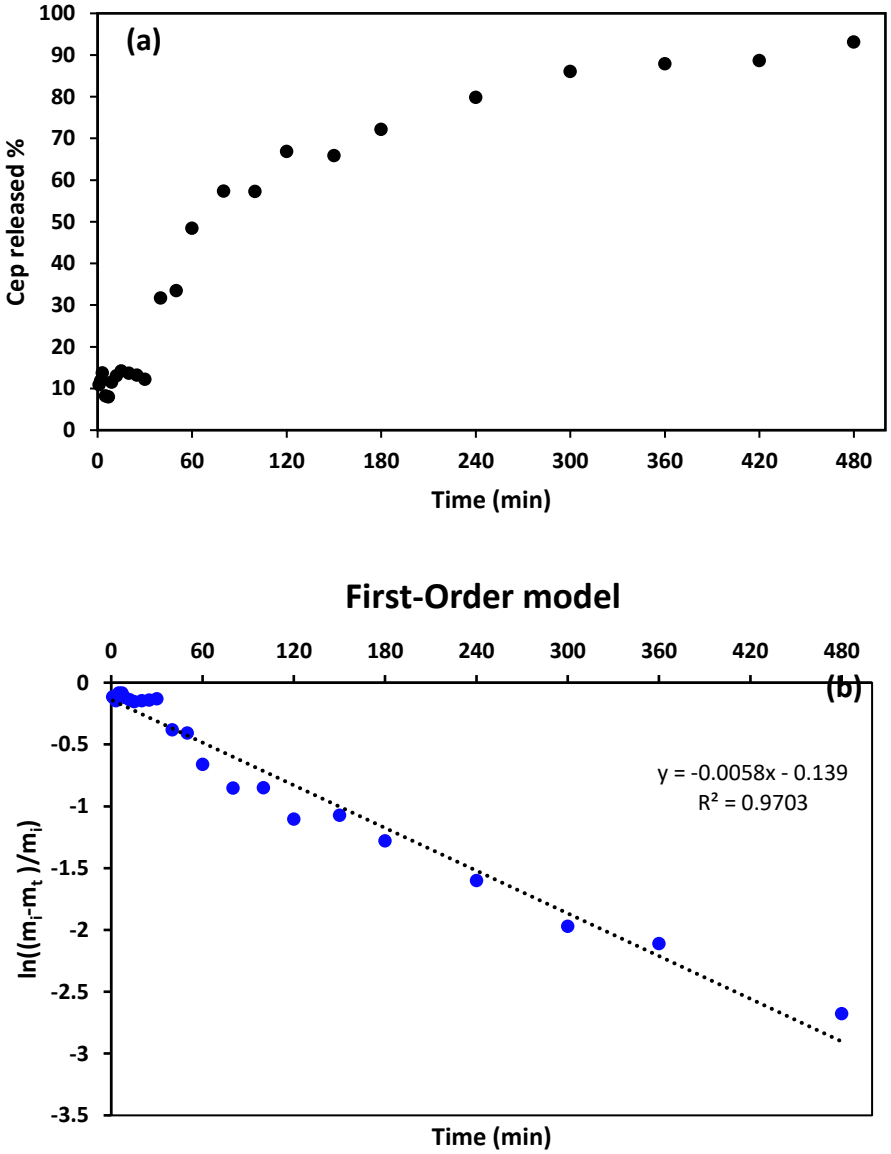


Figure III.31 (a) Release profile of cep from hydrogel beads in pH 7.4 at 37°C, **(b)** linear plot of first-order kinetic modal.

III.2.3.5 Antibacterial activity evaluation

The antibacterial effect of cephalexin-loaded beads was tested via agar disc diffusion method. This approach allows more contact with the microorganisms to test the efficiency of the drug diffusion [101]. Free-cephalexin beads has shown no effect on either of the tested strains **(Figure III.32)**, which aligns with the findings of Alvarez-Lorenzo et al.[102] who reported the lack of antibacterial activity of calcium alginate gel beads. Nevertheless, the calcium alginate beads did not interfere with cephalexin antibacterial properties. In fact, cephalexin-loaded beads were effective against *Staphylococcus aureus* which was highly sensitive compared to *Escherichia coli* tested strain (moderately sensitive) **(Table III.8)**. It is well reported that cephalexin has good antibacterial activity against Gram positive bacteria and moderate one toward Gram negative ones [103]. These results showed that cephalexin diffusion occurred in normal way from the polymer matrix and the encapsulation did not alter the beta lactam and R-group, which are the active groups of Cephalexin. Its antibacterial effect remained similar to that of free cephalexin against *S. aureus*. In contrast, Bhaskara Rao et al.[104] reported in their study a reduced antibacterial efficiency of cephalexin conjugated to Silica microparticles compared to the free form after 24 h of incubation. It is worth to mention that the synthesized cephalexin-loaded beads maintained their effectiveness against both strains after 9 months of storage at room temperature, demonstrating their good stability. Ozseker and Akkaya [105] reported a decrease in the antibacterial activity of tetracycline-immobilized calcium alginate beads when stored at a temperature of 25 °C over a period of 3 months.

Table III.8 Inhibition zone values of free and cephalexin-loaded hydrogel beads.

Sample	Code	Diameters of inhibition zones (mm)	
		Escherichia coli	***Staphylococcus aureus***
Free-cephalexin beads	F	0	0
Loaded-cephalexin beads	L	6.5±0.71	13±1.41
Positive control	CL 30µg	11±1.41	13.5±0.70

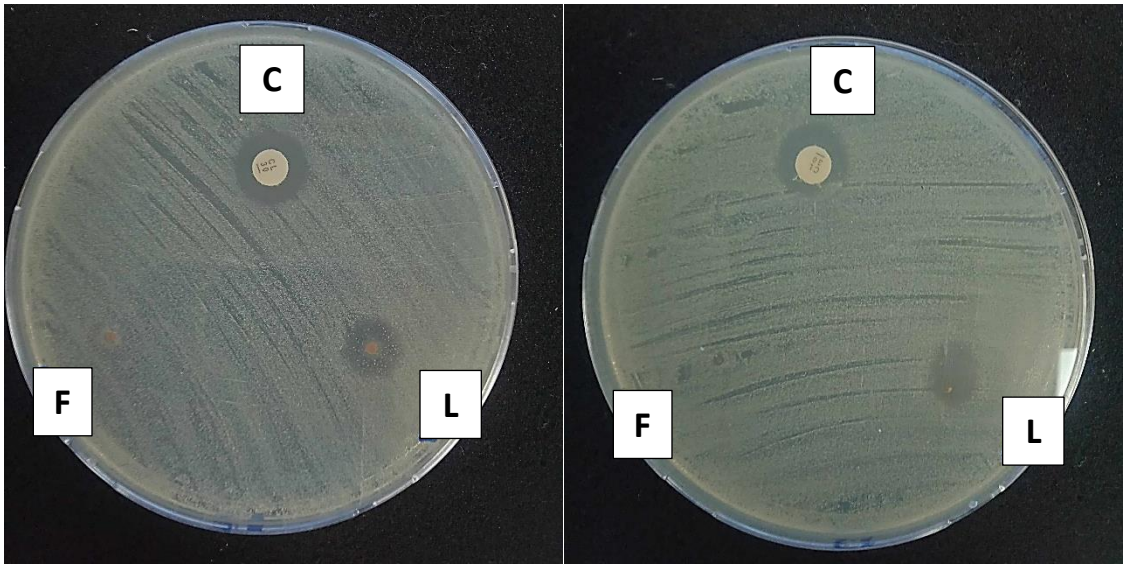


Figure III.32 Antibacterial activity of synthesized hydrogel beads.

III.2.4 Conclusion

The characterization and application of various new algae-based materials have been discussed in this section. Firstly, he introduction of ester group on extracted sodium alginate by reaction with maleic anhydride has successfully carried out according to FT-IR, XRD and TGA/DSC analysis data and DS value. This chemical modification resulted in a morphology and thermal stability change. Furthermore, the visible appearance and the antioxidant activity of sodium alginate have been enhanced.

Secondly, the preparation of nanoemulsion coating based on sodium alginate and date seed oil was well conducted. The mixture remained homogenous and stable over more than 30 days according to the value of zeta potential which was less than -30mV. It was found that the coating was effective for a long time with the inhibition of spoilage and dryness of coated strawberries compared to uncoated ones.

Thirdly, the encapsulation of cephalexin has successfully conducted. The obtained hydrogel beads have an average particle size of 807µm, a moderate entrapment efficiency (51.45 %), a good swelling behavior (300%) in pH 7.4 and low swelling in acidic medium. First- order kinetics was the best followed modal for cephalexin release. It has been demonstrated via antibacterial assays against *Escherichia coli* and *Staphylococcus aureus* that the microencapsulation has maintained the effectiveness of cephalexin.

III.3 References

[1] A. Kumar *et al.*, "Exploitation of seaweed functionality for the development of food products," *Food Bioprocess Technol.*, vol. 16, no. 9, pp. 1873–1903, 2023, doi: 10.1007/s11947-023-03023-2.

[2] A. K. Patel *et al.*, "Algal polysaccharides: current status and future prospects," *Phytochem. Rev.*, vol. 22, no. 4, pp. 1167–1196, 2023, doi: 10.1007/s11101-021-09799-5.

[3] P. Schiener, K. D. Black, M. S. Stanley, and D. H. Green, "The seasonal variation in the chemical composition of the kelp species Laminaria digitata, Laminaria hyperborea, Saccharina latissima and Alaria esculenta," *J. Appl. Phycol.*, vol. 27, no. 1, pp. 363–373, 2015, doi: 10.1007/s10811-014-0327-1.

[4] B. Y. S. Hellal and A. Ba, "Checklist of the marine macroalgae of Algerian west coast (Ain Témouchent site)," *Ukr. J. Ecol.*, vol. 11, no. 3, pp. 22–25, 2021, doi: 10.15421/2021.

[5] P. Schiener, K. D. Black, M. S. Stanley, and D. H. Green, "The seasonal variation in the chemical composition of the kelp species Laminaria digitata, Laminaria hyperborea, Saccharina latissima and Alaria esculenta," *J. Appl. Phycol.*, vol. 27, no. 1, pp. 363–373, 2015, doi: 10.1007/s10811-014-0327-1.

[6] V. Ummat, S. P. Sivagnanam, G. Rajauria, C. O'Donnell, and B. K. Tiwari, "Advances in pre-treatment techniques and green extraction technologies for bioactives from seaweeds," *Trends Food Sci. Technol.*, vol. 110, pp. 90–106, 2021, doi: 10.1016/j.tifs.2021.01.018.

[7] A. Mohammed, A. Rivers, D. C. Stuckey, and K. Ward, "Datasets on the optimization of alginate extraction from sargassum biomass using response surface methodology.," *Data Br.*, vol. 31, 2020, doi: 10.1016/j.dib.2020.105837.

[8] S. Y. Chee, P. K. Wong, and C. L. Wong, "Extraction and characterisation of alginate from brown seaweeds (Fucales, Phaeophyceae) collected from Port Dickson, Peninsular Malaysia," *J. Appl. Phycol.*, vol. 23, no. 2, pp. 191–196, 2011, doi: 10.1007/s10811-010-9533-7.

[9] A. Dobrinčić *et al.*, "Advanced technologies for the extraction of marine brown algal polysaccharides," *Mar. Drugs*, vol. 18, no. 3, 2020, doi: 10.3390/md18030168.

[10] S. Sankhla, H. H. Sardar, and S. Neogi, "Greener extraction of highly crystalline and thermally stable cellulose micro-fibers from sugarcane bagasse for cellulose nano-fibrils preparation," *Carbohydr. Polym.*, vol. 251, 2021, doi: 10.1016/j.carbpol.2020.117030.

[11] B. Machado, S. M. Costa, I. Costa, R. Fangueiro, and D. P. Ferreira, "The potential of algae as a source of cellulose and its derivatives for biomedical applications," *Cellulose*, vol. 31, no. 6, pp. 3353–3376, 2024, doi: 10.1007/s10570-024-05816-w.

[12] Z. Zulnazri *et al.*, "Effect of hydrochloric acid hydrolysis under sonication and hydrothermal process to produce cellulose nanocrystals from oil oalm empty fruit bunch (OPEFB)," *Polymers (Basel).*, vol. 16, p. 1866, 2024, doi: 10.3390/polym16131866.

[13] S. Saji, A. Hebden, P. Goswami, and C. Du, "A brief review on the development of

alginate extraction process and its sustainability," *Sustain.*, vol. 14, no. 9, pp. 1–20, 2022, doi: 10.3390/su14095181.

[14] S. Sellimi, N. Kadri, V. Barragan-Montero, H. Laouer, M. Hajji, and M. Nasri, "Fucans from a Tunisian brown seaweed Cystoseira barbata: Structural characteristics and antioxidant activity," *Int. J. Biol. Macromol.*, vol. 66, pp. 281–288, 2014, doi: 10.1016/j.ijbiomac.2014.02.041.

[15] S. Sellimi *et al.*, "Structural, physicochemical and antioxidant properties of sodium alginate isolated from a Tunisian brown seaweed," *Int. J. Biol. Macromol.*, vol. 72, pp. 1358–1367, 2015, doi: 10.1016/j.ijbiomac.2014.10.016.

[16] H. H. Ammar, J. Hafsa, D. Le Cerf, A. Bouraoui, and H. Majdoub, "Antioxidant and gastroprotective activities of polysaccharides from the Tunisian brown algae (Cystoseira sedoides)," *J. Tunis. Chem. Soc.*, vol. 18, pp. 80–88, 2016.

[17] N. Hachemi-Benmalek, A. Nouani, and A. Benchabane, "Valorization of brown algae (Cystoseira caespitosa) from local region in Algeria for sodium alginate extraction and their application in the immobilization of microbial pectinases," *Alger. J. Environ. Sci. Technol.*, vol. 5, pp. 1155–1162, 2019.

[18] M. Aitouguinane *et al.*, "Polysaccharides from Moroccan green and brown seaweed and their derivatives stimulate natural defenses in olive tree leaves," *Appl. Sci.*, vol. 12, no. 17, p. 8842, 2022, doi: 10.3390/app12178842.

[19] A. K. Siddhanta *et al.*, "The cellulose contents of Indian seaweeds," *J. Appl. Phycol.*, vol. 23, no. 5, pp. 919–923, 2011, doi: 10.1007/s10811-010-9599-2.

[20] A. Benslima *et al.*, "Brown seaweed Cystoseira schiffneri as a promising source of sulfated fucans: Seasonal variability of structural, chemical, and antioxidant properties," *Food Sci. Nutr.*, vol. 9, no. 3, pp. 1551–1563, 2021, doi: 10.1002/fsn3.2130.

[21] H. R. Fletcher, P. Biller, A. B. Ross, and J. M. M. Adams, "The seasonal variation of fucoidan within three species of brown macroalgae," *Algal Res.*, vol. 22, pp. 79–86, 2017, doi: 10.1016/j.algal.2016.10.015.

[22] A. Benslima *et al.*, "The brown seaweed Cystoseira schiffneri as a source of sodium alginate: Chemical and structural characterization, and antioxidant activities," *Food Biosci.*, vol. 40, 2021, doi: 10.1016/j.fbio.2020.100873.

[23] Z. Belattmania *et al.*, "Seasonal patterns of growth, alginate content and block structure of the alien invader Sargassum muticum (Fucales, Ochrophyta) from the Atlantic coast of Morocco," *Bot. Mar.*, vol. 65, no. 1, pp. 69–78, 2022, doi: 10.1515/bot-2021-0050.

[24] A. F. Tarchoun, D. Trache, and T. M. Klapötke, "Microcrystalline cellulose from Posidonia oceanica brown algae : Extraction and characterization," *Int. J. Biol. Macromol.*, vol. 138, pp. 837–845, 2019, doi: 10.1016/j.ijbiomac.2019.07.176.

[25] M. Habibi, M. Golmakani, and M. H. Eskandari, "Potential prebiotic and antibacterial activities of fucoidan from Laminaria japonica," *Int. J. Biol. Macromol.*, vol. 268, p. 131776, 2024, doi: 10.1016/j.ijbiomac.2024.131776.

[26] A. Faidi *et al.*, "Application of sodium alginate extracted from a Tunisian brown algae Padina pavonica for essential oil encapsulation : Microspheres preparation , characterization and in vitro release study," *Int. J. Biol. Macromol.*, vol. 136, pp. 386–394, 2019, doi: 10.1016/j.ijbiomac.2019.06.023.

[27] L. Chávez-Guerrero, A. Toxqui-Terán, and O. Pérez-Camacho, "One-pot isolation of nanocellulose using pelagic Sargassum spp. from the Caribbean coastline," *J. Appl. Phycol.*, vol. 34, no. 1, pp. 637–645, 2022, doi: 10.1007/s10811-021-02643-5.

[28] D. M. S. A. Salem and M. M. Ismail, "Characterization of cellulose and cellulose nanofibers isolated from various seaweed species," *Egypt. J. Aquat. Res.*, vol. 48, no. 4, pp. 307–313, 2022, doi: 10.1016/j.ejar.2021.11.001.

[29] B. Luo *et al.*, "Physicochemical characterization and antitumor activity of fucoidan and its degraded products from Sargassum hemiphyllum (Turner) C. Agardh," *Molecules*, vol. 28, no. 6, p. 2610, 2023, doi: 10.3390/molecules28062610.

[30] H. Terea *et al.*, "Characterization, biological, and antimicrobial properties of nanocellulose isolated from peanut shells (Arachis hypogaea L.)," *Biomass Convers. Biorefinery*, vol. 14, no. 23, pp. 30435–30445, 2023, doi: 10.1007/s13399-023-04792-8.

[31] S. Singh, K. K. Gaikwad, S. Park, and Y. S. Lee, "Microwave-assisted step reduced extraction of seaweed (Gelidiella aceroso) cellulose nanocrystals," *Int. J. Biol. Macromol.*, vol. 99, pp. 506–510, 2017, doi: 10.1016/j.ijbiomac.2017.03.004.

[32] R. Al Monla, Z. Dassouki, N. Sari-Chmayssem, H. Mawlawi, and H. Gali-Muhtasib, "Fucoidan and Alginate from the Brown Algae Colpomenia sinuosa and Their Combination with Vitamin C Trigger Apoptosis in Colon Cancer," *Molecules*, vol. 27, no. 2, 2022, doi: 10.3390/molecules27020358.

[33] F. Hentati *et al.*, "Structural characterization and antioxidant activity of water-soluble polysaccharides from the Tunisian brown seaweed Cystoseira compressa," *Carbohydr. Polym.*, vol. 198, pp. 589–600, 2018, doi: https://doi.org/10.1016/j.carbpol.2018.06.098.

[34] K. Sakugawa, A. Ikeda, A. Takemura, and H. Ono, "Simplified method for estimation of composition of alginates by FTIR," *J. Appl. Polym. Sci.*, vol. 93, no. 3, pp. 1372–1377, 2004, doi: 10.1002/app.20589.

[35] N. Perumal, S. Indran, S. Divya, and D. Suchart, "Isolation of Microcrystalline Cellulose from Valoniopsis pachynema Green Macroalgae : Physicochemical , Thermal , Morphological , and Mechanical Characterization for Biofilm Applications," *Waste and Biomass Valorization*, vol. 15, no. 3, pp. 1247–1266, 2024, doi: 10.1007/s12649-023-02228-y.

[36] H. Doh, M. Hyeock, and W. Scott, "Physicochemical characteristics of cellulose nanocrystals isolated from seaweed biomass," *Food Hydrocoll.*, vol. 102, p. 105542, 2020, doi: 10.1016/j.foodhyd.2019.105542.

[37] H. Fouad, L. K. Kian, M. Jawaid, M. D. Alotaibi, O. Y. Alothman, and M. Hashem, "Characterization of microcrystalline cellulose isolated from conocarpus fiber," *Polymers (Basel).*, vol. 12, no. 12, p. 2926, 2020, doi: 10.3390/polym12122926.

[38] Z. Belattmania, E. A. Samir, E. Sabbar, and A. Mortadi, "Spectroscopic and rheological characterization of sodium alginate extracted from three Phaeophycean seaweeds (Dictyopteris polypodioides , Dilophus ligulatus and Halopteris scoparia ... Spectroscopic and rheological characterization of sodium alginate ex," *J. Mater. Environ. Sci.*, vol. 6, no. 6, pp. 1654–1662, 2015.

[39] N. A. R. Osman, T. O. Suliman, and K. A. Osman, "Characterization of native alginates of common alginophytes from the red sea coast of Sudan," *Int. J. Second. Metab.*, vol. 7, no. 4, pp. 266–274, 2020, doi: 10.21448/ijsm.685864.

[40] S. H. Ptak, A. L. Hjuler, S. I. Ditlevsen, X. Fretté, M. Errico, and K. V. Christensen, "The effect of seasonality and geographic location on sulphated polysaccharides from brown algae," *Aquac. Res.*, vol. 52, no. 12, pp. 6235–6243, 2021, doi: 10.1111/are.15485.

[41] S. Kaidi *et al.*, "Isolation and Structural Characterization of Alginates from the Kelp Species Laminaria ochroleuca and Saccorhiza polyschides from the Atlantic Coast of Morocco," *Colloids and Interfaces*, vol. 6, no. 4, p. 51, 2022, doi: 10.3390/colloids6040051.

[42] B. Mabate and B. I. Pletschke, "Sequential and enzyme-assisted extraction of algal bioproducts from Ecklonia maxima," *Enzyme Microb. Technol.*, vol. 173, p. 110364, 2024, doi: 10.1016/j.enzmictec.2023.110364.

[43] X. Zhao, X. Wang, and T. Lou, "Preparation of fibrous chitosan/sodium alginate composite foams for the adsorption of cationic and anionic dyes," *J. Hazard. Mater.*, vol. 403, p. 124054, 2021, doi: 10.1016/j.jhazmat.2020.124054.

[44] S. Sayin *et al.*, "Characterization and evaluation of the antimicrobial properties of algal alginate; a potential natural protective for cosmetics," *J. Res. Pharm.*, vol. 26, no. 1, pp. 198–209, 2022, doi: 10.29228/jrp.117.

[45] Z. Kassab, H. Ben youcef, H. Hannache, and M. El Achaby, "Isolation of cellulose nanocrystals from various lignocellulosic materials: Physico-chemical characterization and Application in Polymer Composites Development," *Mater. Today Proc.*, vol. 13, pp. 964–973, 2019, doi: 10.1016/j.matpr.2019.04.061.

[46] R. S. Baghel, P. Suthar, T. K. Gajaria, S. Bhattacharya, A. Anil, and C. R. K. Reddy, "Seaweed biorefinery: A sustainable process for valorising the biomass of brown seaweed," *J. Clean. Prod.*, vol. 263, 2020, doi: 10.1016/j.jclepro.2020.121359.

[47] L. Segal, J. J. Creely, A. E. Martin, Jr., and C. M. Conrad, "An empirical method for estimating the degree of crystallinity of native cellulose using the X-Ray diffractometer," *Text. Res. J.*, vol. 29, no. 10, pp. 786–794, 1959, doi: 10.1177/004051755902901003.

[48] A. D. French and S. M. Cintron, "Cellulose polymorphy , crystallite size , and the Segal Crystallinity Index," *Cellulose*, vol. 20, pp. 583–588, 2013, doi: 10.1007/s10570-012-9833-y.

[49] J. Matusiak, U. Maciołek, M. Kosińska-Pezda, D. Sternik, J. Orzeł, and E. Grządka, "Textural and thermal properties of the novel fucoidan/nano-oxides hybrid materials with cosmetic, pharmaceutical and environmental potential," *Int. J. Mol. Sci.*, vol. 23, no. 2, p.

805, 2022, doi: 10.3390/ijms23020805.

[50] K. Anastasakis, A. B. Ross, and J. M. Jones, "Pyrolysis behaviour of the main carbohydrates of brown macro-algae," *Fuel*, vol. 90, no. 2, pp. 598–607, 2011, doi: 10.1016/j.fuel.2010.09.023.

[51] A. J. Antonisamy and K. Rajendran, "Comparative study on the extraction methods, characterization, and bioactivity of crude fucoidan, a polysaccharide derived from Sargassum ilicifolium," *Biochem. Eng. J.*, vol. 209, p. 109398, 2024, doi: 10.1016/j.bej.2024.109398.

[52] R. Pereira, A. Tojeira, D. C. Vaz, A. Mendes, and P. Bártolo, "Preparation and characterization of films based on alginate and aloe vera," *Int. J. Polym. Anal. Charact.*, vol. 16, no. 7, pp. 449–464, 2011, doi: 10.1080/1023666X.2011.599923.

[53] J. S. Rowbotham, P. W. Dyer, H. C. Greenwell, D. Selby, and M. K. Theodorou, "Copper(II)-mediated thermolysis of alginates: A model kinetic study on the influence of metal ions in the thermochemical processing of macroalgae," *Interface Focus*, vol. 3, no. 1, 2013, doi: 10.1098/rsfs.2012.0046.

[54] N. Wahlstrom, U. Edlund, H. Pavia, G. Toth, A. Jaworski, and A. J. Pell, "Cellulose from the green macroalgae Ulva lactuca : isolation , characterization , optotracing , and production of cellulose nanofibrils," *Cellulose*, vol. 27, pp. 3707–3725, 2020, doi: 10.1007/s10570-020-03029-5.

[55] D. K. B. Lee, D. Hyun, K. P. Kang, and J. Jeun, "Preparation of nanocellulose from a kenaf core using E-beam irradiation and acid hydrolysis," *Cellulose*, vol. 23, no. 5, pp. 3039–3049, 2016, doi: 10.1007/s10570-016-1037-4.

[56] K. Sonia, K. S. Meena, and D. Rajesh, "Structural Characterization, Biological Evaluation and Molecular Docking Studies of Fucoidan Isolated From Brown Marine Algae," *J. Adv. Sci. Res.*, vol. 12, no. 04 Suppl 1, pp. 90–100, 2021, doi: 10.55218/jasr.s1202112409.

[57] O. Roger, N. Kervarec, and J. Ratiskol, "Structural studies of the main exopolysaccharide produced by the deep-sea bacterium Alteromonas infernus," *Carbohydr. Res.*, vol. 339, pp. 2371–2380, 2004, doi: 10.1016/j.carres.2004.07.021.

[58] A. Zayed *et al.*, "Phenomenological investigation of the cytotoxic activity of fucoidan isolated from Fucus vesiculosus," *Process Biochem.*, vol. 81, pp. 182–187, 2019, doi: 10.1016/j.procbio.2019.03.026.

[59] A. Zayed, M. El-Aasr, A. R. S. Ibrahim, and R. Ulber, "Fucoidan characterization: Determination of purity and physicochemical and chemical properties," *Mar. Drugs*, vol. 18, no. 11, pp. 1–31, 2020, doi: 10.3390/md18110571.

[60] M. N. G. Amin, T. Rosenau, and B. Stefan, "The structure of fucoidan by linkage analysis tailored for fucose in four algae species : Fucus serratus , Fucus evanescens , Fucus vesiculosus and Laminaria hyperborea," *Carbohydr. Polym. Technol. Appl.*, vol. 7, p. 100455, 2024, doi: 10.1016/j.carpta.2024.100455.

[61] P. S. Birgersson, A. S. Chahal, L. J. Klau, H. Bratsberg, Ø. Arlov, and F. L. Aachmann, "Structural characterization and immunomodulating assessment of ultra-purified water

extracted fucoidans from Saccharina latissima , Alaria esculenta and Laminaria hyperborea," *Carbohydr. Polym.*, vol. 343, p. 122448, 2024, doi: 10.1016/j.carbpol.2024.122448.

[62] R. A. Hamouda, F. A. K. Qarabai, F. S. Shahabuddin, T. M. Al-Shaikh, and R. R. Makharita, "Antibacterial activity of Ulva/nanocellulose and Ulva/Ag/cellulose nanocomposites and both blended with fluoride against bacteria causing dental decay.," *Polymers (Basel).*, vol. 15, no. 4, p. 1047, 2023, doi: 10.3390/polym15041047.

[63] M. M. El-Sheekh, W. E. Yousuf, E. R. Kenawy, and T. M. Mohamed, "Biosynthesis of cellulose from Ulva lactuca , manufacture of nanocellulose and its application as antimicrobial polymer," *Sci. Rep.*, vol. 13, no. 1, p. 10188, 2023, doi: https://doi.org/10.1038/s41598-023-37287-7.

[64] N. I. Abdo, Y. M. Tufik, and S. M. Abobakr, "A comparison of nano-celluloses prepared with various terms of time and sulfuric acid concentration from bagasse derived cellulose : Physicochemical characteristics and process optimization," *Curr. Res. Green Sustain. Chem.*, vol. 6, p. 100365, 2023, doi: 10.1016/j.crgsc.2023.100365.

[65] H. Terea, "Application of cellulose / ZnO nanocomposite on the removal of toxic pollutants from aqueous solutions," Universityof Kasdi Merbah- Ouergla, 2024. doi: 10.13140/RG.2.2.20226.04802.

[66] S. Honary and F. Zahir, "Effect of zeta potential on the properties of nano-drug delivery systems - A review (Part 2)," *Trop. J. Pharm. Res.*, vol. 12, no. 2, pp. 255–264, 2013, doi: 10.4314/tjpr.v12i2.19.

[67] H. Yunhai, A. Eyþórsdóttir, and S. M. Scully, "In vitro antibacterial activity of fucoidan islolated from Ascophyllum nodosum and Laminaria digitata," Iceland: Nations University Fisheries Training Programme, 2018.

[68] W. Janik *et al.*, "Modulation of physicochemical properties and antimicrobial activity of sodium alginate films through the use of chestnut extract and plasticizers," *Sci. Rep.*, vol. 13, no. 1, p. 11530, 2023, doi: 10.1038/s41598-023-38794-3.

[69] N. Halib *et al.*, "Potential applications of nanocellulose-containing materials in the biomedical field," *Materials (Basel).*, vol. 10, no. 8, p. 977, 2017, doi: 10.3390/ma10080977.

[70] X. Chen, Q. Zhu, C. Liu, D. Li, H. Yan, and Q. Lin, "Esterification of alginate with alkyl bromides of different carbon chain lengths via the bimolecular nucleophilic substitution reaction: Synthesis, characterization, and controlled release performance," *Polymers (Basel).*, vol. 13, no. 19, p. 3351, 2021, doi: 10.3390/polym13193351.

[71] J. P. Soares, J. E. Santos, G. O. Chierice, and E. T. G. Cavalheiro, "Thermal behavior of alginic acid and its sodium salt," vol. 29, no. 2, pp. 53–56, 2004.

[72] L. Xiaochao, L. Dongtao, S. Xuefeng, and L. Tao, "Development and performance study of coal seam water injection permeation enhancer based on polymer modification," *China Min. Mag.*, vol. 32, no. 12, pp. 177–183, 2023, doi: 10.12075/j.issn.1004-4051.20230187.

[73] K. Madhusudana Rao, K. S. V Krishna Rao, P. Sudhakar, K. Chowdoji Rao, and M. C. S.

Subha, “Synthesis and Characterization of biodegradable Poly (Vinyl caprolactam) grafted on to sodium alginate and its microgels for controlled release studies of an anticancer drug,” vol. 3, no. 06, pp. 61–69, 2013, doi: 10.7324/JAPS.2013.3609.

[74] Y. Zuo, J. Gu, L. Yang, Z. Qiao, H. Tan, and Y. Zhang, “Synthesis and characterization of maleic anhydride esterified corn starch by the dry method,” *Int. J. Biol. Macromol.*, vol. 62, pp. 241–247, 2013, doi: 10.1016/j.ijbiomac.2013.08.032.

[75] C. T. Mei, L. Y. Jiang, M. M. Jiang, X. L. Zhou, and H. Huang, “Modification of cellulose extracted from waste newspaper,” *IOP Conf. Ser. Earth Environ. Sci.*, vol. 295, no. 3, p. 032009, 2019, doi: 10.1088/1755-1315/295/3/032009.

[76] V. Bátori *et al.*, “Synthesis and characterization of Maleic Anhydridegrafted orange waste for potential use in biocomposites,” *BioResources*, vol. 13, no. 3, pp. 4986–4997, 2019, doi: 10.15376/biores.13.3.4986-4997.

[77] Y. Zhou *et al.*, “Preparation and characterization of κ-carrageenan modified with maleic anhydride and its application in films,” *Mar. Drugs*, vol. 19, no. 9, p. 486, 2021, doi: 10.3390/md19090486.

[78] P. A. R. Fernandes and M. A. Coimbra, “The antioxidant activity of polysaccharides: A structure-function relationship overview,” *Carbohydr. Polym.*, vol. 314, p. 120965, 2023, doi: 10.1016/j.carbpol.2023.120965.

[79] L. Bai *et al.*, “Antioxidant activities of natural polysaccharides and their derivatives for biomedical and medicinal applications,” *Antioxidants*, vol. 11, no. 12, p. 2491, 2022, doi: 10.3390/antiox11122491.

[80] M. Şen, “Effects of molecular weight and ratio of guluronic acid to mannuronic acid on the antioxidant properties of sodium alginate fractions prepared by radiation-induced degradation,” *Appl. Radiat. Isot.*, vol. 69, no. 1, pp. 126–129, 2011, doi: 10.1016/j.apradiso.2010.08.017.

[81] X. Xiong, M. Li, J. Xie, B. Xue, and T. Sun, “Preparation and antioxidant activity of xanthan oligosaccharides derivatives with similar substituting degrees,” *Food Chem.*, vol. 164, pp. 7–11, 2014, doi: 10.1016/j.foodchem.2014.05.001.

[82] M. D. Ghoora and N. Srividya, “Effect of Packaging and Coating Technique on Postharvest Quality and Shelf Life of Raphanus sativus L. and Hibiscus sabdariffa L. Microgreens,” *Foods*, vol. 9, no. 5, p. 653, 2020, doi: 10.3390/foods9050653.

[83] S. A. A. Mohamed, M. El-Sakhawy, and M. A. M. El-Sakhawy, “Polysaccharides, Protein and Lipid -Based Natural Edible Films in Food Packaging: A Review,” *Carbohydr. Polym.*, vol. 238, p. 116178, 2020, doi: 10.1016/j.carbpol.2020.116178.

[84] J. G. de Oliveira Filho, M. Miranda, M. D. Ferreira, and A. Plotto, “Nanoemulsions as Edible Coatings : A Potential Strategy for Fresh Fruits and Vegetables Preservation,” *Foods*, vol. 10, p. 2438, 2021, doi: 10.3390/foods10102438.

[85] J. M. Sousa *et al.*, “Chitosan grafted with maleic anhydride and ethylenediamine: Preparation, characterization, computational study, antibacterial and cytotoxic properties,” *Mater. Chem. Phys.*, vol. 287, p. 126301, 2022, doi:

10.1016/j.matchemphys.2022.126301.

[86] C. Santos *et al.*, "Green nanotechnology for the development of nanoparticles based on alginate associated with essential and vegetable oils for application in fruits and seeds protection," *Int. J. Biol. Macromol.*, vol. 232, p. 123351, 2023, doi: 10.1016/j.ijbiomac.2023.123351.

[87] J. Li, S. Y. Kim, X. Chen, and H. J. Park, "Calcium-alginate beads loaded with gallic acid: Preparation and characterization," *LWT - Food Sci. Technol.*, vol. 68, pp. 667–673, 2016, doi: 10.1016/j.lwt.2016.01.012.

[88] S. R. Dalal, M. H. Hussein, N. E. A. El-Naggar, S. I. Mostafa, and S. A. Shaaban-Dessuuki, "Characterization of alginate extracted from Sargassum latifolium and its use in Chlorella vulgaris growth promotion and riboflavin drug delivery," *Sci. Rep.*, vol. 11, no. 1, p. 16741, 2021, doi: 10.1038/s41598-021-96202-0.

[89] Z. Khoshdouni Farahani, M. Mousavi, S. M. Seyedain Ardebili, and H. Bakhoda, "Modification of sodium alginate by octenyl succinic anhydride to fabricate beads for encapsulating jujube extract," *Curr. Res. Food Sci.*, vol. 5, pp. 157–166, 2022, doi: 10.1016/j.crfs.2021.11.014.

[90] M. S. Seyed Dorraji, M. H. Rasoulifard, S. Madadi, M. Doosti, H. Chiti, and S. N. Mousavi, "Synthesis and evaluation of the efficiency of antibacterial hydrogel beads based on the sodium alginate–ferula gum for delayed release of quercetin," *Polym. Bull.*, vol. 78, no. 7, pp. 3667–3685, 2021, doi: 10.1007/s00289-020-03293-2.

[91] J. Vijay, J. Sahadevan, R. Prabhakaran, and R. Gilhotra, "Formulation and evaluation of cephalexin extended-release matrix tablets using hydroxy propyl methyl cellulose as rate-controlling polymer," *J. Young Pharm.*, vol. 4, no. 1, pp. 3–12, 2012, doi: 10.4103/0975-1483.93570.

[92] W. Chaisri, W. Hennink, and S. Okonogi, "Preparation and Characterization of Cephalexin Loaded PLGA Microspheres," *Curr. Drug Deliv.*, vol. 6, no. 1, pp. 69–75, 2009, doi: 10.2174/156720109787048186.

[93] S. Barkhordari and M. Yadollahi, "Applied Clay Science Carboxymethyl cellulose capsulated layered double hydroxides / drug nanohybrids for Cephalexin oral delivery," *Appl. Clay Sci.*, vol. 121, pp. 77–85, 2016, doi: 10.1016/j.clay.2015.12.026.

[94] D. Kundu and T. Banerjee, "Development of microcrystalline cellulose based hydrogels for the in vitro delivery of Cephalexin," *Heliyon*, vol. 6, no. 1, 2020, doi: 10.1016/j.heliyon.2019.e03027.

[95] G. Owusu-Ababio and J. A. Rogers, "Formulation, and release kinetics of cephalexin monohydrate from biodegradable polymeric microspheres," *J. Microencapsul.*, vol. 13, no. 2, pp. 195–205, 1996, doi: 10.3109/02652049609052907.

[96] S. Dash, P. N. Murthy, L. Nath, and P. Chowdhury, "Kinetic modeling on drug release from controlled drug delivery systems," *Acta Pol. Pharm. - Drug Res.*, vol. 67, no. 3, pp. 217–223, 2010.

[97] L. BENNABI, "Etude de la dégradation de copolymères blends à base du

polycaprolactone et d'ethylcellulose. Microencapsulation et étude de la libération de substances actives," Université Djillali Liabes, Sidi Bel-Abbes, 2017.

[98] T. Do Mai Tran *et al.*, "Preparation and characterization of chitosan/fish scale collagen/lovastatin nanocomposites," *J. Polym. Environ.*, vol. 28, no. 11, pp. 2851–2863, 2020, doi: 10.1007/s10924-020-01819-3.

[99] B. Sipos, M. Benei, G. Katona, and I. Csóka, "Optimization and characterization of sodium alginate beads providing extended release for antidiabetic drugs," *Molecules*, vol. 28, no. 19, p. 6980, 2023, doi: 10.3390/molecules28196980.

[100] C. Armutcu and S. Piskin, "Evaluation of controlled hydroxychloroquine releasing performance from calcium-alginate beads," *Hittite J. Sci. Eng.*, vol. 8, no. 3, pp. 255–263, 2021, doi: 10.17350/HJSE19030000236.

[101] W. Al-Gethami and N. Al-Qasmi, "Antimicrobial activity of Ca-alginate/chitosan nanocomposite loaded with camptothecin," *Polymers (Basel).*, vol. 13, p. 3559, 2021, doi: 10.3390/polym13203559.

[102] C. Alvarez-lorenzo, B. Blanco-fernandez, A. M. Puga, and A. Concheiro, "Crosslinked ionic polysaccharides for stimuli-sensitive drug delivery ☆," *Adv. Drug Deliv. Rev.*, vol. 65, pp. 1148–1171, 2013, doi: 10.1016/j.addr.2013.04.016.

[103] N. Sultana and M. S. Arayne, "In vitro activity of cefadroxil, cephalexin, cefatrizine and cefpirome in presence of essential and trace elements," *Pak. J. Pharm. Sci.*, vol. 20, no. 4, pp. 305–310, 2007.

[104] B. V Bhaskara Rao, R. Mukherji, G. Shitre, F. Alam, A. A. Prabhune, and S. N. Kale, "Controlled release of antimicrobial Cephalexin drug from silica microparticles," *Mater. Sci. Eng. C*, vol. 34, pp. 9–14, 2014, doi: 10.1016/j.msec.2013.10.002.

[105] E. E. Ozseker and A. Akkaya, "Development of a new antibacterial biomaterial by tetracycline immobilization on calcium-alginate beads," *Carbohydr. Polym.*, vol. 151, pp. 441–451, 2016, doi: 10.1016/j.carbpol.2016.05.073.

General Conclusion

General Conclusion

This research paper contributes to the analysis of Cystoseira stricta brown algae biomass for ash and moisture content, yield and properties of fucoidan, sodium alginate and cellulose in addition to microcrystalline cellulose.

As far as we know, this is the first time dealing with the extraction of polysaccharides from western Algerian Cystoseira stricta macroalgae. This is considered as an effective and sustainable way for algae exploitation and the synthesis of bio-based materials.

The utilized sequential process proved effective in extracting four different polysaccharides with reliable and reproducible results. It was found that higher content of ash was measured during September and the moisture content was almost equal between September and February. Different particle size, S/L ratio and harvesting period in extraction are known to affect the yield and properties of polysaccharides. The optimum sample particle size was found to be 150µm and S/L ratio of 1:30. February is the best period to extract fucoidan and alginate, contrary to cellulose, with high yield compared to harvesting in September.

Several characterization methods were employed in order to analyse our products. FTIR analysis showed distinctive bands of different polysaccharides confirming the identity of the desired products to be extracted.

XRD analysis provided information about the crystallinity of our products where it was found that all the extracted polysaccharides have a semi-crystalline character which tend to have good thermal resistance confirmed by data obtained from TGA/DSC analysis.

SEM and EDX analysis of the C. stricta polysaccharides have given worthy information about the surface morphology and the composition of the products revealing their purity.

Acid hydrolysis of cellulose was found to be effective to produce microcrystalline cellulose with enhanced properties confirmed by the above-mentioned analysis in addition to DLS which has disclosed its micro-sizing and its stability in aqueous suspension.

Fucoidan, cellulose and MCC have given a promising antibacterial effect against *S. aureus* and *E. coli* whereas, sodium alginate has shown a weak inherent antibacterial activity.

The extracted products serve as a versatile precursor in the development of new materials with favourable properties and tailored functionalities. Sodium alginate has been chosen to the synthesis of derived materials notably maleated alginate with enhanced antioxidant activity, nanocoating to protect and enhance the shelf-life of strawberries and hydrogel for cephalexin encapsulation.

These bio-based materials have been successfully synthesized and characterized by FT-IR, XRD, TGA/DSC and SEM.

The chemical modification of sodium alginate resulted in a morphology and thermal stability change. Furthermore, the visible appearance and the antioxidant activity of the row material have been enhanced.

The protective effect of the prepared nanoscale emulsion on fresh strawberries was evaluated over time. The results were promising where it was found that the coating was stable and effective to protect fruits from dehydration, oxidation and rot.

Concerning the encapsulation, the prepared cephalexin-loaded beads were micro-sized spheres with good values of encapsulation efficiency and drug loading. The release kinetics of cephalexin from hydrogel beads was best fitted by the first-order modal equation and the matter transfer was through Fickian diffusion process. The encapsulation of cephalexin into our extracted alginate hydrogel was prolonged the drug release, enhanced its availability and maintained its efficiency.

Future research should be expanded based on these preliminary results. As a perspective, other species and classes of algae can be exploited for a sustainable valorisation of this natural resource. The application scope of algal polysaccharides may be broadened for other domains such us the purification and depollution of water, development of biodegradable composites and films. Further, these polysaccharides alone or combined, row or modified could be excellent carriers for the delivery of other drugs, encapsulation of essential oils and nutrients.

Appendix

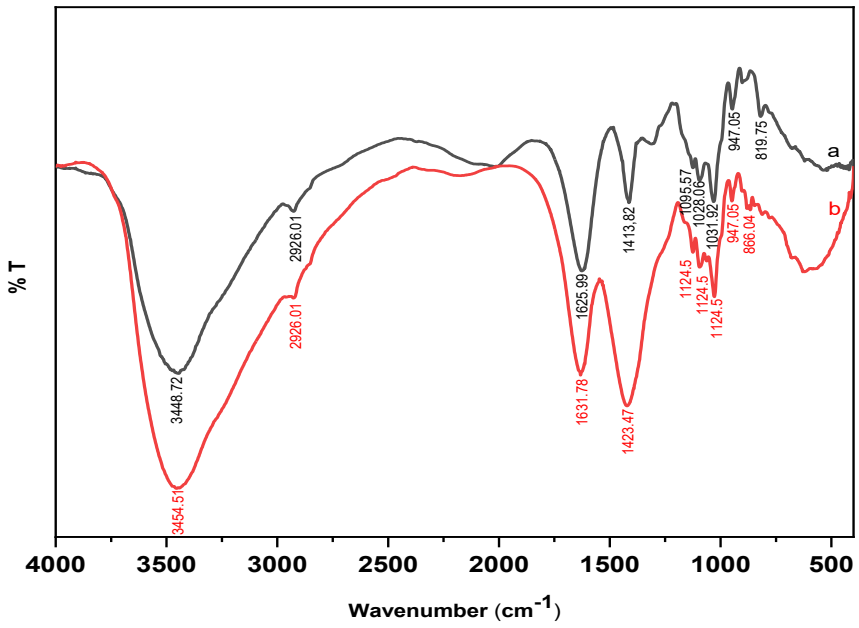


Figure. FTIR spectrum of **(a)** commercial and **(b)** Cystoseira stricta extracted sodium alginate.

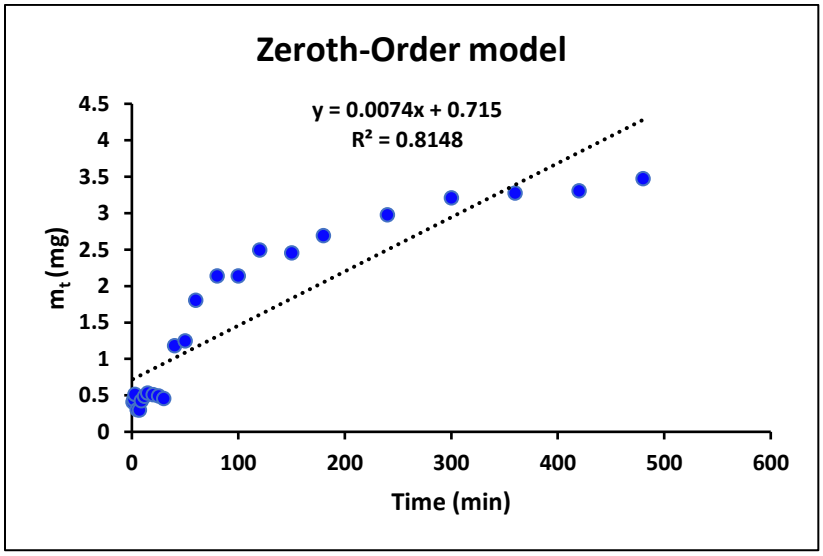


Figure. Cephalexin release data fitted to zero-order kinetic model.

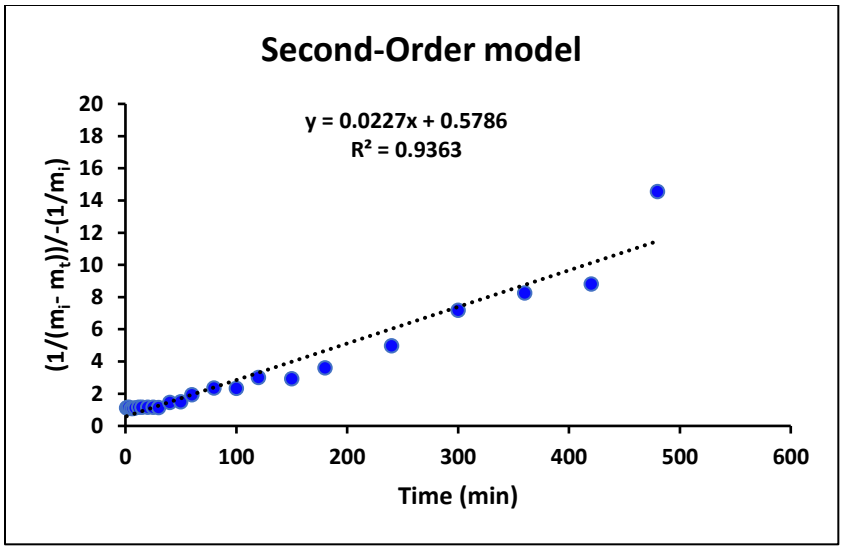


Figure. Cephalexin release data fitted to second-order kinetic model.

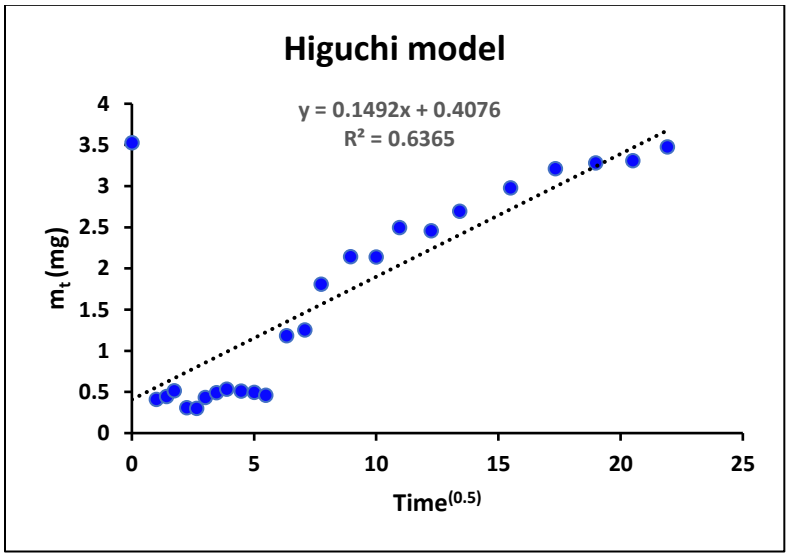


Figure. Cephalexin release data fitted to Higuchi kinetic model.

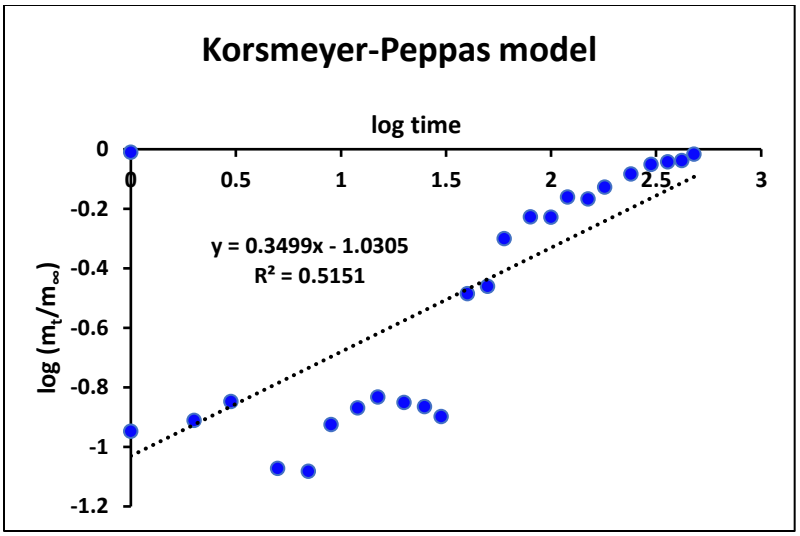


Figure. Cephalexin release data fitted to Korsmeyer-Peppas kinetic model.

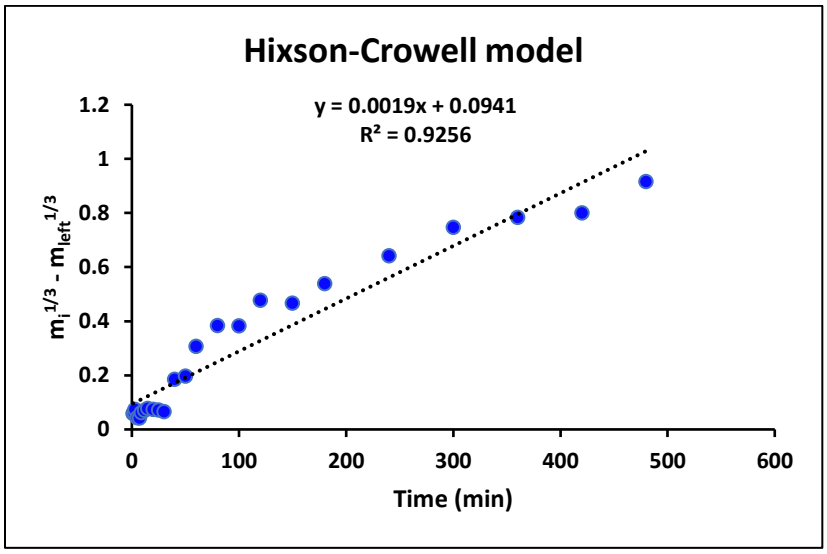


Figure. Cephalexin release data fitted to Hixon-Crowell kinetic model.

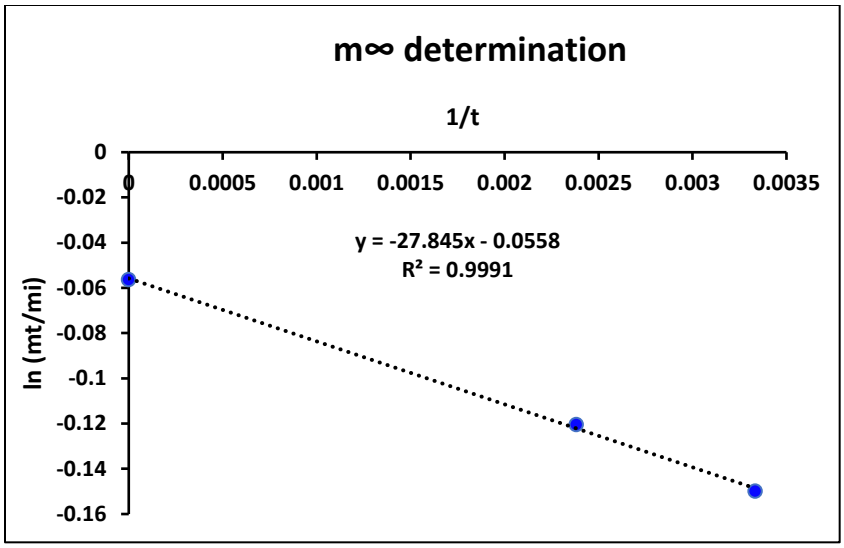


Figure. Plotting for the determination of m_{∞}.

Check for updates

JOURNAL OF
Bioactive and Compatible Polymers

Original article

Journal of Bioactive and Compatible Polymers
1–18
© The Author(s) 2026
Article reuse guidelines:
sagepub.com/journals-permissions
DOI: 10.1177/08839115251401209
journals.sagepub.com/home/jbc
Sage

Elaboration and characterization of maleated sodium alginate derivative from west Algerian algae biomass with enhanced antioxidant potential

Radhia Elong[1], Mahmoud Belalia[1], Louiza Belkacemi[2], Fouad Mekhalef Benhafsa[3,4,5] and Bouchama Abdelghani[3,6]

Abstract

The present study aimed to characterize *Cystoseira stricta* sodium alginate and its maleated derivative for potential use in food preservation. The alginate was extracted from the brown alga *Cystoseira stricta*, harvested from west Algerian coast (35°49′N/0°01′W). The sodium alginate was grafted with maleic anhydride to obtain maleated sodium alginate. The native and grafted sodium alginate were analyzed using FTIR, XRD, SEM, DSC, TGA, X-ray, and EDX. Their antioxidant potential was evaluated using DPPH scavenging activity. Additionally, a nanoemulsion based on maleated sodium alginate and date seed oil was synthesized and applied as an edible functional coating for delaying strawberries' spoilage. The extraction of sodium alginate resulted in good yield (37.52%) with a β-D-mannuronic acid /α-L-guluronic acid (M/G) ratio of 0.80. The grafting of sodium alginate with maleic anhydride has been successfully executed and confirmed by infrared analysis and DSC. The degree of substitution was estimated to 93%. The crystallinity becomes greater according to x-ray diffraction data. Thermal analysis indicated that maleated sodium

[1]Laboratoire Structure, Elaboration et Application des Matériaux Moléculaires (SEAMM), Department of Chemistry, Faculté de Sciences Exactes et de l'Informatique, Abdelhamid Ibn Badisuniversity, Mostaganem, Algeria
[2]Laboratory of Agricultural, Agri-food Production Techniques and Sustainable Development, Higher School of Agronomy of Mostaganem, Mostaganem, Algeria
[3]Centre de Recherche Scientifique et Technique en Analyses Physico-chimiques (CRAPC). Zone Industrielle, BP 384 Bou-Ismail, Tipaza, Algeria
[4]Unité de Recherche en Analyses Physico-Chimiques des Milieux Fluides et Sols (URAPC-MFS/ CRAPC), 11, Chemin Doudou Mokhtar, Ben Aknoun – Alger, Algeria
[5]Laboratory of Advanced Materials and Physicochemistry for the Environment and Health (MAPES), Djillali Liabes University, P.B. 89 Sidi Bel Abbes, Algeria
[6]Plateau Technique d'Analyses Physico-Chimiques, PTAPC-Mostaganem, Algeria

Corresponding author:
Mahmoud Belalia, Laboratoire Structure, Elaboration et Application des Matériaux Moléculaires (SEAMM), Department of Chemistry, Faculté de Sciences Exactes et de l'Informatique, Abdelhamid Ibn Badisuniversity, Mostaganem 27000, Algeria.
Email: mahmoud.belalia@univ-mosta.dz

alginate was more thermally stable. The SEM/EDX analyses revealed well defined morphological characteristics and high chemical purity of native and modified sample. The maleated sodium alginate exhibits higher antioxidant activity than native sodium alginate. It was found the maleation cannot improve only the antioxidant ability but also the product esthetic. The prepared nanostructured system demonstrated dispersion stability with a zeta potential of −29.9, as determined by DLS. When applied as an edible coating, it effectively protected and enhanced the shelf-life of fresh strawberries at ambient temperature.

Keywords
Algerian coast, *Cystoseira stricta*, sodium alginate, maleated sodium alginate, modification, antioxidant activity, edible coating

Introduction

Nowadays, environmental awareness is increasing, and the demand for eco-friendly materials is growing faster to replace synthetic ones in numerous industrial applications. Algal biomass has recently gained a great interest from researchers and industries due to its significant potential as a functional ingredient and source of active agents.[1]

Brown algae, or *Phaeophyceae*, are the second most abundant group of marine algae.[2] They contain a large amount of bioactive components, mostly carbohydrates in the form of sulfated and non-sulfated polysaccharides.[1] Seaweed polysaccharides differ significantly from the terrestrial plant polysaccharides, and their composition and properties vary even between the algae species and within the same species.[2] In fact, their chemical composition is influenced by the environmental conditions, growth location, and harvesting season.[3] Crude polysaccharides extracted from brown seaweeds were reported to exhibit higher antioxidant activities with high levels of sulfate and polyphenols than that of green and red seaweeds.[4]

Alginate is the main polysaccharide present in the brown algae cell walls.[5] It is the only polysaccharide that naturally contains carboxyl groups in each constituent residue.[6] Alginate is a water-soluble polymer made up of linear β-D-mannuronic acid (M block) and α-L-guluronic acid (G block), linked in the position 1,4 (Figure 1).[7] Alginate can react with divalent cations via its free carboxylate groups, producing a gel.[8] The physicochemical properties of alginate depend on the proportion and distribution pattern of M and G blocks. Alginate with a high value of M/G ratio (>1) forms soft and elastic gels, while that with a weak value of M/G (<1) forms a mechanically stable, strong, and brittle gel.[9] The U.S. Food and Drug Administration (FDA) classifies food-grade sodium alginate as GRAS (generally regarded as safe) and lists its usage as an emulsifier, stabilizer, thickener, and gelling agent.[10] These techno-functional properties are attributable to the availability of hydroxyl groups in the C_2 and C_3 positions, which promotes the reactivity of sodium alginate with other moieties. Indeed, the alginate structure displays numerous free available hydroxyl groups, allowing the incorporation of a wide range of functional groups into the polysaccharide backbone.[11] Alginate derivatization via hydroxyl groups gives alginate derivatives particular properties, making possible their use in a variety of applications.[11] Maleic anhydride is a reactive additive that has been used as a grafting agent in different biomolecules such as proteins and enzymes to enhance their chemical biological properties.[12]

To our knowledge, this is the first work focusing on the chemical modification of sodium alginate extracted from *Cystoseira stricta* species with maleic anhydride. The objective was to develop a novel sodium alginate derivative with improved chemical and biological properties in order to apply it in food preservation, among other applications.

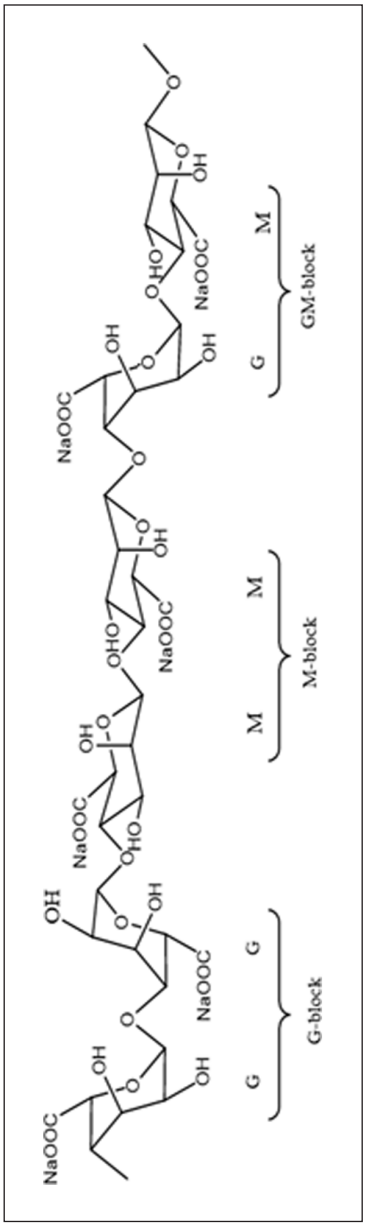


Figure 1. Structure of sodium alginate.

Materials and methods

Materials

Calcium Chloride dihydrate (Merck), (1-Hexadecyl) trimethylammonium bromide, 98% (Alfa Aesar), Sodium carbonate, Sodium hydroxide pellets > 98% (Merck), Acetic acid (Biochem), acetone 99% (Organics), Ethanol 96% (Specilab), Maleic anhydride, were all used without further purification.

Plant material preparation

The brown seaweed *Cystoseira stricta* was collected from Stidia shore (35°49′N/0°01′W) on the western Algerian coast during February 2022. The alga was washed several times with tap water to remove epiphytes and sand, then with distilled water. The sample was shade-dried to constant weight, then milled with an electric grinder. The algal powder was sieved to obtain a fine particle size of 150 µm using a CISA BA200N compact digital electromagnetic sieve shaker. The fine powder was preserved at room temperature away from humidity and light for further extraction and analysis.

Moisture content and ash determination

Moisture content was determined by placing the samples in the crucibles and drying them at 105 ± 1°C until a constant weight was achieved. After this, the same crucibles were placed in a muffle furnace at 575 ± 1°C for 4 h for ash content determination. The moisture and ash content were determined on three replicates. The moisture and ash content were calculated according to Farzanah et al.[13] as follows:

$$\text{MC}, \% = \left(1 - \frac{W_d}{W_i}\right) \times 100 \quad (1)$$

$$\text{Ash}, \% = \frac{W_r}{W_d} \times 100 \quad (2)$$

Where W_i is the initial weight of sample, W_d is the weight of samples after drying at 105°C and W_r is the weight of residues after drying at 575°C. All measurements were conducted at a resolution of ±0.0001 g.

Sodium alginate extraction

Pre-treatment. Algal powder was soaked in ethanol/chloroform/distilled water (4:2:1, v/v/v) for 15 min under ultrasonic agitation, then left overnight at room temperature under simple magnetic stirring in order to remove low molecular weight compounds such as pigments and proteins. The residue was separated by filtration using Whatman filters, washed with acetone, and finally oven-dried at 30°C.[14]

Alginate extraction. The pre-treated sample was mixed with an aqueous solution of 2% $CaCl_2$ at a ratio of 1:30 (w/v) at 85°C with regular stirring for 5h. After cooling to room temperature, the mixture was centrifuged, and the calcium alginate remaining in the residual seaweed was converted to the water-soluble sodium alginate using a 3% aqueous sodium carbonate solution (3.3%, w/v) and incubated at 70°C for 5 h. Then, the mixture was cooled at room temperature and centrifuged for 20 min. The supernatant was recovered and mixed with cold ethanol to precipitate Na-alginate (HO-alg).[5] This later was dried, milled, and kept in a hermetic container for further analyses and uses. Each experiment was repeated in triplicate for reliable results.

Sodium alginate modification

The maleation of extracted sodium alginate was conducted according to a modified method of Belalia et al.[15] One gram of sodium alginate (HO-alg) was mixed with 10 mL of 20% NaOH aqueous solution and stirred at room temperature. After 4 h, ethanol was added to crystallize the product. This later was filtered, rinsed with ethanol, and dried overnight (NaO-alg). One gram of NaO-alg was mixed with 10 mL of distilled water, 2.5 mL of triethylamine, and

1.5 g of maleic anhydride, and stirred for 90 min at 80°C. After cooling to room temperature, 10 mL of 1M acetic acid solution was added to the mixture kept under stirring for a further 2 h. The resulting product (Malg) was recovered by recrystallization in ethanol, filtration, and drying, then subjected to an alkaline treatment with saturated sodium carbonate aqueous solution for 2 h at room temperature. The final product was recovered and finally dried (NaMalg). The whole chemical reaction process is summarized in Figure 2.

Determination of the degree of substitution

The degree of maleation of sodium alginate was determined by the titration method as reported by Wardhani et al.[16] with slight modifications. Sodium alginate or maleated sodium alginate (500 mg) was reacted with excess NaOH (10 mL, 0.1 N) overnight at room temperature to hydrolyze the ester groups. The remaining NaOH molecules were then back-titrated with 0.1N HCl solution using phenolphthalein as an indicator. The degree of substitution was calculated as follows (equation (3)):

$$\mathrm{DS} = \frac{M_a \times C\left(V_0 - V\right) \times 10^{-3}}{m - M_b \times C\left(V_0 - V\right)} \tag{3}$$

Where m is the sample mass, M_a and M_b are the molecular weight of sodium alginate repeating unit (198 g/mol) and acyl group, respectively, V_0 and V are the titration consumed volumes of hydrogen chloride by native and modified sodium alginate, respectively, C is the hydrogen chloride molar concentration.

Characterizations

The FT-IR spectra were recorded using a spectrophotometer (Shimadzu-IR Prestige-21) in the range of 400–4000 nm^{-1}. Sample were mixed and ground with KBr and pressed with Specas press 10 ton load configuration. The XRD (Rigaku-Smartlab) radiation Cu-Kα/1.54186 Å operating at the diffraction angle 2θ range from 4° to 40° at 40 KV and 50 mA with scanning rate 2°/min. The morphological analysis of native and modified extracted sodium alginate was carried out using Desktop Scanning Electron Microscope (SEM) (thermoscientific Phenom Pharos G2) coupled with an energy dispersive spectroscopy (EDS) using high vaccum mode (0.10 Pa) and acceleration voltage of 10–15 kV. The samples were priory coated with Gold-Palladium layer after 3 purge cycles using a sputter (Leica EM ACE200) for 30 s at a current of 30 mA. Simultaneous DSC and TGA measurements were carried out with (TA SDT650) analyzer. 5–10 mg of samples were heated at a ramping rate of 10 C°/min under nitrogen flow of 50 mL/min.

Antioxidant activity evaluation

The 1,1-diphenyl-2-picrylhydrazine DPPH radical scavenging assay was conducted as described by Belkacemi et al.[17] with slight modifications. A volume of 1950 µL of 0.08 mM DPPH solution in ethanol was added to 50 µL of HO-alg or NaMAlg solutions in distilled water at varying concentrations. The absorbance was measured after 30 min at 517 nm using a spectrophotometer (analytic jena SPECORD 210 PLUS). Control reaction (without sample solution) and blanks (without DPPH solution) were also prepared. Ascorbic acid was used as a standard. The inhibition percentage of DPPH was calculated using the following equation:

$$Inhibition\left(\%\right) = \frac{\left(A_C - A_S\right)}{A_C} \times 100 \tag{4}$$

Where A_c is the control reaction absorbance and A_s is the absorbance in presence of the sample or standard. The 50% inhibition concentration (IC_{50}) was determined by linear regression analysis. The results are the mean of three repetitions.

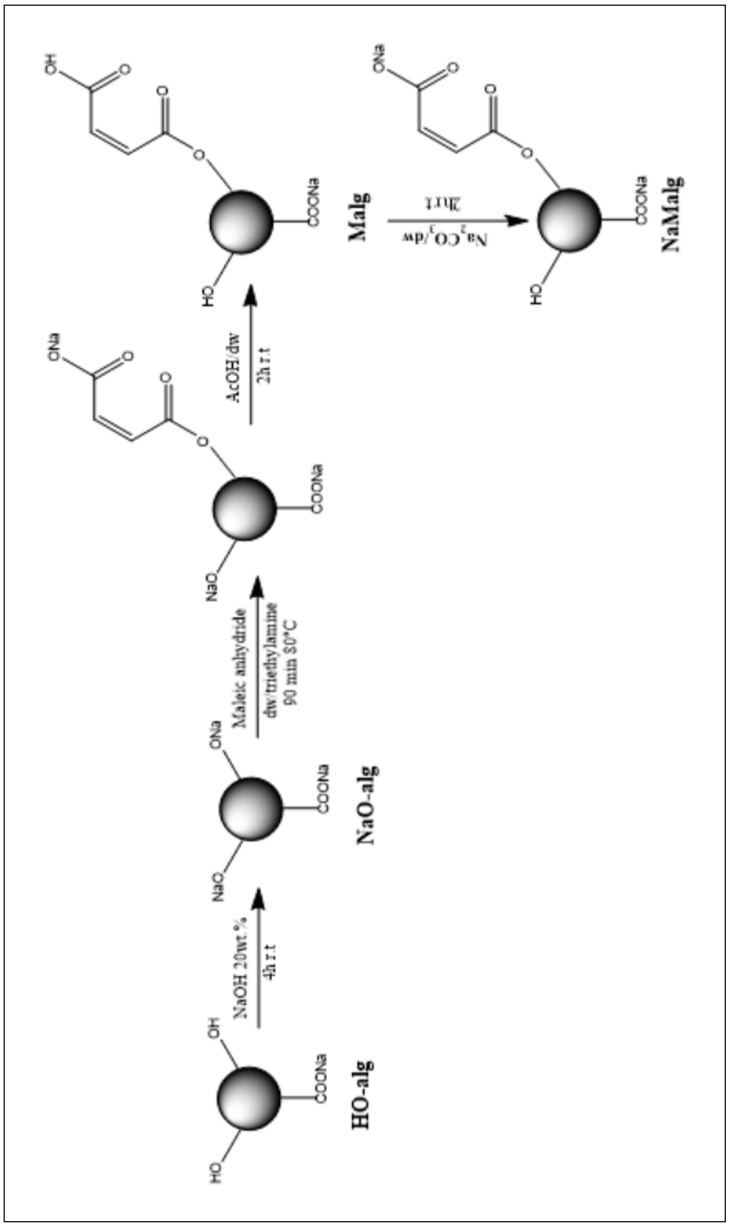


Figure 2. Schematic diagram of sodium alginate modification.

Preparation and application of maleated sodium alginate-date seed oil-based oil-in-water nanoemulsion

Nanoemulsion preparation. The nanoemulsion of maleated sodium alginate was prepared using date seed oil (DSO) purchased from Inovapalm company (Algeria). The DSO was extracted from date seeds of the *Phoenix dactylifera* species cultivated in Tolga (Biskra, Algeria). Three hundred milligrams of DSO were dissolved in 150 µL of ethanol to prepare oil phase. In parallel, the aqueous phase containing 300 mg of NaMalg and 30 mL of distilled water was prepared under slight heating and stirring for 2 h. After that, 300 mg of Tween 80 was added to the mixture and stirred at room temperature. After 10 min of stirring, the mixture was poured slowly into the lipophilic organic phase for 30 min under gentle stirring. The nanoemulsion was stabilized by sonication for 15 min. Finally, crosslinking was achieved by adding 10 mL of 0.002 g/mL $CaCl_2$ aqueous solution to obtain a viscous solution.[18] The same steps were followed to prepare nanoemulsion (control) with sodium alginate and date seed oil.

Protective effect evaluation of the nanoemulsion. The synthesized nanoemulsion was applied as an edible functional coating for strawberry protection from spoilage. A thin layer of the nanocoating was applied on the entire surface of fresh strawberries, of comparable size using a brush (spreading technique). Each sample was placed separately in a sterile container and kept over 14 days at room temperature. Uncoated samples were used as a control for comparison in the same conditions. All samples were imaged daily over the period of study. The Zeta potential and Z average were analyzed by Horiba nano-Partica SZ-100V2 analyzer using 1% coating suspension in ultrapure water.

Results and discussion

Moisture content and ash determination

Cystoseira brown alga was ground and sieved into 150 µm powder to ensure the uniformity of the powdered seaweed. The moisture content of the raw material reached 6.69 ± 0.11%, and the ash content was 35.86 ± 3.03%.

Sodium alginate extraction yield

The pretreatment process before biomolecule extraction is of great importance to enhance the exposure of target compounds to the extraction solvent and to remove excess color and undesired molecules. The use of ultrasonication before or during extraction is crucial for cell wall disruption to allow solvent to penetrate the surface area of algal powder and improve thereby the extraction yield.[19]

In the process of sodium alginate extraction from *Cystoseira stricta*, an aqueous solution of $CaCl_2$ was used to convert sodium alginate contained in the cell wall of alga into water-insoluble calcium alginate, which was removed together with solid seaweed residues. Sodium carbonate was then used to solubilize alginate into water-soluble sodium salt form. The final product was purified by ethanol precipitation to remove low molecular weight impurities from the polysaccharide.[4] The extraction yield reached in this study (37.52 ± 1.22%) is one of the highest yields reported in the literature for *Cystoseira* species and other species (Table 1). It seems that the solid loading ratio used in the present study enhanced the extraction yield without altering the structure of alginate. According to Saji et al.,[20] seaweed loading ratio, together with the pre-treatment and time extraction, significantly improves the extraction efficiency.

Characterization

Physical appearance of native and modified sodium alginate. The brown color of extracted native sodium alginate lightened after grafting it with maleic anhydride, noticeably improving the product's visual appearance (Figure 3). This natural lightening avoided the utilization of toxic reagents, such as formaldehyde, in the bleaching step during the extraction process, which can badly influence the rheological and physicochemical properties of alginate.[26] The lightening of maleic sodium alginate would be

Table 1. Alginate content and M/G ratio of different species.

Species	Harvesting site	M/G ratio	Alginate content%	Reference
Cystoseira barbata	Kerkennah Island (Sfax, Tunisia)	0.59	9.9	Sellimi et al.[21]
Cystoseira compressa	Kerkennah Island (Sfax, Tunisia)	0.65	21.65 ± 1.5	Hentati et al.[22]
Cystoseira crinita	Bulgarian Black Sea Coast	1.018	20.18 ± 1.7	Kokova et al.[23]
Dictyota dichotoma	Red Sea Coast of Sudan	0.92	8.8 ± 2.12	Abdel and Osman[9]
Hormophysa cuneiformis		0.97	19.1 ± 1.62	
Padina pavonica		0.93	7.99 ± 2.60	
Turbinaria ornata		1.01	14.3 ± 1.2	
Laminaria digitata	Isle of Seil, Scotland		34.6 ± 3.1	Ptak et al.[24]
Laminaria hyperborean			33.2 ± 3.8	
Saccharina latissimi			28.5 ± 3.9	
Alaria esculenta			37.4 ± 4.0	
Laminaria ochroleuca (blade)	Atlantic Coast of Morocco		28.96 ± 0.20	Kaidi et al.[25]
Laminaria ochroleuca (stipe)		1.38	49.80 ± 2.40	
Saccorhiza polyschides (blade)		1.62	20.19 ± 2.00	
Saccorhiza polyschides (stipe)		2.14	26.28 ± 0.08	
Cystoseira stricta	Stidia Algerian coast	0.81	37.52 ± 1.22	The present work

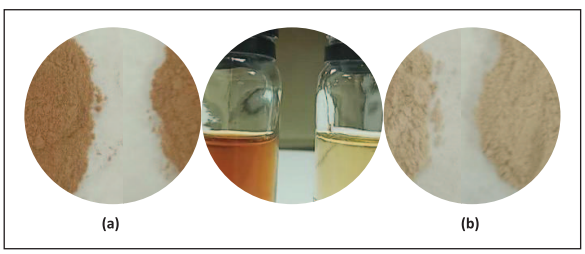


Figure 3. Physical appearance of (a) crude and (b) modified sodium alginate.

useful in the preparation of gel film or nanoemulsion for food coating. At this fact, Ye et al.[27] reported that maleic anhydride grafted to agar significantly improved agar gel transparency.

FT-IR analysis. The alginate extract was characterized by the means of FTIR. Figure 4 shows the spectra of native and modified sodium alginate. The bands around 3454, 2926, 1631, 1423, 1095, 1028, and 947 cm^{-1} are related to O-H bond stretching vibration, C-H bond stretching vibration, COO-asymmetric and symmetric stretching vibration, C-O-C stretching vibration of mannuronic and guluronic units and C–O stretching vibration of uronic acid residues, respectively. The spectrum of extracted sodium alginate, which was not significantly different from that of the commercial one, hence confirming the purity of the sample.

The proportion and distribution of mannuronic (M) and guluronic (G) units (M/G ratio) affect the physicochemical properties of sodium

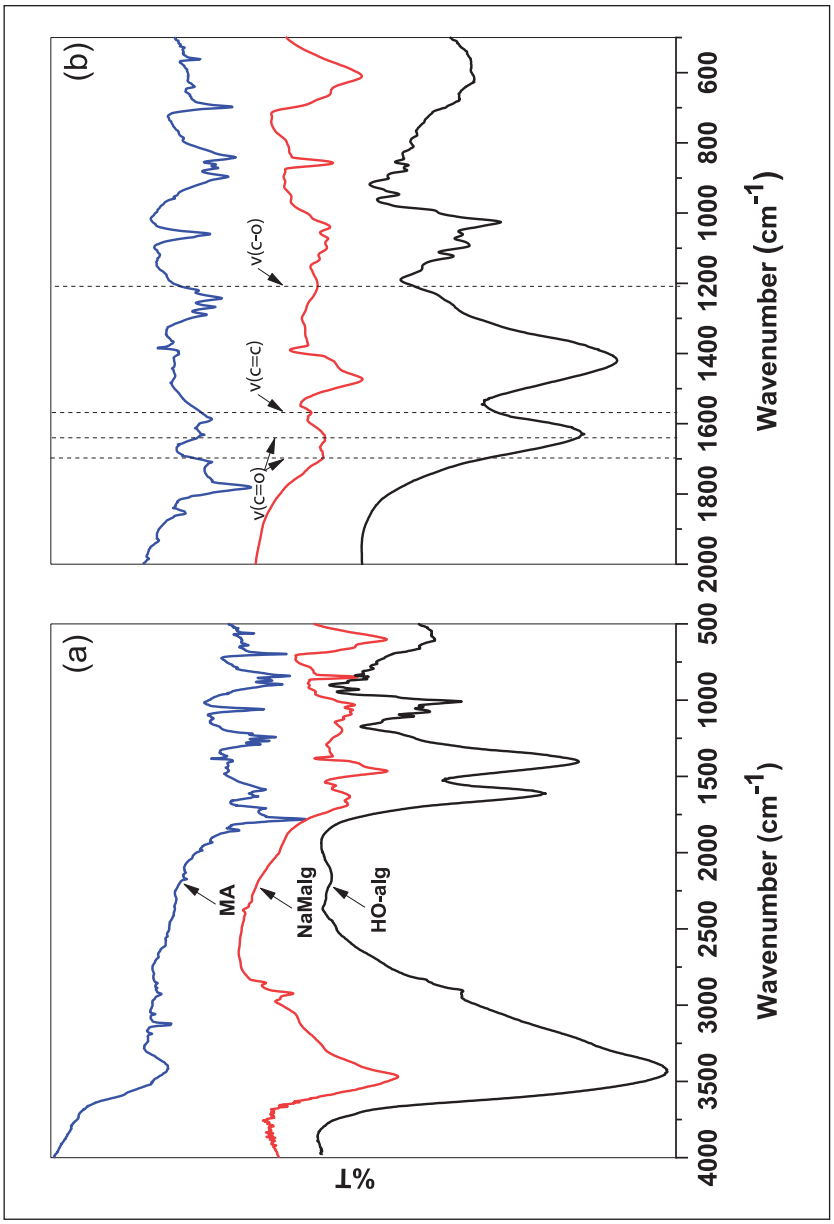


Figure 4. FTIR spectra of maleic anhydride, crude and maleated sodium alginate (a), zoom of the 2000–500 cm^{-1} region (b).

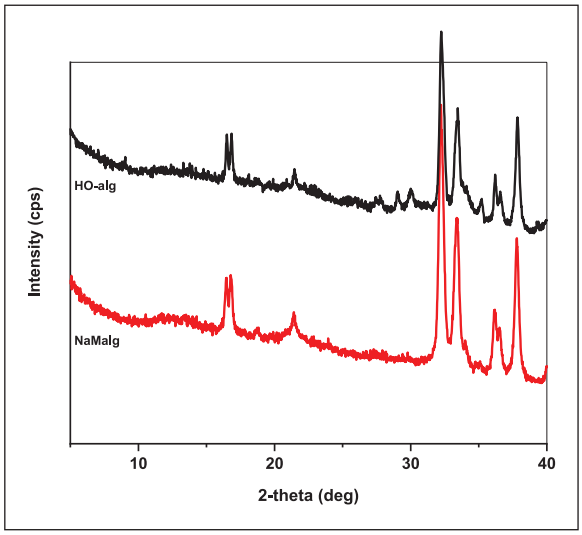


Figure 5. XRD patterns of native and modified sodium alginate.

alginate solutions. This parameter was estimated by Sakugawa et al.[28] using FTIR by calculating the ratio between the absorbance reading at the frequencies of M and G units. According to the calculation, the Na-Alginate's M/G atio of the current study was lower compared to those reported for different algal species, except for *Cystoseira barbata* and *Cystoseira compressa* (Table 1). The characteristic absorption peaks of sodium alginate were maintained after chemical modification, with the emergence of a new band at 1560 cm^{-1} assigned to the maleic anhydride double bond. Two stretching vibration bands of ester carbonyl appeared near 1686 cm^{-1} and the maleic carboxyl C=O bond at 1626 cm^{-1} overlapped with the C=O stretching band of alginate. This indicates the successful maleic anhydride grafting into sodium alginate chains.

X-ray diffraction (XRD). The diffractogram (Figure 5) shows the major crystalline peaks of sodium alginate at 16.84° and 21.45°. According to the study performed by Zhao et al.,[29] the intense crystalline peak at 32° is ascribed to (2 0 0) planes. The chemical modification induced a slight increase in the intensity of the characteristic peaks, and they became slightly broader while maintaining the general pattern of pure alginate. Similar observations were reported by Chen et al.[30] about crystal structures of alginate derivatives obtained through esterification.

SEM/EDX analysis. The SEM analysis (Figure 6) of native alginate revealed a rough surface with visible voids. At higher magnifications, different alignments of thin and small-sized rods were observed distributed homogenously at the surface. Functionalization of alginate with maleic anhydride resulted in a morphology change characterized by the presence of several bundles of parallel rods. These later became thicker and greater compared to the HO-alg structure, which can be attributed to the covalent bonding of maleic anhydride resulting in the modification of the internal polymeric chain order of sodium alginate.

The EDX analysis (Figure 7) provided details on the elemental composition of samples. The surface of both HO-alg and NaMalg contained C, O and Na atoms in different proportions with no characteristic peaks of impurities such as heavy metals (Arsenic, lead).

Thermal analysis. The TGA and DSC thermograms of modified and unmodified extracted

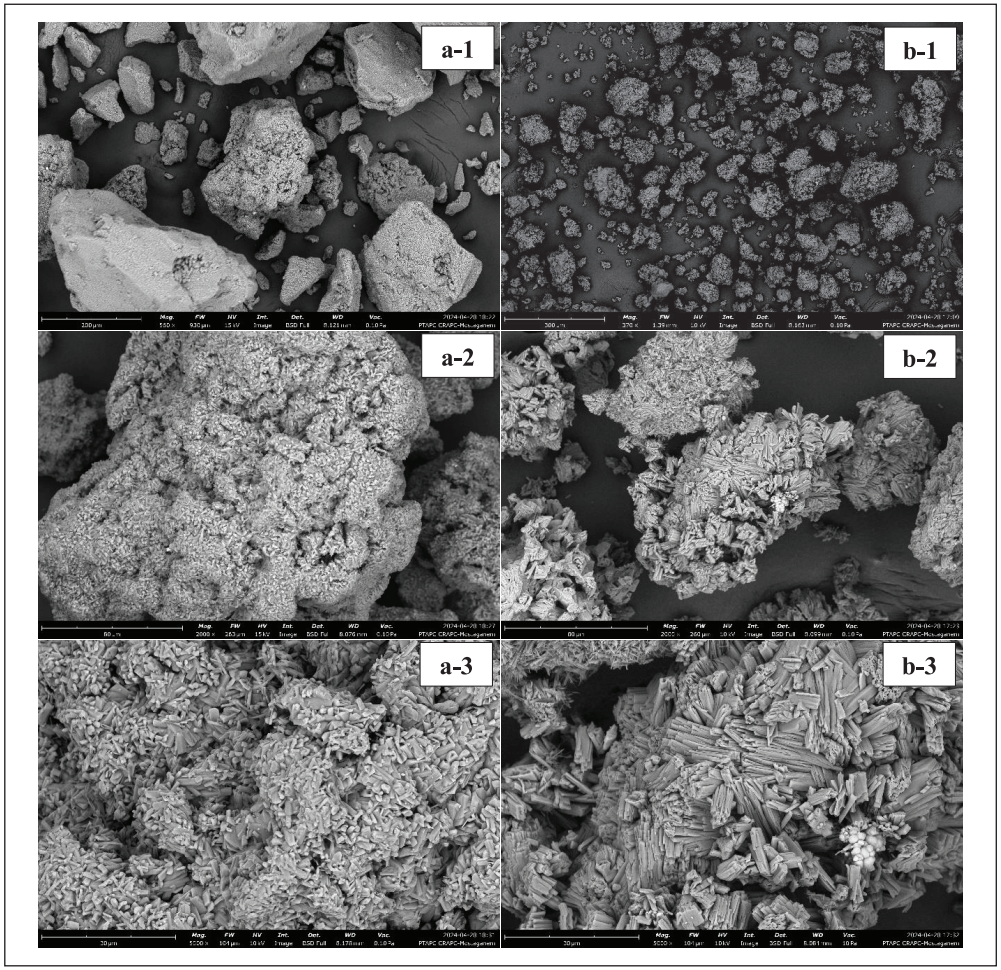


Figure 6. SEM images of native and modified alginate (a-1) HO-alg (200 µm), (a-2) HO-alg (80 µm) and (a-3) HO-alg (30 µm), (b-1) NaMalg (300 µm), (b-2) NaMalg (80 µm) and (b-3) NaMalg (30 µm).

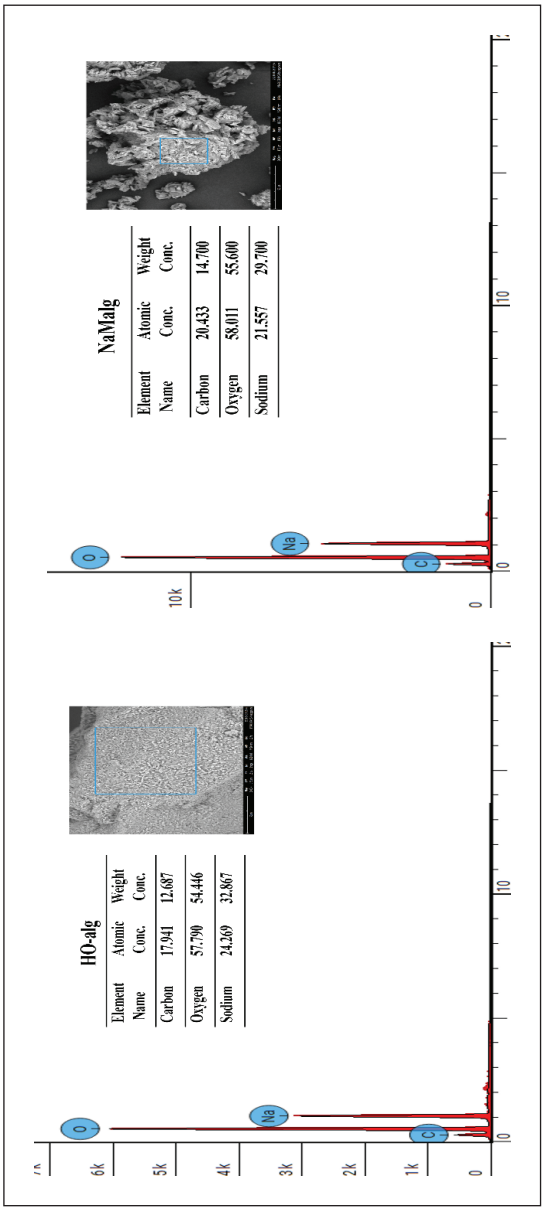


Figure 7. EDX images of native and modified.

sodium alginate are depicted in Figure 8. By plotting the differentiate of TGA curves, three stages have been noticed. The first one, recorded between 50°C and 170°C, was attributed to non-bonded than adsorbed water molecules evaporation. The second stage corresponded to polymer chain degradation at 254°C (modified) and 245°C (native) and the release of intermediate substances. The later showed degradation curves from 300 up to 1000°C. The temperatures of 50% weight loss were 417°C (modified) and 732°C (native). These findings corresponded well with the value ranges previously mentioned in the work of Benslima et al.[31]

The DSC curves in Figure 8(b) revealed clearly the thermal phase transitions occurring within samples. The first endothermic peak in the HO-alg curve is mainly caused by water evaporation. A second endothermic peak around 140°C, followed by an exothermic peak at 245°C, indicated a thermal decomposition process of native alginate.[32] Concerning the NaMalg curve, there is no obvious endothermic peak around 140°C, indicating the improvement of the thermal stability of alginate within this stage after modification.[33] The exothermic peak was shifted to a higher temperature after modification with MA. This temperature increasing confirmed the sodium alginate chain modification. Madhusudana Rao et al.[34] also demonstrated that the exothermic peak temperature increased after grafting poly(vinyl caprolactam) onto sodium alginate chains.

Determination of the degree of substitution

The degree of substitution (DS) value of the maleated alginate was found to be 0.9297 ± 0.33. This implies that almost 93% of the hydroxyl groups present in the alginate polysaccharide have undergone an esterification reaction with maleic anhydride. The synthesis of maleic anhydride esterified sodium alginate has not been previously reported prior to this work. However, maleic anhydride was used for the modification of other polysaccharides such as corn starch,[35] cellulose,[36] pectin,[37] and κ-carrageenan.[38] The DS has reached 0.3386, 0.38, 0.6657, and 0.032, respectively.

Antioxidant activity test

The scavenging activity of the DPPH radical is among the frequent methods used for the first screen of the antioxidant properties of polysaccharides because of its simplicity, low cost, and rapid outcomes.[39] In the present study, both native and modified sodium alginate were assessed for their DPPH scavenging ability. The native sodium alginate recorded a very high IC_{50} value (223.95 mg/mL), indicating its very weak DPPH radical-scavenging ability. The low M/G ratio (0.80) of the unmodified sodium alginate could negatively influence the DPPH antioxidant activity. As reported by Bai et al.,[40] the antioxidant properties of polysaccharides are significantly affected by their proportion of monosaccharide components. In this regard, it was reported that the fraction with higher M/G has more potent antioxidant activity.[41] Maleic anhydride esterification of sodium alginate significantly reduced the IC_{50} to 55.6 mg/ml ($p < 0.001$), confirming its favorable effect on increasing the DPPH antioxidant activity of the NaMalg polymer. Similarly, Xiong et al.[42] found that grafting maleic anhydride onto xanthan oligosaccharides enhanced their DPPH radical-scavenging activity.

Protective effect evaluation of maleated sodium alginate-date seed oil-based oil-in-water nanoemulsion

Nowadays, edible coatings are used as a strategy to preserve the postharvest quality of many fresh fruits and vegetables and extend their shelf life.[43] Polysaccharides are among the biomolecules being recently used as a sustainable material in coatings.[44] As polysaccharides, the alginate has good gas and mechanical barrier properties, however, its hydrophilic nature makes it a poor moisture barrier.[45] The objective was to assess the effect of grafting sodium alginate with maleic anhydride on the efficiency of nanoemulsion on strawberry preservation. The nanoemulsions were assessed for their

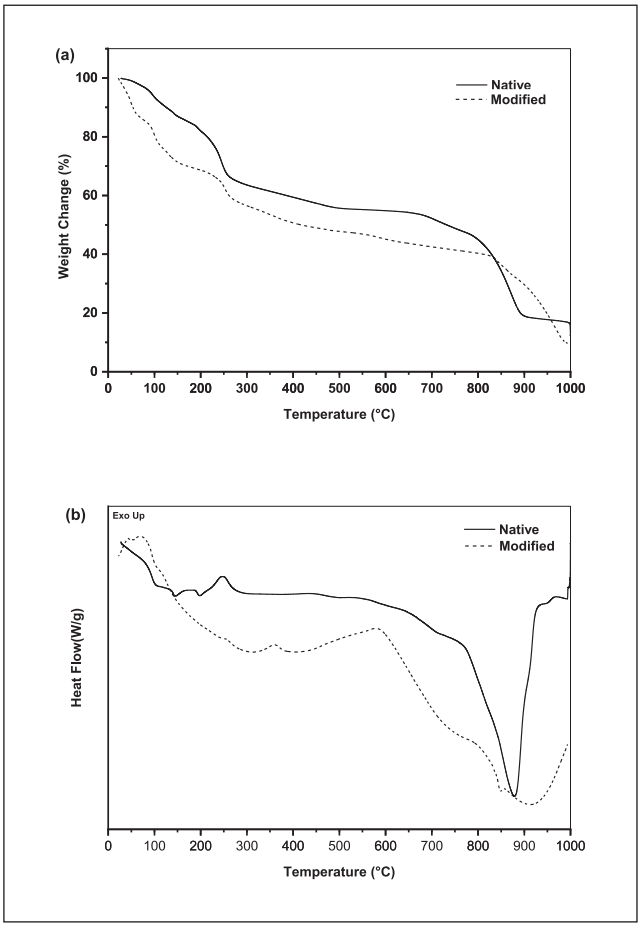


Figure 8. TGA (a) and DSC (b) curves of native and modified sodium alginate.

Table 2. Characteristics of maleated sodium alginate-date seed oil-based nanoemulsion.

Peak no.	S.P. area ratio	Mean particle diameter (nm)	SD	Z average (nm)	PI	Mean zeta potential (mV) at 25°C
1	0.51	191	37.9	461.8	0.546	−29.9
2	0.49	1413.7	286.4			

1: date seed oil-based nanoemulsion; 2: maleated sodium alginate-date seed oil-based nanoemulsion.
PI: polydispersity index, SD: standard deviation.

dimensions and physical stability using DLS. The outcomes are reported in Table 2. Their zeta potential of about ±30 mV is indicative of adequate stability of the system as mentioned by Honary and Zahir.[46]

The results of nanoemulsion protective effect on strawberries are shown in Figure 9. The uncoated samples developed spoilage on their surface within only 5 days, and lost water as were totally covered by mold at the sixth day

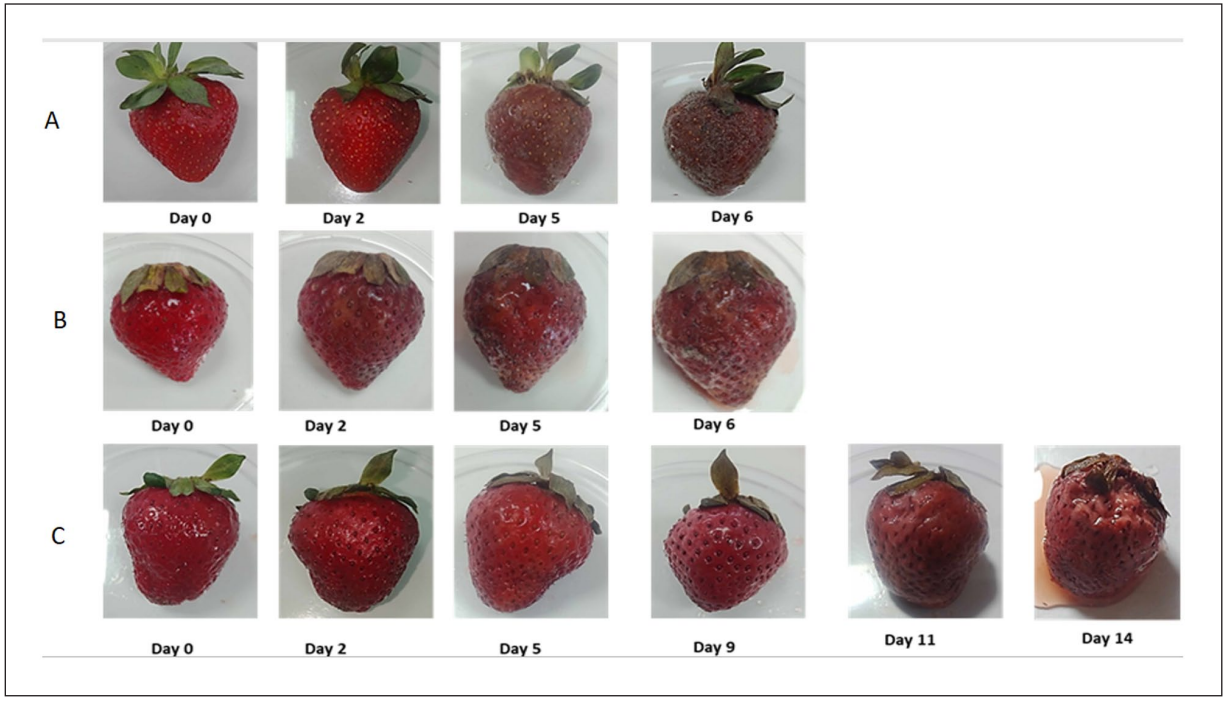


Figure 9. Nanoemulsion coating effect on strawberries over the time at room temperature ((a) uncoated strawberries; (b) coated strawberries with sodium alginate-based nanoemulsion; (c) coated strawberries with maleated sodium alginate-based nanoemulsion).

of storage at room temperature. Meanwhile, there was no change of the texture of the coated samples with the maleated sodium alginate-date seed oil nanoemulsion till the 11th day, whereas, the sample coated with sodium alginate-date seed oil nanoemulsion displayed a noticeable deterioration starting already at the fifth day. The incorporation of maleic anhydride as hydrophobic group contributed to the delaying of strawberries' spoilage. In this regard, Sousa et al.[47] reported that incorporating anhydrides in the molecular chain of chitosan has been shown to provide better antimicrobial properties. Besides, the nano-sized oil droplets dispersed in the alginate network provided a hydrophobic barrier that reduces moisture loss from the fruit surface. This kept fruit freshness, reduced textural changes and expended shelf-life. Those results are in agreement with the results of Santos et al.[18] which indicated that the coating of fruits and seeds with a system of nanoparticles based on alginate associated with essential and vegetable oils inhibited the growth of microorganisms and delayed the fruit maturation.

Conclusion

The present paper reports the extraction of sodium alginate from Algerian *Cystoseira stricta* species. The introduction of the ester group onto the extracted sodium alginate by reaction with maleic anhydride has been successfully carried out as confirmed by FTIR, XRD, and TGA/DSC analysis data and DS value. This chemical modification affected the physical properties, the morphology, and the thermal stability of the sodium alginate maleate derivative. Indeed, it improved the maleate-grafted alginate's color and its antioxidant activity. Furthermore, utilizing maleated alginate-based nanoemulsion and date seed oil as a functional coating was efficient in preventing spoilage and thereby extending the shelf life of coated strawberries when compared to the control ones. This nanostructured system would be suitable for preserving and prolonging the storage life of fruits and vegetables.

Acknowledgments

The authors are grateful for the substantial support provided by the General Direction of Scientific Research and Technology Development (DGRSDT, MESRS, Algeria).

ORCID iD

Mahmoud Belalia https://orcid.org/0000-0003-2812-0947

Author contributions

Radhia Elong did the lab practice and wrote the manuscript. Mahmoud Belalia supervised the study and contributed in writing manuscript. Louiza Belkacemi identified the algae, , and contributed in writing and editing the manuscript. Fouad Mekhalef Benhafsa and Bouchama Abdelghani performed the XRD and SEM/EDX analyses.

Funding

The authors received no financial support for the research, authorship, and/or publication of this article.

Declaration of conflicting interests

The authors declared no potential conflicts of interest with respect to the research, authorship, and/or publication of this article.

References

1. Gullón B, Gagaoua M, Barba FJ, et al. Seaweeds as promising resource of bioactive compounds: overview of novel extraction strategies and design of tailored meat products. *Trends Food Sci Technol* 2020; 100: 1–18.
2. Cunha L and Grenha A. Sulfated seaweed polysaccharides as multifunctional materials in drug delivery applications. *Mar Drugs* 2016; 14(3): 42.
3. Dobrinčić A, Balbino S, Zorić Z, et al. Advanced technologies for the extraction of marine brown algal polysaccharides. *Mar Drugs* 2020; 18(3): 168.
4. Mohd Fauziee NA, Chang LS, Wan Mustapha WA, et al. Functional polysaccharides of fucoidan, laminaran and alginate from Malaysian brown seaweeds (Sargassum polycystum, Turbinaria ornata and Padina boryana). *Int J Biol Macromol* 2021; 167: 1135–1145.

5. Zaki M, Abdul Khalil HPS, Sabaruddin FA, et al. Microbial treatment for nanocellulose extraction from marine algae and its applications as sustainable functional material. *Bioresour Technol Reports* 2021; 16: 10811.
6. Gao X, Zhang Y and Zhao Y. Biosorption and reduction of Au (III) to gold nanoparticles by thiourea modified alginate. *Carbohydr Polym* 2017; 159: 108–115.
7. Usov AI and Zelinsky ND. Chemical structures of algal polysaccharides. In: Domínguez H (ed.) *Functional ingredients from algae food and nutraceuticals*. Woodhead Publishing Series in Food Science, Technology and Nutrition, 2013, pp.23–86.
8. Abang S, Chan ES and Poncelet D. Effects of process variables on the encapsulation of oil in ca-alginate capsules using an inverse gelation technique. *J Microencapsul* 2012; 29(5): 417–428.
9. Abdel N and Osman R. Characterization of native alginates of common alginophytes from the Red Sea Coast of Sudan. *Int J Second Metabolite* 2020; 7(4): 266–274.
10. U.S. Food & Drug Administration. CFR - Code of Federal Regulations Title 21 Part 184, www.accessdata.fda.gov/scripts/cdrh/cfdocs/cfcfr/CFRSearch.cfm?fr=184.1724 (1985, accessed 2 January 2023).
11. Putri AP, Picchioni F, Harjanto S, et al. Alginate modification and lectin-conjugation approach to synthesize the mucoadhesive matrix. *Appl Sci* 2021; 11(24): 11818.
12. Popescu I, Suflet DM, Pelin IM, et al. Biomedical applications of maleic anhydride copolymers. *Rev Roum Chim* 2011; 56(3): 173–188.
13. Farzanah RH, Brudecki GP, Cybulska I, et al. Screening and production of biogas from macro algae biomass of Padina boergesenii, Colpomenia sinuosa, and Ulva sp. In: Bastidas-Oyanedel JR and Schmidt JE (eds) *Biorefinery: integrated sustainable processes for biomass conversion to biomaterials, biofuels, and fertilizers*. Springer, 2019, pp.727–740.
14. Chen S, Sathuvan M, Zhang X, et al. Characterization of polysaccharides from different species of brown seaweed using saccharide mapping and chromatographic analysis. *BMC Chem* 2021; 15(1): 1–11.
15. Belalia M, Bendjelloul M, Aziz A, et al. Surface modification of olive stone waste for enhanced sorption properties of cadmium and lead ions. *Acta Chem Iasi* 2018; 26(2): 281–306.
16. Wardhani DH, Ulya HN, Kumoro AC, et al. Partial hydrophobic modification of alginate using dodecenyl succinic anhydride for fish oil encapsulation. *Acta Sci Pol Technol Aliment* 2022; 21(4): 369–378.
17. Belkacemi L, Belalia M, Djendara A, et al. Antioxidant and antibacterial activities and identification of bioactive compounds of various extracts of Caulerpa racemosa from Algerian coast. *Asian Pac J Trop Biomed* 2020; 10(2): 87–94.
18. Santos C, de Araújo Gonçalves M, de Macedo LF, et al. Green nanotechnology for the development of nanoparticles based on alginate associated with essential and vegetable oils for application in fruits and seeds protection. *Int J Biol Macromol* 2023; 232: 123351.
19. Ummat V, Sivagnanam SP, Rajauria G, et al. Advances in pre-treatment techniques and green extraction technologies for bioactives from seaweeds. *Trends Food Sci Technol* 2021; 110: 90–106.
20. Saji S, Hebden A, Goswami P, et al. A brief review on the development of alginate extraction process and its sustainability. *Sustainability* 2022; 14(9): 1–20.
21. Sellimi S, Younes I, Ayed HB, et al. Structural, physicochemical and antioxidant properties of sodium alginate isolated from a Tunisian brown seaweed. *Int J Biol Macromol* 2015; 72: 1358–1367.
22. Hentati F, Delattre C, Ursu AV, et al. Structural characterization and antioxidant activity of water-soluble polysaccharides from the Tunisian brown seaweed Cystoseira compressa. *Carbohydr Polym* 2018; 198: 589–600.
23. Kokova V, Lukova P, Baldzhieva A, et al. Extraction, structural characterization, and in vivo anti-inflammatory effect of alginate from Cystoseira crinita (Desf.) Borry harvested in the Bulgarian Black Sea. *Mar Drugs* 2023; 21(4): 245.
24. Ptak SH, Hjuler AL, Ditlevsen SI, et al. The effect of seasonality and geographic location on sulphated polysaccharides from brown algae. *Aquac Res* 2021; 52(12): 6235–6243.
25. Kaidi S, Bentiss F, Jama C, et al. Isolation and structural characterization of alginates from the kelp species Laminaria ochroleuca and saccorhiza polyschides from the Atlantic Coast of

Morocco. *Colloids and interfaces* 2022; 6(4): 51.
26. Mohammed A, Rivers A, Stuckey DC, et al. Datasets on the optimization of alginate extraction from sargassum biomass using response surface methodology. *Data Brief* 2020; 31: 105837.
27. Ye S, Zhang Y, Chen J, et al. Synthesis and properties of maleic anhydride-modified agar with reversibly controlled gel strength. *Int J Biol Macromol* 2022; 201: 364–377.
28. Sakugawa K, Ikeda A, Takemura A, et al. Simplified method for estimation of composition of alginates by FTIR. *J Appl Polym Sci* 2004; 93(3): 1372–1377.
29. Zhao X, Wang X and Lou T. Preparation of fibrous chitosan/sodium alginate composite foams for the adsorption of cationic and anionic dyes. *J Hazard Mater* 2021; 403: 124054.
30. Chen X, Zhu Q, Liu C, et al. Esterification of alginate with alkyl bromides of different carbon chain lengths via the bimolecular nucleophilic substitution reaction: synthesis, characterization, and controlled release performance. *Polymers* 2021; 13(19): 3351.
31. Benslima A, Sellimi S, Hamdi M, et al. The brown seaweed Cystoseira schiffneri as a source of sodium alginate: Chemical and structural characterization, and antioxidant activities. *Food Biosci* 2021; 40: 100873.
32. Soares JDP, Dos Santos JE, Chierice GO, et al. Thermal behavior of alginic acid and its sodium salt. *Eclet Quim* 2004; 29(2): 57–63.
33. Xiaochao L, Dongtao L, Xuefeng S, et al. Development and performance study of coal seam water injection permeation enhancer based on polymer modification. *China Min Mag* 2023; 32(12): 177–183.
34. Madhusudana Rao K, Krishna Rao KSV, Sudhakar P, et al. Synthesis and characterization of biodegradable poly (vinyl caprolactam) grafted on to sodium alginate and its microgels for controlled release studies of an anticancer drug. *J Appl Pharm Sci* 2013; 3(6): 61–69.
35. Zuo Y, Gu J, Yang L, et al. Synthesis and characterization of maleic anhydride esterified corn starch by the dry method. *Int J Biol Macromol* 2013; 62: 241–247.
36. Mei CT, Jiang LY, Jiang MM, et al. Modification of cellulose extracted from waste newspaper. *IOP Conf Ser Earth Environ Sci* 2019; 295(3): 032009.
37. Bátori V, Jabbari M, Srivastava RK, et al. Synthesis and characterization of maleic anhydride-grafted orange waste for potential use in biocomposites. *BioResources* 2018; 13(3): 4986–4997.
38. Zhou Y, Chen FQ, Chen S, et al. Preparation and characterization of κ-carrageenan modified with maleic anhydride and its application in films. *Mar Drugs* 2021; 19(9): 486.
39. Fernandes PAR and Coimbra MA. The antioxidant activity of polysaccharides: A structure-function relationship overview. *Carbohydr Polym* 2023; 314: 120965.
40. Bai L, Xu D, Zhou YM, et al. Antioxidant activities of natural polysaccharides and their derivatives for biomedical and medicinal applications. *Antioxidants* 2022; 11: 2491.
41. Sen M. Effects of molecular weight and ratio of guluronic acid to mannuronic acid on the antioxidant properties of sodium alginate fractions prepared by radiation-induced degradation. *Appl Radiat Isot* 2011; 69: 126–129.
42. Xiong X, Li M, Xie J, et al. Preparation and antioxidant activity of xanthan. oligosaccharides derivatives with similar substituting degrees. *Food Chem* 2014; 164: 7–11.
43. Ghoora MD and Srividya N. Effect of packaging and coating technique on postharvest quality and shelf life of Raphanus sativus L. and Hibiscus sabdariffa L. Microgreens. *Foods* 2020; 9(5): 653.
44. Mohamed SAA, El-Sakhawy M and El-Sakhawy MA. Polysaccharides, protein and lipid -based natural edible films in food packaging: a review. *Carbohydr Polym* 2020; 238: 116178.
45. de Oliveira Filho JG, Miranda M, Ferreira MD, et al. Nanoemulsions as edible coatings: a potential strategy for fresh fruits and vegetables preservation. *Foods* 2021; 10(10): 2438.
46. Honary S and Zahir F. Effect of zeta potential on the properties of nano-drug delivery systems - a review (Part 2). *Trop J Pharm Res* 2013; 12(2): 255–264.
47. Sousa JM, Vieira ACC, Costa MP, et al. Chitosan grafted with maleic anhydride and ethylenediamine: preparation, characterization, computational study, antibacterial and cytotoxic properties. *Mater Chem Phys* 2022; 287: 126301.